

Titre: Nouveaux additifs pour les réfractaires en service à plus de 1200°C
Title:

Auteur: Minghua Zhang
Author:

Date: 2004

Type: Mémoire ou thèse / Dissertation or Thesis

Référence: Zhang, M. (2004). Nouveaux additifs pour les réfractaires en service à plus de 1200°C [Mémoire de maîtrise, École Polytechnique de Montréal]. PolyPublie.
Citation: <https://publications.polymtl.ca/7208/>

 **Document en libre accès dans PolyPublie**
Open Access document in PolyPublie

URL de PolyPublie: <https://publications.polymtl.ca/7208/>
PolyPublie URL:

**Directeurs de
recherche:** Claude Allaire
Advisors:

Programme: Non spécifié
Program:

UNIVERSITÉ DE MONTRÉAL

ÉCOLE POLYTECHNIQUE DE MONTRÉAL

**NOUVEAUX ADDITIFS POUR LES RÉFRACTAIRES
EN SERVICE À PLUS DE 1200°C**

MINGHUA ZHANG

DÉPARTEMENT DE GÉNIE PHYSIQUE
ÉCOLE POLYTECHNIQUE DE MONTRÉAL

MÉMOIRE PRÉSENTÉ EN VUE DE L'OBTENTION DU DIPLÔME DE
MAITRISE ES SCIENCES APPLIQUÉES
(GÉNIE MÉTALLURGIQUE)

LE 31 MARS 2004



National Library
of Canada

Bibliothèque nationale
du Canada

Acquisitions and
Bibliographic Services

Acquisitions et
services bibliographiques

395 Wellington Street
Ottawa ON K1A 0N4
Canada

395, rue Wellington
Ottawa ON K1A 0N4
Canada

Your file *Votre référence*

ISBN: 0-612-91974-9

Our file *Notre référence*

ISBN: 0-612-91974-9

The author has granted a non-exclusive licence allowing the National Library of Canada to reproduce, loan, distribute or sell copies of this thesis in microform, paper or electronic formats.

L'auteur a accordé une licence non exclusive permettant à la Bibliothèque nationale du Canada de reproduire, prêter, distribuer ou vendre des copies de cette thèse sous la forme de microfiche/film, de reproduction sur papier ou sur format électronique.

The author retains ownership of the copyright in this thesis. Neither the thesis nor substantial extracts from it may be printed or otherwise reproduced without the author's permission.

L'auteur conserve la propriété du droit d'auteur qui protège cette thèse. Ni la thèse ni des extraits substantiels de celle-ci ne doivent être imprimés ou autrement reproduits sans son autorisation.

In compliance with the Canadian Privacy Act some supporting forms may have been removed from this dissertation.

Conformément à la loi canadienne sur la protection de la vie privée, quelques formulaires secondaires ont été enlevés de ce manuscrit.

While these forms may be included in the document page count, their removal does not represent any loss of content from the dissertation.

Bien que ces formulaires aient inclus dans la pagination, il n'y aura aucun contenu manquant.

Canada

UNIVERSITÉ DE MONTRÉAL

ÉCOLE POLYTECHNIQUE DE MONTRÉAL

Ce mémoire est intitulé:

**NOUVEAUX ADDITIFS POUR LES RÉFRACTAIRES
EN SERVICE À PLUS DE 1200°C**

Présenté par: ZHANG Minghua

En vue de l'obtention du diplôme de: Maîtrise és sciences appliquées

A été dûment accepté par le jury d'examen constitué de:

Pr. RIGAUD Michel, président

Pr. ALLAIRE Claude, membre et directeur de recherche

Pr. CHARTRAND Patrice, membre

ACKNOWLEDGEMENTS

I express my extreme sense of gratitude to my research supervisor Professor Claude Allaire, Department of Engineering Physics, Ecole Polytechnique of Montreal, for his guidance, stimulating discussions, intellectual inspiration, encouragement, sound advice and good teaching during this course of study.

My appreciation to Professor Michel Rigaud, for creating a friendly and pleasant learning atmosphere.

I am thankful to Saied Afshar, for his support and help for experimental work.

I like to express my sincere thanks to Dr. Kannabiran Sankaranarayanan for his valuable help in the period of thesis writing, Vincent Ébacher and Redouane Megateli for helping me with the French translation of the abstract.

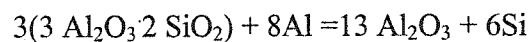
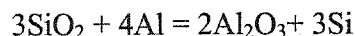
Furthermore, I would like to thank all my colleagues and friends at CIREP, including Jean-Philippe Bouchard, Huiqing HE, Roger PELLETIER, Vladimir Kovac, Stefan PALCO, Eugène PARANSKY, Xianxin ZHOU, Jingguo GAO, Huguette Rioux, Thérèse CRISSON, Yassine DOUCHE, Fangbao YE, Emmanuel DIVRY, and Christophe BAUBERT.

Finally, I am extremely grateful to my family members for their constant support, affection and sacrifices during the course of this research.

RÉSUMÉ

IL est bien connu que les fours de fusion et de maintien de l'aluminium sont divisés en 3 zones. Le revêtement réfractaire au-dessus de la ligne de métal est exposé à de hautes températures et est attaqué par la croissance du corindon. La température dans cette zone atteint habituellement plus de 1000°C et parfois même 1400°C. Le mécanisme de corrosion par lequel agit le corindon dépend de la température, de la pression partielle d'oxygène et de la composition de l'alliage métallique.

La dégradation d'alumino-siliceux par l'aluminium liquide est connue depuis longtemps. Cette détérioration est plus prononcée lorsque des éléments d'alliage tels que le magnésium et le zinc sont présents dans l'aluminium en fusion. Il est rapporté que l'aluminium liquide réduit la silice et les constituants du réfractaire alumino-siliceux (par exemple, la mullite) à un état métallique lors de la conversion de l'aluminium en corindon. Ces types de réaction peuvent être représentés comme suit :



La conversion des réfractaires alumino-siliceux, aussi appelée corrosion, peut causer plusieurs problèmes tels qu'une chute de leurs propriétés mécaniques, une contamination du bain métallique, une perte d'aluminium ainsi que d'importantes pertes de chaleur. C'est pourquoi, plusieurs tentatives ont été réalisées pour améliorer la résistance de ces réfractaires envers la pénétration et l'attaque chimique de l'aluminium.

Jusqu'à maintenant, la recherche au CIREP s'est concentrée sur les additifs pour des conditions de service de moins de 1200°C. Cependant, dans les fours de refonte, la température de service peut dépasser 1200°C pour diminuer le temps requis pour la fusion. Les additifs en usage jusqu'à maintenant ne peuvent résister convenablement à

des températures dépassant environ 1100°C. Ainsi, des additifs sont nécessaires pour protéger les réfractaires à des températures de plus de 1200°C.

Une nouvelle méthode a été développée pour le test de corrosion par le corindon à 1200°C. Elle permet de simuler la corrosion des réfractaires par le corindon tel qu'il se forme habituellement sur les parois des fours de maintien et de refonte de l'aluminium. Avec cette nouvelle méthode, il sera possible de choisir avec beaucoup plus de confiance le revêtement réfractaire le plus approprié pour les fours de traitement de l'aluminium.

À l'aide de cette méthode, quelques nouveaux additifs ont été développés pour augmenter la résistance des alumino-siliceux à des alliages Al-5%Mg-5%Zn. Afin de comprendre le mécanisme de corrosion, des techniques telles que la diffraction des rayons X (XRD), la porosimétrie au mercure et la microscopie optique ont été utilisées.

Quatre nouveaux genres d'additifs ont été identifiés.

Ils impliquent la présence de bore ou sont constitués de AlPO_4 , d'oxydes d'alcalino-terreux et d'oxydes de terres rares.

Les additifs à base de bore (BN, B_4C , ZrB_2 , CaB_6 et TiB_2) favorisent la formation des phases cristallines $\text{B}_2\text{O}_3\text{-Al}_2\text{O}_3$.

Les oxydes d'alcalino-terreux et de terres rares peuvent réagir avec la silice pour produire des nouvelles phases cristallines telles que l'anorthite ($\text{CaO}\cdot\text{Al}_2\text{O}_3\cdot 2\text{SiO}_2$), l'anorthite de baryum ($\text{BaO}\cdot\text{Al}_2\text{O}_3\cdot 2\text{SiO}_2$) et le $\text{Y}_2\text{O}_3\cdot\text{SiO}_2$. Ces transformations réduisent la quantité de silice libre dans la matrice des réfractaires. Ces nouvelles phases assurent donc la protection des réfractaires puisqu'elles font en sorte qu'il n'y ait plus de réaction entre la silice et l'aluminium.

Dans le cas du AlPO_4 , il n'y a pas de formation de nouvelle phase. AlPO_4 ne se décompose pas et ne réagit pas avec le SiO_2 .

En ce qui concerne l'effet du sodium, du phosphore et du bore sur la résistance à la corrosion par l'alliage Al-5%Mg-5%Zn de la silice vitreuse, cette dernière est plus résistante à la corrosion lorsqu'elle contient du bore ou du phosphore que lorsqu'elle contient du sodium.

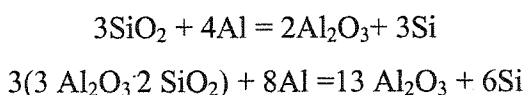
La structure des pores et la porosité n'ont pas un rôle bien défini sur la corrosion.

Les tests de corrosion exécutés avec des échantillons préparés de fines particules réfractaires confirment l'efficacité des additifs à base de bore sur la protection des réfractaires contre la croissance du corindon.

ABSTRACT

It is well known that aluminum holding and melting furnaces are divided into 3 zones. Refractory lining above the metal line are exposed to high temperature, and are subjected to corundum attack. The temperature in this zone is usually more than 1000°C, up to 1400°C sometimes. The corundum corrosion mechanism depends on the temperature, the oxygen partial pressure and the composition of the alloy.

The degradation of alumino-silicates by aluminum attack has long been known. This deterioration is more pronounced when alloying elements such as magnesium and zinc are present in molten aluminum. It is reported that liquid aluminum reduces silica and its bearing constituents of the alumino-silicate refractories (e.g., mullite) to a metallic state along with the conversion of aluminum to corundum. These types of reaction can be represented as:



The conversion of alumino-silicate refractories, also referred to as corrosion, can cause several problems, such as a sharp decrease in the mechanical properties of the refractory, contamination of the molten bath, aluminum loss, and enormous heat loss. Several attempts have been focused to improve the resistance of these refractories to aluminum attack and penetration.

Research to date at CIREP has focused on additives for service conditions less than 1200°C. In remelt and recycling furnaces, service temperature may exceed 1200°C to

speed up melt rate. Additives so far in use are known to not survive beyond about 1100°C. Additives are needed to protect refractory at temperatures in excess of 1200°C.

A new method for corundum corrosion test at 1200°C, which allows corroding refractory materials with the corundum that is usually formed on the walls of aluminium melting and holding furnaces has been developed. With this new method, it should be possible to select the most appropriate refractory lining for aluminum treatment furnaces, with much more confidence.

Through this new method, some new additives to increase the resistance of aluminosilicate refractories by molten Al-5%Mg-5%Zn alloys were developed. In order to understand the corrosion mechanism, XRD, mercury porosimetry and optical micrography were used as characterizing tools.

Four kinds of new additives were identified.

These involve the presence of boron or are made of AlPO_4 , alkaline earth oxides and rare earth oxide.

Addition of boron-based additives (BN , B_4C , ZrB_2 , CaB_6 and TiB_2) favors the formation of B_2O_3 - Al_2O_3 crystalline phases.

Alkaline earth metal oxides and rare earth oxides can react with silica, and new crystalline phases such as anorthite ($\text{CaO}\cdot\text{Al}_2\text{O}_3\cdot 2\text{SiO}_2$), barium anorthite ($\text{BaO}\cdot\text{Al}_2\text{O}_3\cdot 2\text{SiO}_2$), and $\text{Y}_2\text{O}_3\cdot\text{SiO}_2$ are formed. These transformations reduce the amount of free silica within the matrix of refractories. Refractory protection is achieved by these new crystalline phases, which prevent reaction between silica and aluminium metal.

In case of AlPO_4 , there is no new phase is formed. AlPO_4 does not be decomposed, and does not react with SiO_2 .

Regarding the effect of sodium, phosphorus and boron in silica glasses, on their resistance to corrosion by Al-5%Mg-5%Zn alloy, boron-bearing and phosphorus-bearing silica glasses are more resistant to corrosion than ordinary sodium-bearing glasses.

Pore structure and porosity don't have a well-defined role on corrosion.

The corrosion tests performed with the samples prepared from the fine refractory particles confirm the efficiency of boron-based additives on the protection of refractories against corundum attack.

TABLE OF CONTENTS

ACKNOWLEDGMENTS	v
RÉSUMÉ	vi
ABSTRACT	ix
TABLE OF CONTENTS	xii
LIST OF TABLES	xvii
LIST OF FIGURES	xviii

INTRODUCTION	1
---------------------------	---

CHAPTER 1: LITERATURE REVIEW

1.1. Aluminium Industry & Refractory.....	3
1.1.1. Aluminium Industry.....	3
1.1.1.1. The Chemical Process.....	3
1.1.1.2. The Electrolytic Process.....	4
1.1.1.3. Casting and Fabricating.....	4
1.1.2. Treatment Furnace and Refractory.....	6
1.1.2.1. Higher Production Rates.....	6
1.1.2.2. Wide Range of Aluminium Alloys.....	6
1.1.2.3. Recycled Scrap.....	7
1.1.2.4. Importance of Developing Refractories for Better Performance.....	7
1.2. Refractory.....	8
1.3. Corrosion of Refractory by Molten Aluminium.....	10

1.3.1. Corrosion Mechanism of Refractory by Molten Aluminium	10
1.3.2. Conventional Corrosion Test	13
1.3.2.1. The CIREP Immersion Test	13
1.3.2.2. The CIREP Bellyband Test	14
1.4. Corrosion Resistance Improvement of Refractory	15
1.4.1. Influence of Pore Size on Aluminium Penetration	15
1.4.2. Effect of Chemical Composition of Refractory Aggregates on Corrosion Resistance to Molten Aluminium	17
1.4.3. Improving Low Cement Castables by Non-Wetting Additives	19
1.5. Goal and Objectives	21
1.5.1. Improved Non-wetting Additives	21
1.5.2. Improved Testing Set-up	25

CHAPTER 2: A NEW PROCEDURE TO EVALUATE THE RESISTANCE OF REFRACTORIES TO EXTERNAL CORUNDUM GROWTH

2.1.	
Introduction	26
2.2. Corundum Mushroom Formation	27
2.2.1. Experimental Procedure	27
2.2.2. Results and Discussion	30
2.2.2.1. Effect of Test Temperature	30
2.2.2.2. Effect of Oxygen Partial Pressure	31
2.2.2.3. Effect of Soaking Time	32
2.2.2.4. Effect of Metal Amount	32
2.2.2.5. Effect of SiO ₂ Powder Incubator	33

2.2.3. Problems to Be Solved	33
2.2.3.1. Creating a Rich Oxygen Atmosphere and Getting A Stable Air Flow Control	33
2.2.3.2. Preventing Corundum Grows along the Seal between Refractory Sample and Alumina Crucible	34
2.2.3.3. Corundum Grows Through Crucible Wall	34
2.2.4. Conclusions	34
2.3. Optimization of the New Corrosion Test Method	35
2.3.1. Introduction	35
2.3.2. Experimental Procedure	35
2.3.2.1. Oxidization Procedure	35
2.3.2.2. Cutting and Comparison	36
2.3.3. Results and Discussion	36
2.3.3.1. Effect of Corundum Mushroom Size and Alloy Oxidized Extent	36
2.3.3.2. Effect of Soaking Time and Testing Temperature	38
2.3.3.3. Effect of the Furnace Types	39
2.3.3.4. Effect of Different Alloys	41
2.3.3.5. Property of Additives	41
2.3.4. Problems	43
2.3.4.1. Minimization of Corundum Growing around the Crucible	43
2.3.4.2. Furnaces	43
2.3.5. Summary	43
2.4. Improvement of the New Method of Corundum Corrosion Test	47
APPENDIX	50

CHAPTER 3: NOVEL ADDITIVES

3.1. Boron-bearing Compounds and AlPO_4	52
3.1.1. Introduction	52
3.1.2. Experimental Procedures	53
3.1.2.1. Sample Preparation	53
3.1.2.2. Porosity, Density and Amount of Water	54
3.1.2.3. Corrosion Tests	54
3.1.2.4. Characterization Techniques	55
3.1.2.4.1. Pore Size Distribution Analysis	55
3.1.2.4.2. X-Ray Diffraction Analysis	56
3.1.2.4.3. Optical Microscopy (OM) and Scanning Electron Microscopy (SEM)	56
3.1.3. Results and Discussion	56
3.1.3.1. Corrosion Tests	56
3.1.3.2. Porosity, Density and Amount of Water	58
3.1.3.3. Pore Size Distribution Analysis	59
3.1.3.4. X-Ray Diffraction Analyses	64
3.1.3.5. Micrograph Analyses (OM, SEM)	66
3.1.4. Conclusions	70
3.2. Alkaline Earth Metal Oxides and Rare Earth Oxides	77
3.2.1. Introduction	77
3.2.2. Experimental Procedures	77
3.2.3. Results and Discussion	77
3.2.3.1. Corrosion Tests	77
3.2.3.2. Porosity and Density	79
3.2.3.3. Pore Size Distribution	80

3.2.3.4. X-Ray Diffraction Analysis	81
3.2.3.5. Microstructure analysis (Optical Micrograph)	84
3.2.3.6. Thermodynamic and Kinetic Analysis	86
3.2.4. Conclusions	88
CHAPTER 4: THE CORROSION RESISTANCE OF SILICA GLASSES TO MOLTEN ALUMINUM	
4.1. Introduction	89
4.2. Materials and Properties	90
4.3. Test and Results	91
4.4. Discussion	96
4.5. Conclusions	100
CHAPTER 5: GENERAL CONCLUSIONS	101
REFERENCES	104

LIST OF TABLES

Table 1.1: Industry Condition of Each Zone	10
Table 2.1: Effect of Test Temperature on Corundum Mushroom	30
Table 2.2: Effect of Oxygen Partial Pressure on Corundum Mushroom	31
Table 2.3: Effect of Oxygen Partial Pressure on Corundum Mushroom	31
Table 2.4: Effect of Soaking Time on Corundum Mushroom	32
Table 2.5: Effect of SiO ₂ Powder Incubator on Corundum Mushroom	33
Table 2.6: Effect of Corundum Mushroom Size and Alloy Oxidized Extent	37
Table 2.7: Effect of Soaking Time and Testing Temperature	39
Table 2.8: Effect of Different Furnaces on Corrosion Results	40
Table 2.9: Corrosion Rating of Product C-7080-4 with Different Additives	41
Table 3.1.1: Castables Chemical Composition	53
Table 3.1.2: Porosity and Density after 1200°C×5hrs Heat-treatment	58
Table 3.1.3: Mineralogical Phases Analysis for C-6070-3 Samples	64
Table 3.1.4: Mineralogical Phases Analysis for C-7080-4 Samples	65
Table 3.2.1: Porosity and Density after 1200°C×5hrs Heat-treatment	79
Table 3.2.2: Mineralogical Phases Analysis for C-6070-3 Samples	82
Table 4.1: Coordination Number and Bond Strength of Oxides	98

LIST OF FIGURES

Figure 1.1: Aluminium Production	5
Figure 1.2: Three Zones in Aluminium Treatment Furnace Lining, according to Allaire	10
Figure 1.3: Schematic Diagram of Molten Aluminium Alloy on a Silicate-containing Refractory	12
Figure 1.4: CIREP Immersion Test Set-up	13
Figure 1.5: CIREP Bellyband Test set-up	14
Figure 1.6: Effect of the Chemical Composition of the Aggregates on the Corrosion Behavior of the Samples	18
Figure 2.1: Refractory Resistance to Corundum Growth Set-up	28
Figure 2.2: Bottom-Open-Furnace Set-up	29
Figure 2.3: Top-Open -Furnace Set-up	36
Figure 2.4: After Alloy Oxidized Completely	44
Figure 2.5: Corroded Sample C-7080-4+5%SiC	44
Figure 2.6: Corroded Sample C-7080-4+5%CMS	45
Figure 2.7: Corroded Sample C-7080-4+5%C3MS2	45
Figure 2.8: Corroded Sample C-7080-4+5%Y ₂ O ₃	45
Figure 2.9: Corroded Sample C-7080-4+5%ZrB ₂	45
Figure 2.10: Corroded Sample C-7080-4+5%C2S	46
Figure 2.11: Corroded Sample C-7080-4+5%T-30	46
Figure 2.12: Corroded Sample C-7080-4+5%CAS	46
Figure 2.13: Corroded Sample C-7080-4+5%HfO ₂	46
Figure 2.14: Corroded Sample C-7080-4+5%CMS	46
Figure 2.15: Corroded Sample C-7080-4+5%Talc	46
Figure 2.16: Corroded Sample C-7080-4+5%SiC	47

Figure 2.17: Equipment of New Method for Corundum Corrosion	48
Figure 2.18: Picture of New Method for Corundum Corrosion	49
Figure 2.19: Before and After Test	49
Figure 3.1.1: Potential Corundum Corrosion Area in Refractory Sample	54
Figure 3.1.2: Corundum Corrosion Test Results: C-6070-3 Series and C-7080 Series	57
Figure 3.1.3: Pore Size Distribution for C-7080-4 With or Without Additives	60
Figure 3.1.4: Pore Size Distribution for C-6070-3 With or Without Additives	61
Figure 3.1.5: Pore Size Distribution for C-6070-3 With or Without AlPO_4	62
Figure 3.1.6: SEM Observation Shows $9\text{Al}_2\text{O}_3 \cdot 2\text{B}_2\text{O}_3$ (needle like) in C-7080-4+5% CaB_6 Sample After $1200^\circ\text{C} \times 5\text{hrs}$	67
Figure 3.1.7: C-6070-3 new corundum after ox-re	71
Figure 3.1.8: C-6070-3 direct oxidization corundum layer structure	71
Figure 3.1.9: C-6070-3 area between direct oxidization corundum and ox-re corundum	71
Figure 3.1.10: C-6070-3 refractory attacked by corundum and molten Al	71
Figure 3.1.11: C-6070-3+5% TiB_2 corroded area with more pores and cracks and regular	71
Figure 3.1.12: C-6070-3+5% TiB_2 oxidized area and regular	71
Figure 3.1.13: C-7080-4 Refractory corroded by corundum $\times 5$	72
Figure 3.1.14: C-7080-4 Refractory corroded by corundum $\times 10$	72
Figure 3.1.15: C-7080-4+5% ZrB_2 Refractory corroded by corundum(black) $\times 10$	72
Figure 3.1.16: C-7080-4+5% ZrB_2 Refractory corroded by corundum(black) $\times 20$	72
Figure 3.1.17(a) (b): C-7080-4+5% ZrB_2 New phase---glass fibre $\times 50$	72
Figure 3.1.18: C-7080-4+5% CaB_6 Refractory corroded by corundum $\times 10$	73
Figure 3.1.19: C-7080-4+5% CaB_6 Molten Al goes through corundum $\times 10$	73
Figure 3.1.20: C-7080-4+5% B_4C Refractory corroded by corundum(more pores) $\times 50$	73

Figure 3.1.21: C-7080-4+5%CaB ₆ Refractory corroded by corundum ×100 Molten Al goes through channel and attacks inside refractory	73
Figure 3.1.22: C-7080-4+5%CaB ₆ New phase---glass fibre ×500	73
Figure 3.1.23: C-7080-4+5%B ₄ C Molten Al penetrates through capillary channel and new phase (glass fibre) grows ×200	73
Figure 3.1.24: C-7080-4+5%B ₄ C New phase---glass fibre is formed (a)×20 (b)×100	74
Figure 3.1.25: C-7080-4+5%BN Refractory corroded by corundum through re-ox reaction corundum, and stops at a pore ×500	74
Figure 3.1.26: C-7080-4+5%BN Corundum is formed in a Molten Al penetrates closed pore ×200	74
Figure 3.1.27: C-7080-4+5%BN contaminated refractory inside (caused by molten Al penetration) ×100	74
Figure 3.1.28: C-7080-4+5%BN New phase is formed in a pore ×500	74
Figure 3.1.29: C-7080-4+5%B ₄ C Refractory corroded by corundum and molten Al ×50	75
Figure 3.1.30: C-7080-4+5%B ₄ C Refractory corroded by corundum and molten Al ×100	75
Figure 3.1.31: C-7080-4+5%AlPO ₄ Direct Oxidizing Corundum Area ×50	76
Figure 3.1.32: C-7080-4+5%AlPO ₄ Interface between Corroded area and Un-corroded area ×10	76
Figure 3.1.33: C-7080-4+5%AlPO ₄ Interface between Corroded area and Un-corroded area ×20	76
Figure 3.1.34: C-7080-4+5%AlPO ₄ Interface between Corroded area and Un-corroded area ×50	76
Figure 3.1.35: C-7080-4+5%AlPO ₄ Interwine glass fiber in a pore ×20	76
Figure 3.1.36: C-7080-4+5%AlPO ₄ Glass fibres in a pore ×20	76
Figure 3.2.1: Corundum Corrosion Resistance of Low Cement Castable With or Without Oxide-base Additives	78

Figure 3.2.2: Pore size distribution for C-6070-3 with or without additive (Cumulative intrusion vs. Pore size)	80
Figure 3.2.3: Pore size distribution for C-6070-3 with or without additive (Incremental intrusion vs. Pore size)	80
Figure 3.2.4: Pore size distribution for C-7080-4 with or without additive (Cumulative intrusion vs. Pore size)	80
Figure 3.2.5: Pore size distribution for C-7080-4 with or without additive (Incremental intrusion vs. Pore size)	80
Figure 3.2.6: C-7080-4 + 5%Y ₂ O ₃ Interface between corroded area and un-corroded area ×20	84
Figure 3.2.7: C-7080-4 + 5%Y ₂ O ₃ Interface between corroded area and un-corroded area ×50	84
Figure 3.2.8: C-7080-4+5%BaCO ₃ ×50	84
Figure 3.2.9: C-7080-4+5%BaCO ₃ Corroded Area ×50	84
Figure 3.2.10: C-6070-3-5%CaCO ₃ Interface between corroded area and un-corroded area ×20	85
Figure 3.2.11: C-6070-3-5%CaCO ₃ Interface between corroded area and un-corroded area ×50	85
Figure 3.2.12: C-6070-3+5%Dolomite Corroded Area ×20	85
Figure 3.2.13: C-6070-3+5%Dolomite Interface Between Corroded Area and Un-corroded Area ×50	85
Figure 3.2.14: Ellingham diagram for oxides	86
Figure 4.1: Corrosion aspect of W-glass (window glass)	93
Figure 4.2: Pyrex glass	93
Figure 4.3: B ₂ O ₃ (5g) + SiO ₂ (5g)	93
Figure 4.4: B ₄ C (4g) + W-glass (8g)	93
Figure 4.5: P ₂ O ₅ (4g) + W-glass (8g)	94
Figure 4.6: P ₂ O ₅ (3g) + Fumed silica (8g)	94
Figure 4.7: Bone Ash (4g) + W-glass (8g)	94

Figure 4.8: AlPO_4 (3g) + W-glass (6g)	94
Figure 4.9: Stereoscopic view of the three zones analyses: A (dark), B (transition), C (clear)	95
Figure 4.10: Results showing the presence of C, O and Si in the zone A	95
Figure 4.11: Results showing the presence of C, O and Si in the zone B	96
Figure 4.12: Results showing the presence of C, O, Si, Na and Al in the zone C	96
Figure 4.13: Schematic representation of the structure of (a) - ordered crystalline: quartz crystal (b) - random-network glassy form: fused silica glass (c) - sodium silicate glass	97
Figure 4.14: Sketch of the triangular structure of B_2O_3 glass	98
Figure 4.15: Sketch of the tetrahedron structure of P_2O_5 glass	99

INTRODUCTION

The current aluminum treatment furnaces are operated to aim at maximum energy efficiency and thus an increase in the temperature of the liquid metal occurs. Temperatures of 1430°C above the bellyband and 1090°C in the region of the bellyband can be observed. This increase in temperature reduces the viscosity and the surface tension of the liquid metal intensifying a capillary action and the reactions between refractory and aluminum.

The refractory market for the aluminum industry has demanded a constant specialization of products for the different types of equipment. This is due to the change in manufacturing processes, the production of new alloys and the increase in production rates, leading to a much more aggressive corrosion environment for refractory lining. For instance, conventional alumino-silicate refractories or bauxite-based refractories do not perform well, in part due to the formation of a corundum layer and the heavy penetration of aluminum in the microstructure of these refractories. The addition of alkaline salts to the metallic bath to minimize the oxidation reactions and the removal of impurities are additional factors that contribute to the reduction of refractory life.

In the melting of aluminum and its alloys, oxidation always has been of great concern because of the easy formation of aluminum oxide. Many aluminum alloy melting furnaces are gas fired, in air, and atmospheric oxidation plus full combustion and flame impingement often result in prolonged exposure of the refractories to attack and subsequent oxidation. Additionally, molten aluminum is an extremely aggressive medium, and furnace refractory lining, in general, are prone to attack and penetration by the molten metal.

The most common form of attack is the formation of an insidious, tenacious aluminum oxide growth buildup on refractories--known as corundum. When allowed to proceed unchecked, the resulting growth can be severe, and can seriously close off furnace capacity.

In practice, one common way to achieve a better corrosion resistance in case of refractories used to line aluminium furnaces is to add so called "non-wetting" agents, to alumino-silicate castables. Among these additives, BaSO_4 , CaF_2 and AlF_3 are the most common ones. These inorganic compounds are supposed to lower the refractory wettability by aluminium alloys, i.e. to prevent molten alloy infiltration into the refractory.

Although, for more than a decade, the non-wetting agents are used in the alumino-silicate refractories, their beneficial effect is not yet totally understood.

Research to date has focused on additives for service conditions less than 1200°C . In aluminium treatment furnaces, service temperature may exceed 1200°C to speed up melt rate. Additives so far in use are known not to survive beyond about 1100°C . Novel additives are needed to be developed that will protect refractory at temperatures in excess of 1200°C .

The conventional corrosion testing set-ups, CIREP Immersion Test and CIREP Bellyband Test, are capable of evaluating corrosion resistance of refractory material below 1100°C only. Obviously, these methods can not be used to evaluate the corrosion resistance of refractories at temperature in excess of 1200°C .

A new corundum growth test method, which allows to corrode refractory materials with the corundum that is usually formed on the walls of aluminium melting and holding furnaces need to be devised. It should be possible to select the most appropriate refractory lining with much more confidence.

CHAPTER 1: LITERATURE REVIEW

1.1. Aluminium Industry and Refractory

1.1.1. Aluminium Industry

The world's primary aluminium industry produces over 23 millions ton of aluminium metal per year. The metal, supplied as semi products (e.g. ingots), is converted into final products by the aluminium manufacturing industry.

Most of the 23 million tons primary metal comes from approximately 120 aluminium smelters around the world. These smelters account for over 90% of the world production but exclude China which produces between two and three million tonnes per year. In addition to the primary production, more than 7 million tonnes per year of metal is produced by recycling scrap. Almost 100 % of all production scrap is recycled, and over 60 per cent of all old scrap. The proportion of aluminium produced from scrap (so called secondary aluminium) is rising rapidly.

The most important markets for aluminium products are the transport, building and packaging sectors, however aluminium also finds application in electrical and mechanical engineering, office equipment, domestic, applices, lighting, chemistry and pharmaceuticals.

Chemical process, electrolytic process, casting and fabricating are three main processes through which aluminium is made. Two to three tonnes of bauxite are required to produce one ton of alumina and two tonnes of alumina are required to produce one tonne of aluminium metal.

1.1.1.1. The Chemical Process

The first step in the chemical process is to mix crushed bauxite in a solution of hot caustic soda in digesters. This allows the alumina hydrate to be dissolved from the ore. After the red mud residue is removed by decantation and filtration, the caustic solution is

piped into huge tanks, called precipitators, where the alumina hydrate crystallizes. The hydrate is then filtered and sent to calciners to dry under very high temperature and transformed into the fine white powder known as alumina.

1.1.1.2. The Electrolytic Process

Alumina is a compound of aluminum and oxygen. To obtain metal from the alumina, these elements must be separated by electricity in the smelting process. This reaction takes place in large, carbon-lined steel cells or pots, through which a direct current is passed.

The bottom of each pot acts as a cathode or negative electrode. Carbon blocks are suspended in the pot to serve as an anode or positive electrode. Inside the pot, alumina is dissolved in a molten electrolyte, composed mainly of the mineral cryolite. The electrical current passing from the anode to the cathode causes the oxygen in the mixture to react with the carbon anode to form carbon dioxide, while the aluminum settles to the bottom of the pot to be siphoned off.

1.1.1.3. Casting and Fabricating

Before casting into ingot for fabricating, the molten aluminum is treated to ensure cleanliness and purity. Alloying ingredients are usually added to increase strength or provide special properties. Traditionally, the metal is cast into ingots of various shapes, sizes and compositions for a number of uses.

Ingots are converted into sheet, plate or foil products, as well as extruded shapes for engineering and architectural applications.

Value-added foundry alloy ingots for shape castings and unalloyed ingots for remelting are sold mainly to other parties.

In an alternative technique, called continuous casting, molten metal is cast directly into semi-finished form, bypassing the ingot stage. This fabrication method is becoming

more widely used for sheet and foil products, and particularly for rod, which is subsequently drawn into many forms of electrical and mechanical wire. Figure 1.1 shown an overview of the aluminium production procedure.

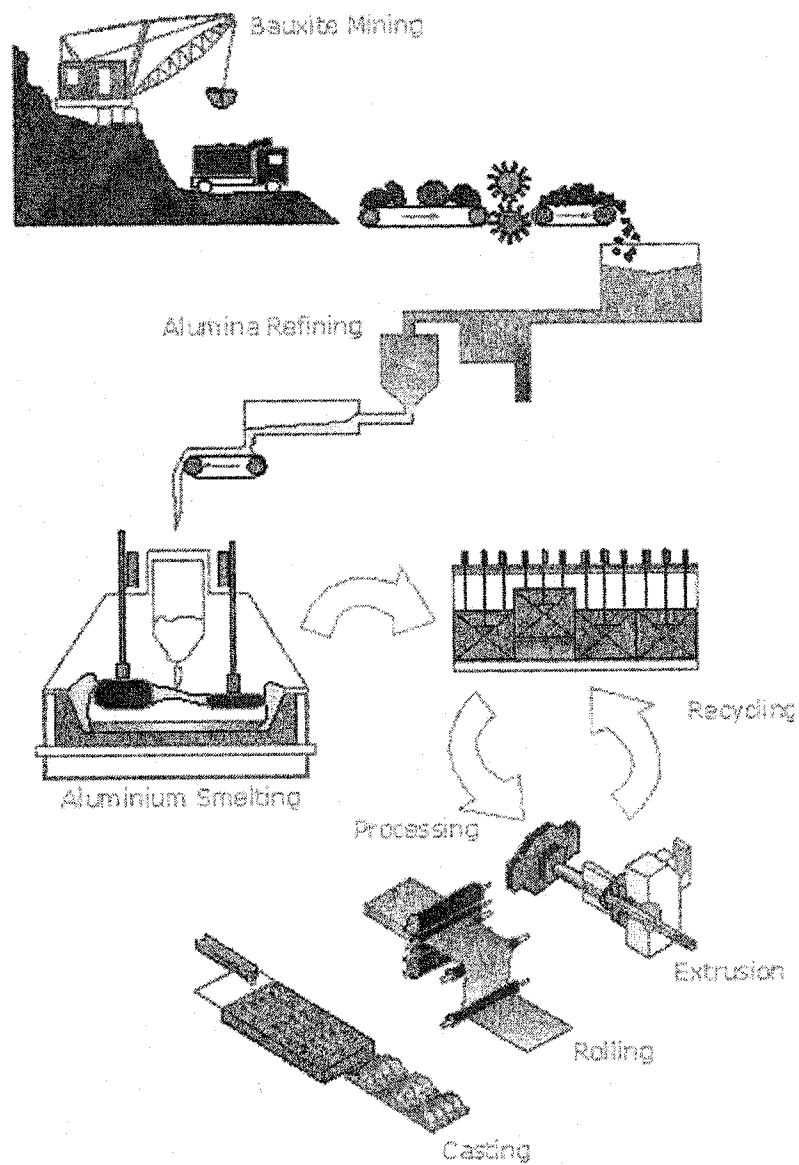


Figure 1.1: Aluminium Production

1.1.2. Treatment Furnace and Refractories

The Melting and Holding Furnaces are used for the treatment of liquid aluminum. They are designed for continuous operation and are suitable for aluminium die-casting and aluminium casting industries. There are three types of furnaces: crucible, shaft and reverberatory. The furnaces offer good temperature uniformity of molten metal coupled with excellent energy savings.

The melting and holding furnace operating practices have changed dramatically during the past several years. A brief review of some of the major changes in melting and holding furnace operation is important to understand refractory performance.

1.1.2.1. Higher Production Rates

The Melting and Holding Furnaces are now being operated at higher production rates than ever before. Improvements in burner technology have resulted in higher fuel input rates to a given furnace. This increased fuel input, which melts more metal, faster, means the furnace operates at high temperatures more frequently, or that the furnace operates consistently at higher temperatures. Refractories below the melt line may not see any appreciable temperature increase, but the bellyband or cross line materials will see the high operating temperatures. This area is where the most severe chemical reactions occur between the refractory and the molten bath. These reactions are accelerated or promoted at high temperatures.

In addition, as more tonnage is processed through a furnace, the physical abuse from charging and cleaning the furnace is, of course, increased. Both of the above operating practices cause more refractory wear.

1.1.2.2. Wide Range of Aluminium Alloys

Another operating factor that has detrimentally affected conventional refractory performance is processing of wide range of aluminium alloys. High zinc alloys, with their accompanying low melting points are very fluid. The potential exists for these

alloys to penetrate into the open porosity of refractories more easily than alloys with higher melting temperature^[71].

High magnesium alloys are extremely corrosive to refractory linings. At the bath line, the magnesium can burn off at temperatures that exceed 1650°C. This localized exposure to high temperature abuse is very detrimental to refractories^[71].

1.1.2.3. Recycled Scrap

The amount of recycled scrap is increasing every year. Recycled scrap contains relatively high levels of impurities, which are detrimental to furnace refractories.

Many of these impurities are chemically reactive with the refractory materials used as a working lining. In addition, the impurities are usually separated from the molten aluminum bath, and skimmed off as dross. The cleaning equipment used to remove dross is physically abusive to the lining, especially on the sidewalls, ramp and sill.

At most melting facilities throughout the industry, all of these practices or a combination of one or more of them, have served to reduce to some extent the service life of conventional refractories.

1.1.2.4. Importance of Developing Refractories for Better Performance

The upkeep of refractories in melting and holding equipment and in transport crucibles is a constant preoccupation for the foundrymen. In fact, it is important to an operator that the working tool does not fail unexpectedly and cause an abrupt stoppage of production. Refractory wear is inevitable. It is therefore normal to carry out repairs from time to time and occasionally a total replacement. It is essential that these interventions come within a maintenance programme established in advance and that they do not upset manufacturing processes that are operated on tight schedule. A good choice of refractories and a good installation are two essential parameters for ensuring the best possible quality of a lining. The life of the refractory lining is of very great interest to the foundrymen. Another aspect also merits consideration when judging refractory quality.

Does the latter risk causing hard particles in the metal or to risk modifying chemical composition of the alloys? One may fear that refractory particles become detached from the wall of the lining and form solid inclusions in the cast metal. One may also be concerned about the formation of corundum or spinel at the refractory interface which lead to hard particles. Lastly, one may fear the dissolution of certain elements from the lining, in the aluminum bath (silicon for example). All of these perturbations in the metal that are due to the refractory are prejudicial to its quality and it is therefore essential to avoid them by correct choice and perfectly controlling the use of the furnaces and other tools.

Refractory with a poor performance may provoke serious damage to the smooth operation of a foundry, such as non-programmed production stoppages and metal contamination and therefore scrapping of parts, without speaking of safety risks. Faced with such significant events, it is necessary to closely examine how refractories behave in contact with aluminum alloys, to what they are subjected, the nature of their defects, how they can be limited, what precautions should be taken, etc.

1.2. Refractory

Refractory materials are heterogeneous and porous ceramics, having a very high melting temperature (up to 1800°C and more). This particular property means that refractories offer a certain mechanical resistance at high temperature. Resistance to high temperatures makes these materials suitable for the construction of linings for the furnaces and kilns of industry. While heat resistance is the primary function of a refractory material, it must also be able to withstand a variety of destructive forces incidental to its use. These include thermal shock resulting from rapid heating and/or cooling, stresses induced by temperature change, pressures from the weights of furnace parts or contents, mechanical wear (abrasion) resulting from such causes as the movement of furnace contents which rage, boil, and splash. They must also withstand chemical attack by heated solids, liquids or gases.

Refractories can be classified on the basis of various criteria but the common practice is dependent upon their chemical nature. Thus there are three types, namely, acid, basic and neutral. Amongst the common refractories, the alumino-silicate refractories, semi-silica and silica bricks belong to the acid group; the magnesite, dolomite, chrome-magnesite, magnesite-chrome and forsterite refractories are of basic variety; and chromite, carbon, graphite and silicon carbide refractories constitute the neutral quality. Refractories can also be classified as shaped and unshaped. Varieties of bricks belong to shaped refractory. Monolithic refractories, also called un-shaped refractories, include castable, ramming mix, gunning mix, plastic mix, mortar, etc.

Castable refractory is an important class of monolithic refractories. It can be defined as a combination of refractory grain and suitable bonding agent that after the addition of a proper liquid, is generally poured into place to form a refractory shape or structure which becomes rigid because of chemical action (ASTM71 1998)^[73]. Refractory castables contain basically coarse and fine fraction. Coarse fraction includes refractory grain such as tabular alumina, fused alumina, andalusite, grog, kyanite, fused mullite, bubble alumina etc. The fine fraction contains calcined alumina, reactive alumina, calcium aluminate cement, microsilica, chrome fine, grog dust, etc.

Refractory requirement for aluminium industry is not large, but is critical, since the refractories determine the efficiency of operation and product quality. Usage of monolithic refractories in aluminium industry has been increasing in major aluminium producing countries.

Refractories are used in three main areas of the aluminum industry: holding and melting furnaces, reduction cells and ring furnaces.

For aluminum melting and holding furnace, most of the refractory lining is made up of alumino-silicate castables. It is subjected to corrosion (in particular at the metal/refractory/atmosphere interface), thermal shock (loading of ingots and scrap,

opening doors, hot spots), mechanical impacts (loading of ingots and scrap, drossing, cleaning) and wear by abrasion/erosion.

1.3. Corrosion of Refractory by Molten Aluminium

The current aluminum melting furnaces are operated to aim at maximum energy efficiency and thus an increase in the temperature of the liquid metal occurs. In holding and melting furnaces, service temperature may exceed 1200°C to speed up melting rate. Temperatures of 1430°C above the metal and 1090°C in the region of bellyband can be observed ^[69]. This increase in temperature reduces the viscosity and the surface tension of the liquid metal intensifying a capillary action and the reactions between refractory and aluminium.

1.3.1. Corrosion Mechanism of Refractory by Molten Aluminium

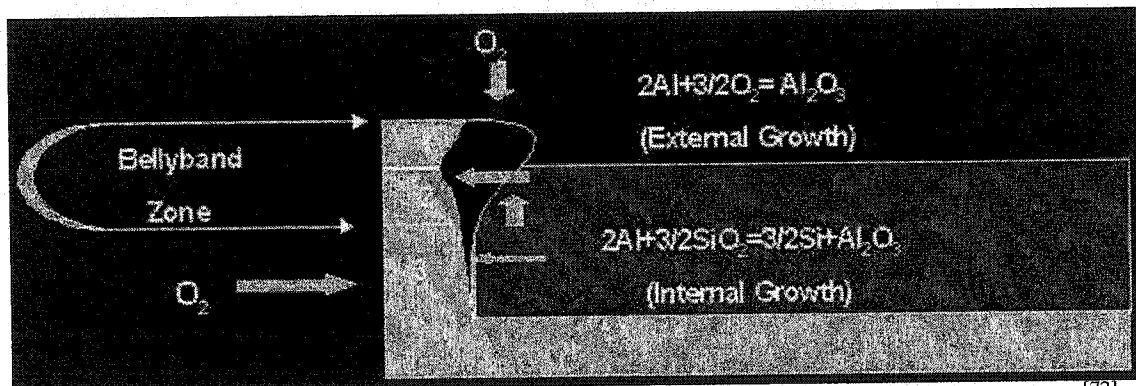
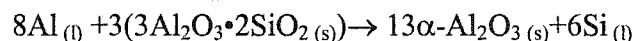
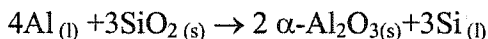


Figure 1.2: Three Zones in Aluminium Treatment Furnace Lining, according to Allaire ^[72]

Table 1.1: Industrial Conditions of Each Zone ^[72]

Industrial Conditions of Each Zone			
Zone	Firing Temperature of the Refractory	Operation Temperature	Oxygen Partial Pressure
1	>1000°C	>1000°C	High
2	>1000°C	<1000°C	Moderate
3	<1000°C	<1000°C	Low

In aluminium industry, the life of melting and holding furnaces is limited by the degradation of the alumino-silicate refractory lining. These furnaces contain pure aluminium and/or aluminium alloys, and also some fluxing agents such as chloride and fluoride salts. The refractories in contact with the liquid metal are subjected to chemical attack by the alloy and/or the fluxing agents. The corrosion phenomenon can be divided in three main zones. The first one is located below the metal line. In this zone, the main cause of corundum growth is the reduction of silica within the refractory lining by the molten aluminium. This phenomenon of corundum formation has been well discussed and it can be shown by the following reactions^[18]:



The bellyband zone is located close to the metal line. Based on the variation of the metal line during operation, the bellyband zone could also be subdivided in two areas. The second zone is a little below the metal line and the third zone is over the metal line.

At the bellyband zone, refractories are exposed to more severe corrosion conditions. Contacting with the alloy and the fluxing agents, the high temperature and the surrounding atmosphere are factors which favour the chemical attack in this zone.

Due to the high affinity of aluminium to oxygen, build-up of corundum on the surface of the refractory lining is easy, especially if the refractory contains free silica^[2].

In bellyband area, the corrosion process, leading to the formation of corundum, takes place in two different ways: The external growth of mushroom like corundum into the melt and the internal growth inside the refractory lining, visible as a dark grey colour layer.

External Growth: The external growth is the result of a direct metal oxidation of the aluminium by the oxygen in the atmosphere. Normally, aluminium forms, due to its high

kinetics, a protective layer of aluminium oxide, which avoids a further oxidation of the metal. This is the reason why corundum growth for pure aluminum is not observed in the same extent like for other alloys, mainly the ones containing magnesium and additives like Zn and Si^[18]. For the magnesium containing alloys, it is the magnesium which prevents the formation of the protective layer by forming a porous spinel layer allowing a continuing growth by oxidation of the metal^[18]. This corundum formed on the surface leads to a continuous reduction of the capacity of the furnace which demand cleaning of the furnace frequently.

Internal Growth: The internal growth of corundum is mainly caused by a red-ox mechanism as described by Figure 1.3.

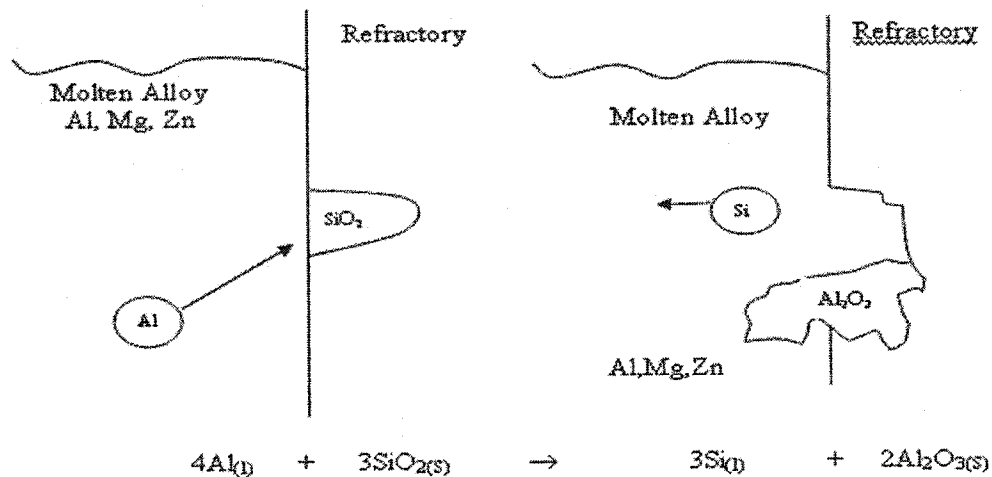


Figure 1.3: Schematic Diagram of Molten Aluminium Alloy on a Silicate-containing Refractory. Alloy is lost by penetration and reaction with the refractory while silicon is released as a contaminant^[70].

Since the furnace conditions differ from one area to another, it is difficult to have a refractory material that resist to corrosion at bellyband zone as well as below it. The challenge facing the research on such refractory materials is to improve the rating of a refractory material in different areas of aluminium holding and melting furnaces. The corrosion therefore results in a decrease in mechanical properties of the refractory,

contamination of the aluminium alloy, and the formation of dross or corundum, which in turns results in a loss of metal. All of this results in considerable loss of refractory material that has to be replaced more frequently, which increases the cost of operation.

1.3.2. Conventional Corrosion Test

There are several methods available for testing the refractories for corrosion, such as the CIREP Standard Immersion Test which is widely used to test the corrosion resistance of the refractories below the metal line, and the CIREP Bellyband Test which tests the refractories for corrosion resistance at the metal line.

1.3.2.1. CIREP Immersion Test

The CIREP Immersion Test is used to evaluate the resistance of refractories to corrosion below the metal line in aluminium treatment furnaces.

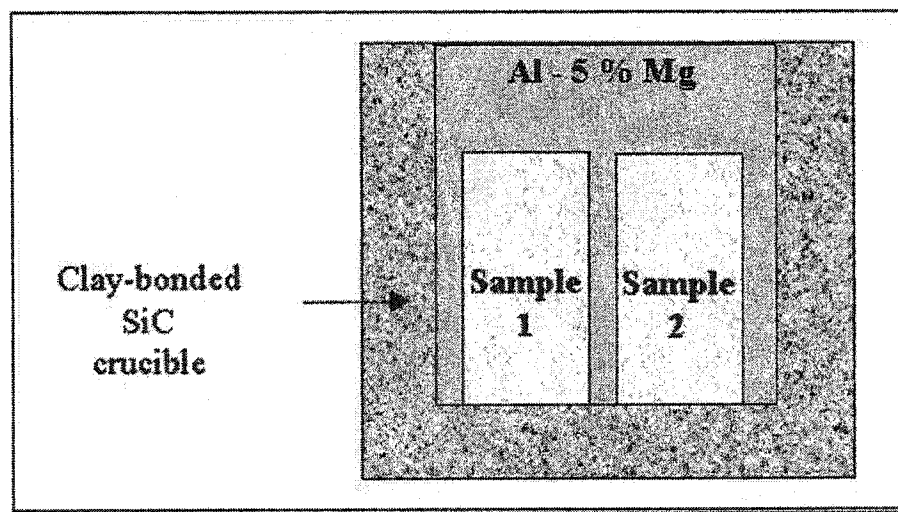


Figure 1.4: CIREP Immersion Test Set-up^[72]

The set-up configuration is shown in Figure 1.4. For each test, two 25 mm x 25 mm x 51 mm samples are immersed in 2 kg of a 5 % (w/w) Mg aluminium alloy maintained at 850°C for four days in a silicon carbide-based crucible. The magnesium level is maintained at 5 % (w/w) by daily additions of this metal to the alloy. Each sample have

no more than five original and at least one cut surfaces. For this immersion tests, the refractory samples are tested in two conditions: 1) pre-fired at 1200 °C, and 2) pre-fired at 815 °C.

1.3.2.2. CIREP Bellyband Test

The CIREP Bellyband Test is used to evaluate the resistance of refractories to corundum attack at the metal line in aluminum treatment furnaces.

The set-up configuration is shown in Figure 1.5. It uses a bottom loading type furnace permitting to achieve a temperature drop from about 1150 to 950°C across the air (atmosphere) interface and the molten aluminum alloy. The latter is contained in the refractory crucible sample which is pre-fired at 1200°C. The crucible sample is cubic with a 7,62 cm edge (a cylinder with the following dimensions may also be used: diameter 7,62 cm, height 7,62 cm). The cavity consists of a hole (3,81 cm diameter x 4,8 cm deep) machined with a diamond tool, thus leaving a 1.9 cm wall minimum thickness. About 90 g of a 5 wt. % Mg alloy is used for each test. This quantity fills two thirds of the cavity. The test is carried out for 4 days (at the soaking temperature).

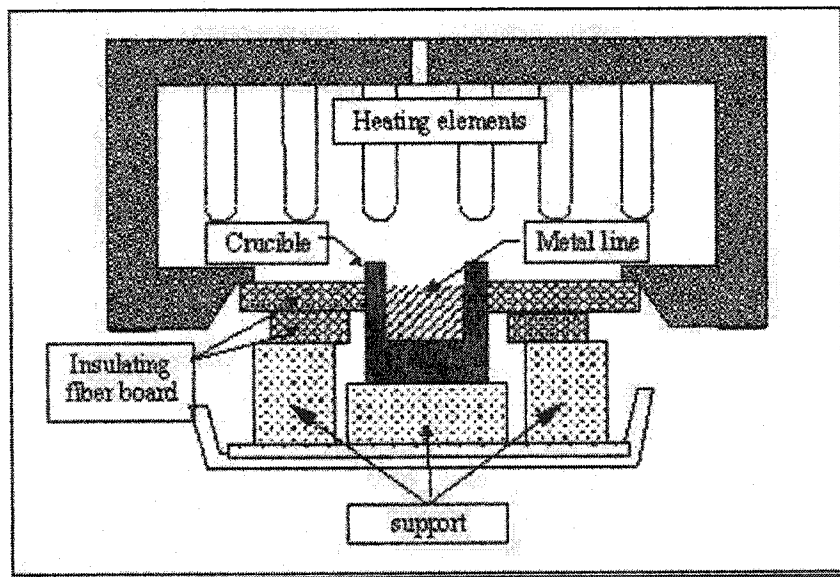


Figure 1.5: CIREP Bellyband Test Set-up^[72]

After the test, the refractory sample is cut longitudinally and two ratings are given according to the extent of metal adherence, penetration and samples friability and/or cracking observed. The first rating is given based on the observation of the portion of the sample that is above the metal line. The second one corresponds to the observation of the sample below the metal line.

1.4. Corrosion Resistance Improvement of Refractory

From theoretical point of view, there are various means to improve corrosion resistance of refractory linings in metallurgical furnaces as given below:

- reducing the active interface between refractory and aggressive melt, i.e. decreasing porosity.
- lowering the melt temperature, i.e. lowering the chemical reaction rate between refractory and alloy and increasing the melt viscosity.
- decreasing the draining rate of the dross along the refractory surface.
- decreasing the atomic diffusion through the reaction layer at the refractory surface.

In practice, there are three common ways to achieve a better corrosion resistance in case of refractories used to line aluminium furnaces. One way is reducing the pore size of refractories, the second way is improving alumina content and restricting SiO_2 in refractories, the last and most common way is to add so called “non-wetting” additives, to alumino-silicate castables, for instance BaSO_4 or CaF_2 ^[19,20,21]. These inorganic compounds are supposed to lower the refractory wettability by aluminium alloys, i.e. to prevent molten alloy infiltration into the refractory^[53].

1.4.1. Influence of Pore Size on Aluminium Penetration

Refractory lining materials for cast house furnaces may be attacked and infiltrated by molten aluminium metal during furnace operation. The wetting of the refractories and physical properties like porosity and pore size distribution of the refractories determine

the extent of the aluminium contact and infiltration. Refractory material open porosity and pore size distribution are of key importance with respect to the penetration and reaction mechanisms of molten aluminium and refractories.

From previous works^[41], it seems that there is a limiting mean pore radius, below which aluminium penetration and attack on alumino-silicate refractories does not take place. According to these works, a best “guestimate” for the maximum pore radius is between 0.5 and 1 μm , meaning that for pores with a diameter exceeding 1.0-2.0 μm , aluminium penetration and subsequent attack on silica in the refractories will take place.

The pore size of the refractory is the most important parameter governing the metal intrusion into the refractory open pore structure. By means of Mercury intrusion method, the pore size distribution of the refractories was characterised, and the aluminium resistance of the investigated alumino-silicate materials was determined by measuring the adherence and penetration/reaction of metal into the sample. The results of investigations are given below^[3,41].

Increasing the pre-firing temperature leads to development of larger pores on the expense of small pores, due to coarsening. A higher content of silica in the refractories will promote this change, due to the action of liquid phase sintering.

For refractory castables containing alumino-silicates there is a clear tendency for reduced aluminium resistance with increasing pore diameter. The investigations indicate that when the pore diameter exceeds 1-2 μm , aluminium penetration and subsequent reactions between metal and refractories occur.

With the above results, as a temporary conclusion, it may be stated that alumino-silicate refractories can be made to resist aluminium attack if the pore radius of the material is kept below 0.5-1.0 μm .

Another research^[66] has developed a structure controlled castables, with a pore diameter of 0.03 to 1 μm . The result have shown that larger diameter pore castables tended to

allow deeper penetration of molten Al-Mg, and for castables with pore diameter controlled to less than $0.1\mu\text{m}$, there was no penetration by molten Al-Mg.

A decrease of pore size accompanies crystallization of the alumina cement hydrate in the matrix (formulated to provide the most dense packing), during curing after casting^[66]. After firing at 1000°C , the hydrate is dehydrated and phase change occurs, leaving a pseudo-crystalline form that decreases the pore size and blocks pore openings.

This research, which was centered on the development of materials with controlled microstructure, led to the development of a castable having enough micropores to prevent the penetration of molten Al-Mg alloy.

Gabis and Victor^[53] have shown that the high corrosion resistant castables could be designed without any corrosion additives. From all their experiments it appears that corrosion is mainly controlled by open size of refractory castables. Castables with very thin pores behave much better than those with bigger pores. Castables with very fine pores (less than $0.25\mu\text{m}$) behave as well as those with "non-wetting" additives. This result indicates that microstructure quality is a first rank castable property.

1.4.2. Effect of Chemical Composition of Refractory Aggregates on Corrosion Resistance to Molten Aluminium

The use of a non-wetting additive is not always a sufficient solution to improve the corrosion resistance of refractories against molten aluminum. Once in contact with liquid aluminum, the coarse refractory aggregates, which do not benefit from the nonwetting additives in the matrix, may be corroded. In some cases, the corrosion of aggregates promotes corrosion in the surrounding matrix, even in the presence of a nonwetting agent. Afshar and Allaire's study^[22] evaluated the corrosion resistance of 15 aggregates commonly used in monolithic refractories and analyzes their effect within a nonwetting matrix. Based on their experimental results, selecting alumino-silicate aggregates that improve the corrosion resistance of castables to aluminum alloys can be designed according to chemical composition.

The corrosion results of the tested aggregates are shown in Figure 1.6. From such representation, three zones, separated by two approximate boundaries, can be distinguished: For the low values of $(\text{SiO}_2 + \text{Fe}_2\text{O}_3 + \text{TiO}_2) / \text{Al}_2\text{O}_3$ ratio and alkali content (zone I: both less than 0.3), aggregates should exhibit a good corrosion resistance. For high value of these parameters (zone III: both more than 0.5), aggregates can be corroded and their corrosion may extend to the refractory matrix. Between these two zones, there is an intermediate zone (zone II), where the aggregate can be subjected to a corrosion process but this corrosion act does not seem to affect the rest of refractory. It is clear that, for aluminum furnaces application, the aggregates situated in zone III are not desirable, considering the fact that the extension of their corrosion to the refractory may decrease the service life of the furnace lining.

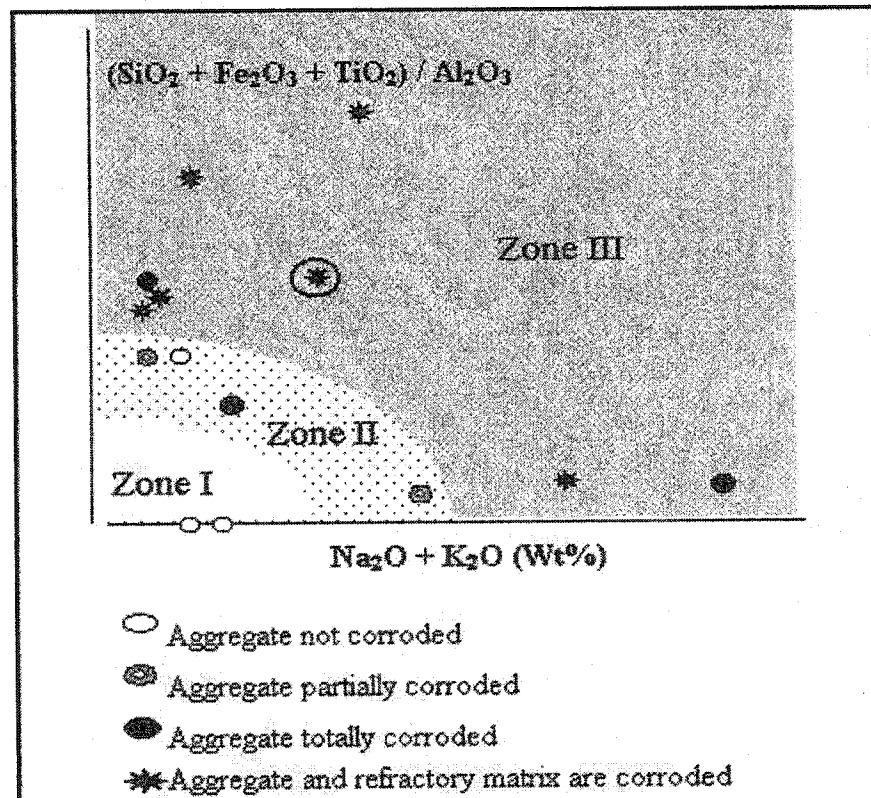


Figure 1.6: Effect of the Chemical Composition of the Aggregates on the Corrosion Behaviour of the Samples^[22].

1.4.3 Improving Low Cement Castables by Non-Wetting Additives

Some specific additives, so called “non-wetting” agents, are generally employed by refractory producers in order to enhance the corrosion resistance of alumino-silicate castables. Among these additives, BaSO_4 , CaF_2 and AlF_3 are the most common ones. Although, more than a decade, the non-wetting agents are used in the alumino-silicate refractories, their beneficial effect is not yet totally understood.

A particular attempt has been made to characterize the proper role of barium sulfate in the protection mechanism of refractories. It has been pointed out that barite, by reacting with alumina and silica among the fine particles of the refractories, forms hexa-celsian and/or celsian in the firing temperature ranging between 900°C to 1200°C ^[19,20,21,26]. Such transformations reduce the amount of free silica within the matrix and should consequently improve the corrosion resistance of the refractory. However, the protective effect of barium sulfate appeared to be significantly reduced for the cause that firing temperatures exceeded 1050°C .

Compared to barium sulfate, the effect of AlF_3 and CaF_2 has been less studied. The experiences carried out on the alumino-silicate ceramics, having a mullite-like composition, have not been conclusive to show the efficiency of the fluoride additives^[20,21]. However, based on the mineralogical analysis results reported^[20,21], it has been postulated that the fluoride additives act as mineralizers, favoring the mullite formation during high temperature firing of alumino-silicate materials.

The efficiency of the three mentioned commercial additives used to protect a low cement castable against aluminum attack was analyzed and compared as follows^[20].

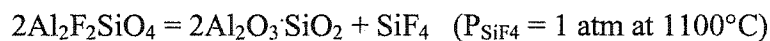
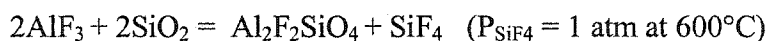
At 7% content, the additives improved the corrosion resistance of the fine portion of the alumino-silicate castable.

Firing temperature influenced differently the protective effect of the additives: with AlF_3 and BaSO_4 , increasing firing temperature reduced the corrosion resistance, while with CaF_2 , an improvement was observed.

The beneficial effect of BaSO₄ was attributed to the formation of some barium aluminosilicate compounds, whose quantity appeared to be proportional to barite content.

It seems that the improvement induced by the addition of AlF₃ is due to its action in converting silica to mullite via fluorotopaz formation.

Based on the thermodynamic calculations and experiments, it is expected that AlF₃ converts a mixture of alumina and silica to mullite via fluorotopaz (Al₂F₂SiO₄) according to following reactions:



Adding CaF₂ favored the anorthite formation. Parallel to corrosion resistance improvement, the amount of anorthite appeared to be increased with firing temperature.

In terms of corrosion resistance improvement, no practical interest was found when the mixes of the additives were used.

From the above work^[20], it can be postulated that the efficiency of non-wetting additives, to protect the castables, is in their potential role in converting silica to some aluminosilicates based crystalline phases that are more resistant to aluminum attack.

It was found that wollastonite (CaO·SiO₂) and barium celsian (BaO·Al₂O₃·2SiO₂) were adequate additives incorporated into refractory materials which resulted in an improved corrosion^[6,14].

It was concluded that the presence of wollastonite in aluminosilicate refractories is more responsible for the improved corrosion resistance^[14]. The first important observation is the decrease in the amount of amorphous phase present in the refractory as wollastonite was added. The second important point is the increase in the amount of anorthite (CAS₂) present in the refractories. It is the anorthite (CAS₂) that would provide the enhanced protection against corrosion. There is also a noticeable decrease in the gas permeability values upon additions of wollastonite.

Adding 3wt% of a Barium Celsian ($\text{BaO}\cdot\text{Al}_2\text{O}_3\cdot 2\text{SiO}_2$) to a typical low cement aluminosilicate refractory castables improved strongly the corrosion resistance against aluminium and cryolite bath^[6]. The low effectiveness of the refractory castables containing 5wt% Barium Celsian ($\text{BaO}\cdot\text{Al}_2\text{O}_3\cdot 2\text{SiO}_2$) maybe related to two factors: (1) the larger pore volume presented by the particular composition; (2) increasing the amount of Barium Celsian ($\text{BaO}\cdot\text{Al}_2\text{O}_3\cdot 2\text{SiO}_2$). It is in fact easier in such a case to form low melting point Barium Silicates with SiO_2 from the refractory^[6].

Research to date has focused on additives for service conditions less than 1200°C . In aluminium treatment furnaces, service temperature may exceed 1200°C to speed up melt rate. Additives so far in use are known not to survive beyond about 1100°C . Additives are needed that will protect refractory at temperatures in excess of 1200°C .

1.5. Goal and Objectives

The goal of this project investigation is to identify the novel additives for refractory castables subjected for service conditions greater than 1200°C in aluminium treatment furnaces. With this goal, the objectives are:

- To optimize the type and amount of additives.
- To explore the role of the additives on corrosion mechanism.
- To improve the corrosion resistance of castable by selecting appropriate additives with respect to operating conditions.

To achieve this goal, an improved testing set-up must be built.

1.5.1. Improved Non-wetting Additives

The focus of many researchers on refractories has been on improving the resistance to aluminium attack. Adding elements or compounds to the refractory has generally resulted in minimizing the reaction with aluminium. More specifically, some additives,

so called “non-wetting” agents, are generally patented and/or investigated, and their primary role is to lower the wettability and/or the reactivity of refractories by molten aluminium and consequently improve the corrosion resistance.

From the extensive literature review, it is understood that the additive to be selected for the particular appropriation must deliver the following function.^[1-12]

- (1) Minimize reaction with molten aluminium;
- (2) Minimize reaction with Al₂O₃-SiO₂ refractories;
- (3) Increase viscosity of glassy phase, and/or new formed phases do not decrease glass phase viscosity;
- (4) Decrease amount of glassy phase;
- (5) Using phases with low melting point to fill the pores, producing higher density during firing or sintering.

On the basis of the principle properties and previous works, the following materials have been selected in this work as additive candidates:

Series I TiO₂, ZrO₂, HfO₂, Cr₂O₃, Mo₂O₃, W₂O₃, V₂O₅, Sc₂O₃, Y₂O₃, ThO₂, La₂O₃, CeO₂, B₂O₃;

Series II B₄C, SiC, Si₃N₄, SIALON, AlN, BN, ZrB₂, CaB₆;

Series III Barium Titanate (BaTiO₃), Calcia Phosphate (Ca₃(PO)₄), CaSO₄, BaZrO₃, Anorthite (Ca₂Si₂O₇), Gehlenite (C₂AS), Aluminum Borate (Al₂O₃·B₂O₃), Aluminum Titanate (Al₂O₃·TiO₂), 2CaO·SiO₂, 3CaO·2SiO₂, CaO·3SiO₂, Forsterite (2MgO·SiO₂);

Series IV Cement Clinker

The reasons for the selection of most of the above materials as candidates go as follows.

- (1) Oxides: TiO₂, ZrO₂, HfO₂, Cr₂O₃, Mo₂O₃, W₂O₃, V₂O₅, B₂O₃

TiO₂. It is expected that low melting point phases in Al₂O₃-SiO₂-TiO₂ system can block the pores, and produce higher density during firing or sintering^[41].

ZrO₂ and Cr₂O₃: Usually, ZrO₂ and Cr₂O₃ are used as additive for corrosion resistance in steel industry and cement industry. It is expected that ZrO₂ and Cr₂O₃ can increase viscosity of glass phase and decrease amounts of glassy phase in structure of refractory castables^[1,2,40].

HfO₂: Ti, Zr and Hf belong to Group IVA in Periodic Table of the Elements. If TiO₂ and ZrO₂ protect alumino-silicate castables from corrosion, HfO₂ may possibly hold the same function.

Mo₂O₃ and WO₃: Cr, Mo, and W belong to Group VIA in Periodic Table of the Elements. If Cr₂O₃ protect alumino-silicate castables from corrosion, Mo₂O₃ and WO₃ may possibly hold the same function. Moreover, Mo₂O₃ reacts with SiO₂ to produce MoSi₂. Consequently, it is expected that Mo₂O₃ can protect free SiO₂ inside castables from molten aluminum attack.

(2) Rare-earth-oxides: Sc₂O₃, Y₂O₃, ThO₂, La₂O₃, CeO₂

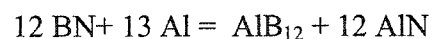
Adding rare-earth-oxides can reduce infiltration possibility and form dense texture^[2,4]. The addition of small amounts of light rare-earth oxides (CeO₂, La₂O₃) dramatically reduced the degree of aluminum alloy attack^[1]. These results need to be confirmed.

(3) Non-oxides: B₄C, SiC, Si₃N₄, SIALON, AlN, BN, ZrB₂, CaB₆

Aluminum and aluminum alloys are prone to very stable nitrides, carbides and borides^[2]. As less reactive (less wetting) materials against molten aluminum, non-oxide materials as silicon carbide (SiC), silicon nitride (Si₃N₄) and graphite are considered to be good candidates^[39]. However, stability in an oxidizing atmosphere should be taken into account.

AlN is stable against Al alloy^[2].

BN is dissolved by aluminum after the following reaction:



At least the reaction product AlN is stable against Al melts. Because of the less wetting tendency of BN in contact with Al melts, very low corrosion rates were achieved by a thin BN layer^[2].

TiB₂ was used as anode block coating in aluminum electrolysis cell. Some people recommended TiB₂ and ZrB₂ as an improvement in lining material for Al melting furnace^[2,4].

(4) Oxide-containing Compounds:

Barium Titanate (BaTiO₃), Calcia Phosphate (Ca₃(PO)₄), CaSO₄ and BaZrO₃: They have similar structure with BaSO₄. For BaSO₄, the beneficial effect was attributed to the formation of some barium alumino-silicate compounds^[20,21]. For these compounds, the formation of barium alumino-silicate compounds and calcium alumino-silicate compounds is expected to improve corrosion resistance against aluminum alloy. Also, phosphate is helpful for retaining smaller pore size^[5].

Anorthite (CaSi₂) and Gehlenite (C₂AS): Barium Celsian (BaO·Al₂O₃·2SiO₂) can improve strongly the corrosion resistance against molten aluminium and cryolite bath, as an additive used in a typical low cement alumino-silicate refractory castables^[6]. Anorthite (CaSi₂) and Gehlenite (C₂AS) have similar structure to Barium Celsian.

Aluminum Borate (Al₂O₃·B₂O₃): According to Japanese researcher^[40], aluminum borate is believed to reduce wettability of refractory by aluminium melt.

Aluminum Titanate (Al₂TiO₅): Some researchers considered Aluminum Titanate (Al₂TiO₅) as a new material for the non-ferrous industry because its outstanding properties such as non-wetting by non-ferrous melts, very low thermal expansion, excellent thermal shock and thermal cycling resistance and good thermal insulation^[9]. On the contrary, Pereira and Baldo's research indicated that the addition of Aluminum Titanate was not effective as expected^[6]. Validation of these results need to be made.

Decalcium Silicate 2CaO·SiO₂, CaO·2SiO₂ and tricalcium Silicate 3CaO·SiO₂: As an additive, wollastonite (CaO·SiO₂) can improve corrosion resistance^[14]. It can be imaged

that $2\text{CaO}\cdot\text{SiO}_2$, $\text{CaO}\cdot 2\text{SiO}_2$, $3\text{CaO}\cdot\text{SiO}_2$, protoenstatite $\text{MgO}\cdot\text{SiO}_2$ and forsterite $\text{MgO}\cdot 2\text{SiO}_2$ have the same property.

(5) Cement Clinker

Portland cement clinker comprises of Tricalcium silicate C_3S (>50%), Dicalcium silicate C_2S (~20%), Tricalcium aluminate C_3A and Tetracalcium aluminoferrite C_4AF . These different compounds have previously been selected.

1.5.2 Improved Testing Set-up

Even though the CIREP Bellyband Test Set-up can be used to evaluate the resistance of refractories to corundum attack, there are some problems which limit its usage well.

First and most important fact is that the service temperature may exceed 1200°C to speed up melt rate in aluminum treatment furnaces where the working temperature of the Bellyband Test Set-up is between 1150 to 950°C . Thus, it can not be used to evaluate the resistance of refractories to corundum attack above the metal line, in such furnaces, for all operating conditions.

Secondly, corundum formation is not always produced during the tests with that set-up since it depends on the composition of the tested sample.

Finally, only two samples can be tested simultaneously with that set-up which involves wastage of more energy and time.

A new external corundum growth test method, which allows corrosion of refractory materials with the corundum that usually form on the walls of aluminium melting and holding furnaces need to be devised. The new test method should allow reproducing such conditions irrespectively of the composition of the tested materials. With the test results, it should be possible to select the most appropriate refractory lining with much more confidence.

CHAPTER 2: A NEW PROCEDURE TO EVALUATE THE RESISTANCE OF REFRACTORIES TO EXTERNAL CORUNDUM GROWTH

2.1. Introduction

Corrosion of refractories at the Bellyband Zone is one of the major causes of lining degradation in holding and melting furnaces for liquid aluminum treatments. Many laboratory experiences, using either a cup test or finger test method, have clearly demonstrated that the direct oxidation of aluminum alloys above the metal line contributes largely in such corrosion process. Moreover, it appeared that the corrosion of refractory samples below the metal line may also have a significant effect on the kinetics of oxidation at the metal/atmosphere interface. Such refractory intervention on corundum growth makes difficult the comparison between the tested refractory samples.

The present chapter proposes a new simple laboratory procedure to evaluate the resistance of refractory samples to corundum growth. The effect of alloying elements, testing temperatures and atmosphere are analyzed. A method to calculate the corroded area in samples, due to the corundum attack, has also been proposed for material classification.

There are several methods available for testing the refractories for corrosion, such as CIREP standard immersion test and CIREP bellyband test which test the refractories for corrosion resistance at the metal line.

It is known that the lining of aluminium melting and holding furnace can be divided into three zones. Each zone are subjected to different industry condition. It is of interest to have different methods for testing the refractories at different areas of the furnace and hence the need for testing refractories designed for the lining is growing rapidly.

The CIREP standard immersion test is widely used to test the corrosion resistance of the refractories below the metal line. The CIREP bellyband test was designed to evaluate the resistance of refractories to corundum attack at the metal line. It uses a bottom loading type furnace permitting to achieve a temperature gradient of about 1150 to 950°C across the air/atmosphere interface and the molten aluminum alloy is contained in the refractory crucible sample which was pre-fired at 1200°C. One limitation observed with this test is the difficulty to evaluate refractories which modify the alloy composition such that corundum growth at the metal line, in crucible, is prevented.

The primary objective of this study is to design a new and simple laboratory experiment to test the corrosion resistance of refractories to corundum attack irrespectively of the nature of the refractory. This new method has been developed to evaluate refractory resistance to corundum growth. The complete experiment details are presented in this chapter. The effect variables such as testing temperature, holding time, oxygen partial pressure, metal amount and incubator are investigated. The problems that occur in testing and countermeasures are also discussed. Larger corundum mushrooms can be got through this new method.

2.2. Corundum Mushroom Formation

2.2.1. Experimental Procedure

Refractory samples, crucibles and aluminum alloys were described before.

Refractory samples: The refractory samples used were square plate with dimension of 50×50mm² and 12 mm height, with a central hole ($\Phi=13\text{mm}$) to favour the air access in the middle top surface of the sample.

Crucibles: Alumina crucible with an internal and external Cr_2O_3 coating was used. Upper inside diameter (I.D): 32mm; Height: 42mm; Bottom inside diameter (I.D): 30mm. Cr_2O_3 powder with sufficient water was mixed to prepare slurry and coated on walls of crucible both inside and outside. The coated crucible was dried in air for 24 hours.

Aluminum alloys: Two kinds of alloys were used. There are Al-5%Mg-5%Zn alloy and 7075 alloy (Al: 90.07, Zn: 5.6, Mg: 2.5, Cu: 1.6 Cr: 0.23). Their weight was about 38g for each test.

Air tight sealing between crucible and refractory was made using alumina slurry. The slurry was prepared by mixing tabular alumina fines ($20\mu\text{m}$) with sufficient water. After drying for 24 hours, the set-up [Figure 2.1] was ready for test.

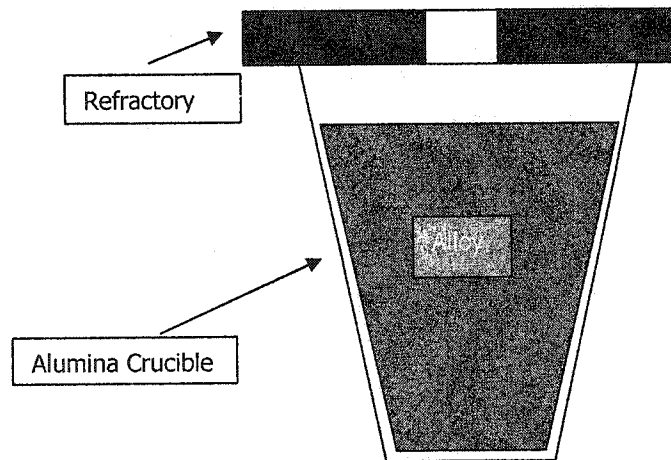


Figure 2.1: Refractory Resistances to Corundum Growth Set-up

Crucible set-ups such as shown in Figure 2.1 were kept in a bottom-open-furnace. The bottom of the furnace was seal lightly with ceramic fibre. This light sealing ensured air flow inside the furnace so as to have oxygen atmosphere.

The crucible set-ups were heated from room temperature to 1200°C with slow heating rate (5°C/min). This slow heating rate avoided cracking of crucible. Samples were soak at 1200°C for different testing times. The testing furnace set-up is shown in Figure 2.2.

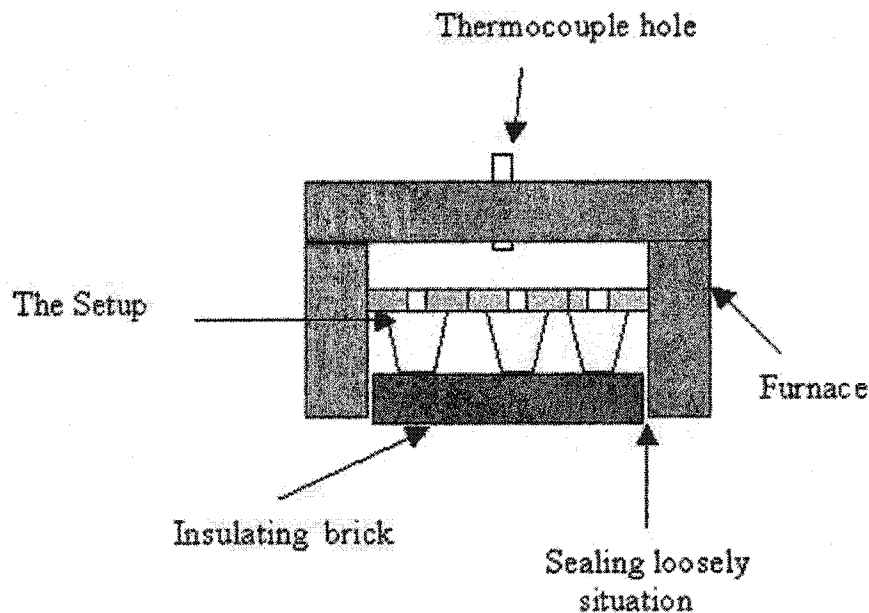


Figure 2.2: Bottom-Open-Furnace Set-up

2.2.2. Results and Discussion

2.2.2.1. Effect of Test Temperature

The effect of test temperature on corundum mushroom growth is presented in Table 2.1. It was shown that corundum growth occurs by direct metal oxidation when the temperature was more than $1150^{\circ}\text{C}^{[13]}$. In the current experiment, the test temperature is varied between 1180 and 1250°C .

Table 2.1: Effect of Test Temperature on Corundum Mushroom

Sample Number	Sealing Condition	Soaking Temperature & Time	Metal in Crucible Volume	Alloy	Result
51, 52, 53	Tight	$1234^{\circ}\text{C}\times 48\text{h}$	1/2 --2/3	7075	Good corundum mushroom
54, 55, 56	Tight	$1217^{\circ}\text{C}\times 50\text{h}$	1/2 --2/3	Al-5%Mg-5%Zn	A little corundum
57,58,59	Loose	(1200-1230) $^{\circ}\text{C}\times 30\text{h}$	1/2 --2/3	Al-5%Mg-5%Zn	Good corundum mushroom
66, 67, 68	Loose	(1212-1222) $^{\circ}\text{C}\times 40\text{h}$	1/2 --2/3	Al-5%Mg-5%Zn	Good corundum mushroom
60, 61, 62	Loose	(1184-1230) $^{\circ}\text{C}\times 21\text{h}$	1/2 --2/3	Al-5%Mg-5%Zn	Good corundum mushroom
57, 58, 59	Loose	$1188^{\circ}\text{C}\times 25\text{h}$	1/2 --2/3	Al-5%Mg-5%Zn	Good corundum mushroom

From Table 2.1, it is observed that with increasing test temperature, good mushroom growth occurs in shorter soaking time.

2.2.2.2. Effect of Oxygen Partial Pressure

The effect of oxygen partial pressure is presented in Table 2.2 and 2.3.

Table 2.2: Effect of Oxygen Partial Pressure on Corundum Mushroom

Sample Number	Sealing Condition	Soaking Temperature & Time	Metal in Crucible Volume	Alloy	Result
2, 5, 9	Tight	(1215-1225) ^o C×72h	3/4 --4/5	7075	Good corundum mushroom
57, 58, 59	Loose	(1200-1230) ^o C×30h	1/2 --2/3	Al-5%Mg-5%Zn	Good corundum mushroom
22, 23, 24	Tight	1286 ^o C×29h	½ --2/3	7075	No mushroom Little corundum

From Table 2.2, it is clear that sufficient air is necessary for good corundum mushroom growth.

Table 2.3: Effect of Oxygen Partial Pressure on Corundum Mushroom

Sample Number	Condition	Hole diameter (Φ) on refractory sample	Result
35	Sealing loosely, 1188 ^o C×25h, (1/2 -- 2/3)metal capacity,7075alloy	25mm	Good mushroom corundum, all metal oxidized
31	idem	13mm	A little metal oxidized, no mushroom

From Table 2.3, it is clear that a bigger hole in refractory sample makes air access into set-up, and metal oxides easily.

2.2.2.3. Effect of Soaking Time

The effect of soaking time on corundum mushroom growth is given in Table 2.4.

Table 2.4: Effect of Soaking Time on Corundum Mushroom

Sample Number	Sealing Condition	Soaking Temperature	Soaking Time	Metal in Crucible Volume	Alloy	Result
1, 4, 7	tight	(1215-1225)°C	30h	3/4 --4/5	7075	2/3 metal is not oxidized
3, 6, 8	Tight	(1215-1225)°C	50h	3/4 --4/5	7075	1/3—1/4 metal is not oxidized
2, 5, 9	Tight	(1215-1225)°C	72h	3/4 --4/5	7075	All metal is oxidized. Good mushroom
60,61,62	Loose	(1184-1230)°C	21h	1/2 --2/3	Al-5%Mg-5%Zn	Good corundum mushroom
63, 64,65	Loose	1220°C	14.5h	1/2 --2/3	Al-5%Mg-5%Zn	A little corundum, no mushroom

From Table 2.4, it is understood that longer soaking time helps metal oxidation.

2.2.2.4. Effect of Metal Amount

In the beginning stage of experiment, metal occupies 3/4--4/5 volume of alumina crucible. It does not show corundum growth easily. Therefore, 1/2 to 2/3 cool metal was easily stuffed in alumina crucible. If test temperature and oxygen partial pressure are suitable, 38±2g metal is appropriate for corundum growing.

2.2.2.5. Effect of SiO₂ Powder Incubator

The role of silica powder on the corundum mushroom growth is presented in Table 2.5. It is observed that 1g SiO₂ powder could effectively incubate corundum growth. Uneven corundum growth has been observed due to non-uniform distribution of SiO₂ powder on alloy surface.

The SiO₂ powder at 0.4g level does not give any valuable information on incubation as its amount is very less.

Table 2.5: Effect of SiO₂ Powder Incubator on Corundum Mushroom

sample	SiO ₂ incubator	Sealing situation	Temperature & time	Metal capacity	Alloy	Result
24, 25, 26	1g	Tight	(1200-1244)°C×50h	3/4 --4/5	7075	All metal oxidized
27, 28, 29	0.4g	Tight	(1215-1234)°C×54h	3/4 --4/5	7075	Small mushroom, a little metal oxidized

2.2.3. Problems to Be Solved:

2.2.3.1. Creating A Rich Oxygen Atmosphere and Getting A Stable Air Flow Control

Our purpose is to get a nice corundum growth. So that rich oxygen atmosphere is important. Big mushroom corundum could easily be got with loose sealing of joint between bottom block and bottom of the furnace, and the holding time is less than 24 hours sometimes. This does not provide quantitative measure on oxygen partial pressure in furnace. Under the same test temperature, good corundum mushroom growth is observed with different soaking time.

2.2.3.2. Preventing Corundum Grows along the Seal between Refractory Sample and Alumina Crucible

Countermeasure: Making crucible upper edge flat and using alumina mortar to seal it; coating Cr_2O_3 powder on mortar surface. Still, corundum growth has been observed occasionally.

2.2.3.3. Corundum Grows Through Crucible Wall

Cr_2O_3 is coated on both inside and outside wall of crucible. This is a valid way to prevent corundum growth through the wall.

2.2.4. Conclusions

In order to evaluate the resistance of refractories to external corundum growth, it is necessary to get nice corundum mushroom firstly.

Good corundum mushroom growth can be achieved under following conditions:

- (1) Between 1220° to 1250°C ;
- (2) Loose sealing of furnace;
- (3) Soaking time of around 40 hours;
- (4) Crucible with more than 50% volume of aluminum alloy.

2.3. Optimization of the New Corrosion Test Method

2.3.1. Introduction

The ways to get larger corundum mushroom growth has been discussed previously. Corundum mushroom represents extent of metal oxidization. It is necessary for refractory to be corroded by corundum from metal oxidation. This part of the study focuses on refractory samples' corrosion and their test conditions through comparing overall cross-sections of the samples. Effect of mushroom size and extent of metal oxidation, soaking temperature and time, type of furnaces, and different alloys are discussed. Some additives added in refractories showing different resistance to corundum growth are also presented.

2.3.2. Experimental Procedure

The set-up shown in Figure 2.1 was used for the experiments. Moreover, two types of furnaces were considered.

2.3.2.1. Oxidization Procedure

The two types of furnaces used were (1) a bottom-open-furnace and (2) a top-open-furnace were described in section 2.2.1.

Nine samples were kept into the furnace with cover of 24mm thick insulating board. The cover was drilled out 9 places (hole's diameter 15mm) to assure good air flow inside the furnace. This promoted oxidation atmosphere inside the furnace. The distance between upper surface of refractory samples and cover was 90mm.

At 1200 °C, samples were soaking for 40 hours.

Figure 2.3 showed the top-open-furnace set-up.

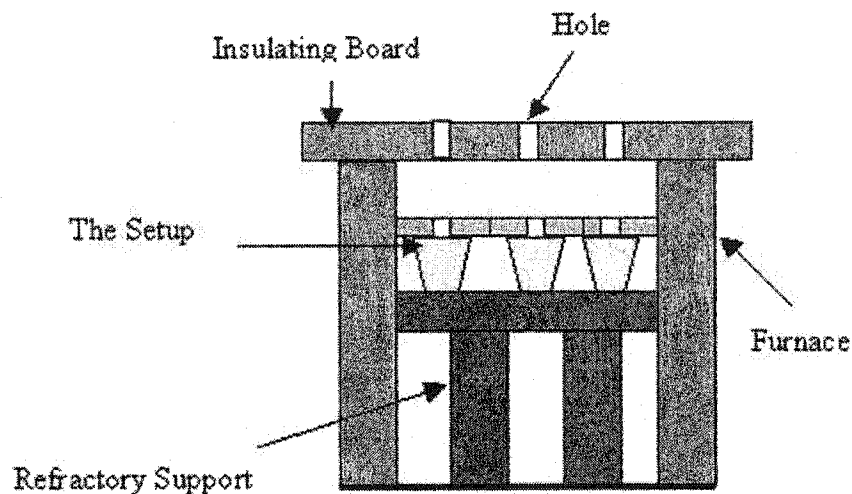


Figure 2.3: Top-Open -Furnace Set-up

2.3.2.2. Cutting and Comparison

After testing, the samples were cut longitudinally, and overall cross-section of the samples was compared.

2.3.3. Results and Discussion

2.3.3.1. Effect of Corundum Mushroom Size and Extent of Alloy Oxidation

It has been shown that corundum growth could be got when temperature is more than $1150^{\circ}\text{C}^{[13]}$. In this experiment, the test temperature is between 1180 and 1250°C (bellyband test furnace). The temperature display in new furnace had shown 1200°C , while the thermocouple measurement inside the furnace was 1160 - 1180°C .

Table 2.6, shows that when more than 70% alloy is oxidized and mushroom diameter is more than 18mm, same refractory materials have the same corroded rating .

Table 2.6: Effect of Corundum Mushroom Size and Extent of Alloy Oxidation

Sample Number	Material	Condition	Mushroom Size (mm) & Oxidized Extent	Corroded Rating
67	C-7080-4+ 5wt%C3MS2	½-2/3, AMZ, (1212-1222)°C×37h, loose sealing, bottom-open-furnace	Φ33×16, 90%	4
217	C-7080-4+ 5wt%C3MS2	½-2/3, AMZ, 1200°C×40h, top-open-furnace	Φ25×12, 100%, little	4
214	C-7080-4+ 5wt%T30	Idem	Φ27×15, 100%	2
218	C-7080-4+ 5wt%T30	Idem	Φ23×9, 100%, some	2
14	C-7080-4+ 5wt%CAS	4/5, 7075, (1190-1225)°C×26h, tight sealing, bottom-open-furnace	Φ25×10, 60%	2
15	C-7080-4+ 5wt%CAS	Idem	Φ20×7, 70%, some	2
22	C-7080-4+ 5wt%CAS	4/5, 7075, 1286°C×29h, tight sealing, bottom-open-furnace	Φ18×23, 60%	2
24	C-7080-4+ 5wt%CAS	Idem	Φ20×6, 90%, much	2 ⁺
60	C-7080-4+ 5wt%SiC	½-2/3, AMZ, (1184-1230)°C×21h, loose sealing, bottom-open-furnace	Φ30×16, 95%	5 ⁺
62	C-7080-4+ 5wt%SiC	Idem	Φ33×11, 95%	4 ⁺

66	C-7080-4+ 5wt%SiC	½-2/3,AMZ,(1212-1222)°C×37h, loose sealing, bottom-open- furnace	Φ30×9, 100%, little	5 ⁻
111	C-7080-4+ 5wt%SiC	½-2/3,AMZ, 1200°C × 40h , top-open-furnace	Φ24×10, 100%, little	5 ⁺
211	C-7080-4+ 5wt%SiC	Idem	Φ29×14, 100%	5 ⁻
212	C-7080-4+ 5wt%SiC	Idem	Φ14×2, 100%, some	5 ⁺
216	C-7080-4+ 5wt%SiC	Idem	Φ20×7, 100%, much	5
219	C-7080-4+ 5wt%SiC	Idem	Φ29×13, 100%	5 ⁺

Note:

“½-2/3,AMZ,(1212-1222)°C×37h, loose sealing, bottom-open-furnace”: volume of metal in crucible, Al-5%Mg-5%Zn alloy or 7075 alloy, soaking temperature and time, sealing condition, type of furnace.

“Φ25×12, 100%, little”: mushroom diameter and height, oxidized percentage, corundum growing around crucible upper.

2.3.3.2. Effect of Soaking Time and Testing Temperature

From Tables 2.6 and 2.7, it is clear that corrosion resistance are independent of soaking time (21-40hrs) and soaking temperature (1160-1250°C) where the corundum mushroom growth is larger with complete metal oxidation.

Actually, in this experiment, the maximum soaking time is 70 hours. Their corrosion results are similar with shorter soaking time samples.

Table 2.7: Effect of Soaking Time and Testing Temperature

Sample	Material	Condition	Mushroom Size (mm) & Extent of Alloy Oxidation	Corroded Rating	Soaking Temperature & Time
61	C-70804+ 5wt%CS	2/3, AMZ, loose, bottom-open-furnace	Φ28×10, 100%	3 ⁺	(1184-1230)°C ×21h
112	C-70804+ 5wt%CS	2/3, AMZ, top-open-furnace	Φ26×14, 100%	4	1200°C ×40h
215	C-70804+ 5wt%CS	2/3, AMZ, top-open-furnace	Φ19×8, 95%	3 ⁺	1200°C ×40h

2.3.3.3. Effect of the Furnace Type

From Tables 2.6, 2.7 and 2.8, it can be seen that under similar testing condition, the change of testing furnace does not have any signification effect on corrosion rating.

However, there are some different between two furnaces.

Larger corundum mushroom is obtained and Al alloy is oxidized completely^[6] under following condition:

- Bottom-open-furnace;
- Test temperature 1220-1250°C;
- Loosing sealing;
- Soaking time of 40 hours;
- Al alloy occupies more than 50% volume of crucible.

Although it has been difficult to fix soaking temperature in bottom-open-furnace, it has not affected the corrosion results.

With top-open-furnace at 1200°C, 40 hours soaking time, the following results are obtained:

- Different size corundum mushrooms;
- Sometimes, ½ to 2/3 volume of alloy (Al-5%Mg-5%Zn) is oxidized completely.
- Some samples does not form corundum mushrooms.
- The measured temperature with thermocouple is 1160-1180°C, though the meter display is 1200°C.

Table 2.8: Effect of Different Furnaces on Corrosion Results

Sample	Material	Mushroom Size (mm) & oxidized extent	Corroded Rating	Condition	Furnace
67	C-7080-4+ 5wt%C3M2	Φ33×16, 95%	4 ⁺	2/3,AMZ,(1212-1222)°C×37h	Loose, bottom-open-furnace
217	C-7080-4+ 5wt%C3M2	Φ25×12, 100%, little	4	2/3,AMZ, 1222°C×40h	top-open-furnace

The top-open-furnace is not a good choice to be used as equipment for Corundum Corrosion Test because (1) some samples do not oxidize due to low oxygen partial pressure and (2) air flow distribution makes corundum infiltrating crucible grow easily. Figure 2.5 to 2.7 show the samples subjected for corrosion testing in bottom-open-furnace. These confirm the fact that corrosion results are not affected by varying soaking time (30-70hrs) or furnaces. In all cases, complete metal oxidation has taken place with good corundum mushroom growth.

The reasonable explanation is that corroded rating is related to extent of metal oxidization, not to oxidization speed.

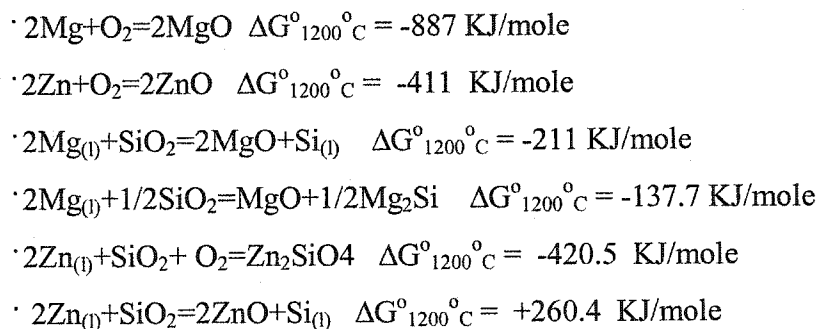
It is known that liquid aluminum infiltrates refractory sample through capillary channel in Al₂O₃/Al composite, then reacts with SiO₂, finally corundum is formed^[18]. Corundum corrosion is stopped after all metal becomes Al₂O₃/Al composite.

2.3.3.4. Effect of Different Alloys

After oxidized, the alloy (Al-5%Mg-5%Zn) become more residue than 7075alloy, and mushroom from 7075 is more smoother. It seems that alloy (Al-5%Mg-5%Zn) oxidizes easilier than 7075.

7075 alloy attacks refractory more seriously than alloy (Al 5%Mg 5%Zn). 7075 alloy is easier than (Al-5%Mg-5%Zn) alloy to form protective deposit. This needs to be confirmed in the future.

From thermodynamic point of view, it is seen that oxidation of Mg and reaction of Zn with SiO₂ (from refractory) is much easier than other reaction. The possible reactions are given below.



2.3.3.5. Property of Additives

After comparing overall results of the test samples, it is understood that additives show different rating of resistance to corundum growth (Figure 2.8--2.16):

Y₂O₃, C₂S, ZrB₂, CAS, Cement clinker T-30, HfO₂, CMS, C₃MS₂, Talc, M₂S, SiC
 GOOD<----->BAD

Table 2.9: Corrosion Rating of Product C-7080-4 with Different Additives

Corroded rating	0	1	2	3	4	5
Additives	Y ₂ O ₃	C ₂ S, ZrB ₂	CAS, Cement clinkerT-30,	HfO ₂ , CMS	C ₃ MS ₂ , Talc, M ₂ S	SiC

SiC may oxidize at temperatures around 1100°C, leading to the formation of SiO₂ followed by its reduction by molten aluminium. In spite of SiC shows excellent resistance to aluminium penetration (815°C×72h) and optimum resistance to alkalis (900°C×2h)^[16], when used as an additive, it does not show good resistance to corundum growth at 1200°C.

Wollastonite (CaO·SiO₂) can improve corrosion resistance^[44]. It is expected 2CaO·SiO₂, CaO·2SiO₂, 3CaO·SiO₂, Anorthite (CaSi₂), Gehlenite (C₂AS), Protoenstatite MgO·SiO₂, Forsterite MgO·2SiO₂, CMS and C₃MS₂ have the same property.

This experiment results has proved CAS and C₂S are good additives. But CMS, C₃MS₂, Talc and M₂S are not showing good resistance to corundum growth. Actually, the mineral composition of CAS, C₂S, CMS, C₃MS₂ and M₂S should be clarified. Further research is required to understand their function in castable matrix after fired at 1200°C.

Portland cement clinker comprises of Tricalcium silicate C₃S (>50%), Dicalcium silicate C₂S (~20%), Tricalcium aluminate C₃A and Tetracalcium aluminoferrite C₄AF(>10%). Usually, it contains 3-5% Fe₂O₃.

White cement specification show its major compounds are C₃S: 56%, C₂S: 22%, C₃A: 11%, C₄AF: 0.7%^[15]. It only contains 0.2% Fe₂O₃.

This dictates that white cement clinker maybe better than cement clinker used as additives. Meanwhile, the binder used in the castable mixes should be less when cement clinker is used as additive.

ZrB₂ plays a positive role in resistance to corundum growth. The reason is not clear. But it maybe explained by following mechanism: additives react with alumina and silica among the fine particles of the refractories, forms new products (e.g. zircon) in the firing

temperature. Such transformations reduce the amount of free silica within the matrix and should consequently improve the corrosion resistance of refractory.

2.3.4: Problems

2.3.4.1. Minimization of Corundum Growth around the Crucible

Some measures have been taken^[20]. They are effective when bottom-open-furnace is used. As for top-open-furnace, new countermeasures should be found in the future.

2.3.4.2. Furnaces

A reasonable air flow distribution inside makes bottom-open-furnace getting a rich oxygen atmosphere, so that larger corundum mushroom growth is achieved and Al alloy oxidize completely^[20].

When top-open-furnace is used, inadequate oxygen partial pressure complete metal oxidation is not possible. Meanwhile, corundum infiltrates crucible wall and grow easily.

With the above results, bottom-open-furnace is selected as the equipment for new method.

2.3.5. Summary

Under the situation of getting larger corundum mushroom with almost complete metal oxidation, same refractory materials have similar corrosion results. This experiment procedure can be used as a new method for evaluation of refractory resistance to corundum growth.

Metal should be oxidized as much as possible. Larger corundum mushroom represents high extent of oxidization. Getting larger corundum mushroom is necessary for this method.

Varying soaking time (30-70hrs) and furnaces (new furnace or bellyband furnace) has not brought out any significant change in corrosion results, when corundum mushroom growth is larger in the complete metal oxidation.

Y_2O_3 , ZrB_2 , CAS, C_2S and Cement clinker T-30 are found to be good additives for corundum corrosion.

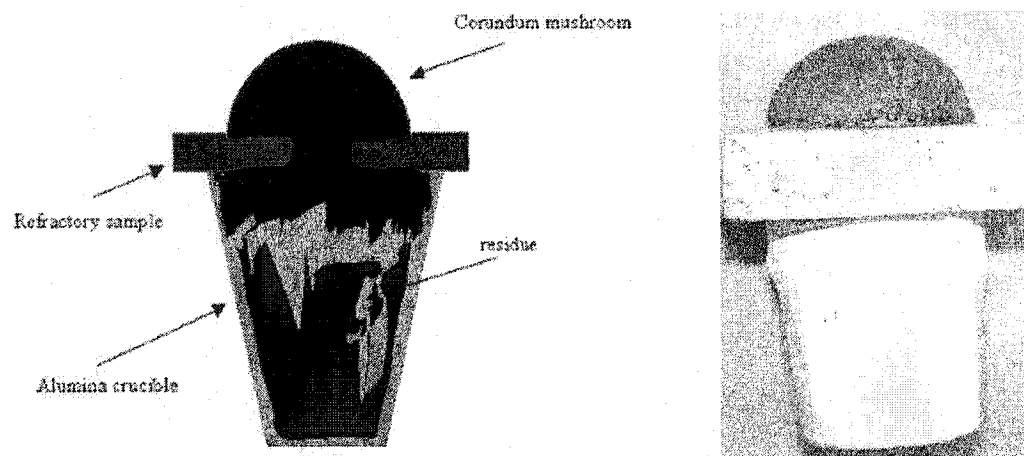


Figure 2.4: After Alloy Oxidized Completely

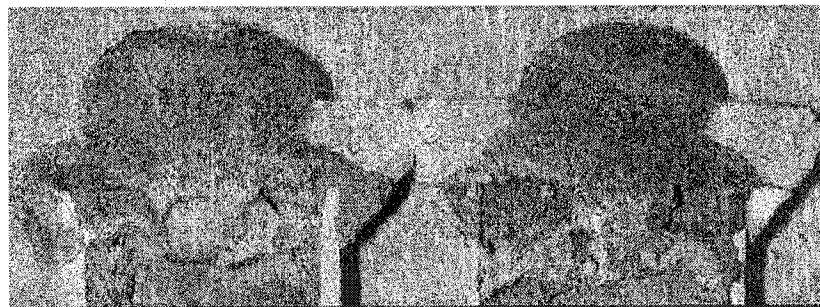


Figure 2.5: left: 66[#] C-7080-4+5%SiC, AMZ, (1212-1222)^oC × 37 h, loose sealing, bottom-open-furnace; right: 111[#] C-7080-4+5%SiC AMZ, 1200^oC × 40h, top-open-furnace



Figure 2.6: left: 112[#] C-7080-4+5%CMS AMZ, 1200°C × 40h , top-open-furnace
right: 61[#] C-7080-4+5%CMS AMZ, (1184-1230)°C × 21 h, loose sealing,
bottom-open-furnace

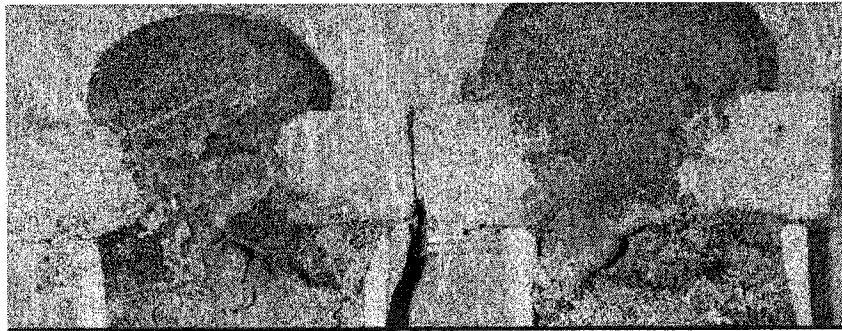


Figure 2.7: left: 217[#] C-7080-4+5%C3MS2, AMZ, 1200°C × 40h, top-open-furnace
right: 67[#] C-7080-4+5%C3MS2, AMZ, (1212-1222)°C × 37h,
loose sealing, bottom-open-furnace

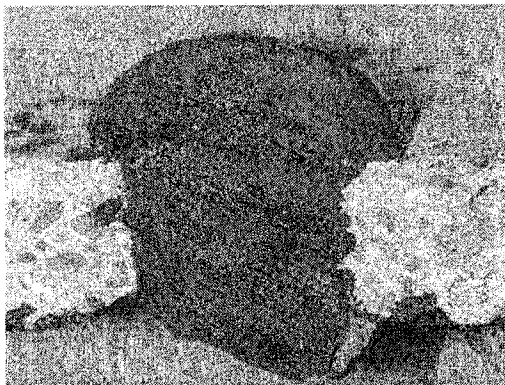


Figure 2.8: C-7080-4+5%Y₂O₃
after 1200°C × 40h, AMZ alloy



Figure 2.9: 68[#] C-7080-4+5%ZrB₂,
after (1212-1222°C) × 37h, AMZ alloy



Figure 2.10: 58# C-7080-4+5%C2S,
after(1200-1230°C)×30h,AMZ alloy



Figure 2.11: 214# C-7080-4+5%T-30(cement
clinker)after1200°C×40h,AMZ alloy



Figure 2.12: 22# C-7080-4+5%CAS,
after1286°C×29h,7075 alloy

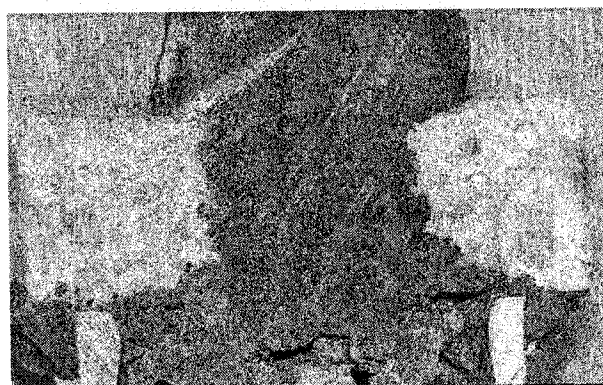


Figure 2.13: 5# C-7080-4+5%HfO₂,
after(1215-1225°C)×70h,7075 alloy



Figure 2.14: 61# C-7080-4+5%CMS,
after(1184-1230°C)×21h,AMZ alloy



Figure 2.15: C-7080-4+5%Talc,
after(1214-1243°C)×72h,7075 alloy



Figure 2.16: C-7080-4+5%SiC, after 1200°C×40h, AMZ alloy

2.4. Improvement of the New Method of Corundum Corrosion Test

Many factors control formation of big corundum mushroom, such as atmosphere, temperature, alloy composition and amount, soaking time, air flow and distribution, and alumina crucible size. The influence of these factors is complex and not easy to be controlled. Thus corundum corrosion test method need to be improved.

Rich-oxygen atmosphere benefits corundum mushroom growing. In order to get bigger mushroom corundum and avoid corundum growing through wall of alumina crucible, a new facility was designated as shown in Figure 2.17.

The new design incorporates a refractory block in the center of the furnace and a compressed air flow system. The compressed air makes furnace full of oxygen that favors corundum mushroom growth. The refractory block disperses the compressed air, keeping a lower partial pressure under the level of refractory samples that are under test, and thus avoid or prevent corundum growing through crucible wall.

With these new measures, Corundum Corrosion Test Method has been improved. It is proven that (1) TiO_2 is a good incubator for corundum growth. (2) Al-5%Mg-5%Zn alloy form corundum mushroom easily than pure Al, Al-5%Mg and Al-5%Mg-7%Si alloy.

It is found that the new method is effective for evaluation of refractory resistance to corundum growth with good repeatability.

Corundum corrosion test conditions go as follows:

- » Refractory sample: $50 \times 50 \times 12 \text{mm}^3$ (refractory sample pre-fired at $1200^\circ\text{C} \times 5\text{hrs}$)
- » 1200°C for 40 hours,
- » Alloy: Al-5%Mg-5%Zn

Nine to twelve refractory samples can be tested each time. The only problem is mushroom corundum could not be grown similarly from each set-up. Three effective same refractory samples are to be used to evaluate corundum corrosion rating.

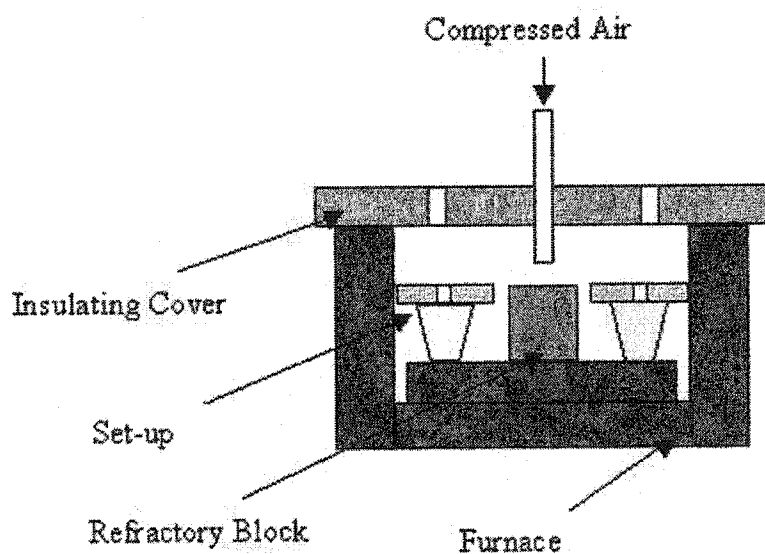


Figure 2.17: Equipment of New Method for Corundum Corrosion

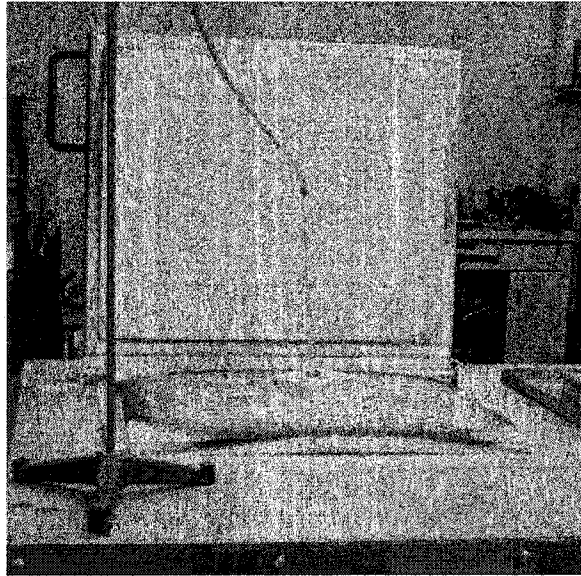


Figure 2.18: Picture of New Method for Corundum Corrosion

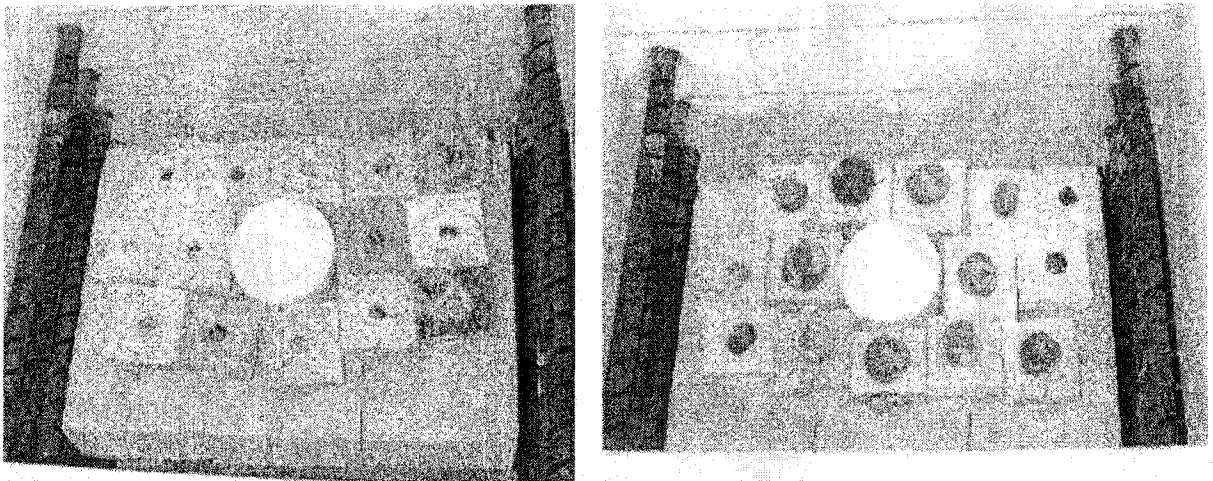








Figure 2.19: Samples Before and After Test

APPENDIX:

2.1 Rating Criteria of the New Method

Rating	Category	Observation
0	"Excellent" resistance	
1	"Good" resistance	
2	"Good to Moderate" resistance	
3	"Moderate" resistance	
4	"Moderate to Poor" resistance	
5	"Poor" resistance	

2.2. Chemical Composition of Additive Materials

Mineral	C2S %	CMS %	CAS %
SiO₂	16.05	30.54	22.21
SiO ₂ -cristobalite-tetragonal	0.00	0.00	13.41
CaCO₃	79.47	57.83	0.00
Ca(Mg,Fe)(CO ₃) ₂	0.00	4.44	0.00
Feldspath-Ca/anorthite	0.12	0.00	1.04
Mg ₄ (OH) ₂ ·3H ₂ O	0.00	7.05	0.00
Fe ₂ O ₃	0.23	0.14	0.00
TiO ₂	0.12	0.00	0.00
Ca ₂ SiO ₄ -larnite	0.00	0.00	26.53
Ca ₂ Al ₂ SiO ₇ -gehlenite	0.00	0.00	14.16
CaO	0.00	0.00	7.45
Ca(AlO ₂) ₂	0.00	0.00	12.22
Ca ₃ Si ₂ O ₇	0.00	0.00	2.98
Total	100.00	100.00	100.00
%Crystalline	79.60	74.80	69.60

CHAPTER 3: NOVEL ADDITIVES

Alumino-silicate materials have traditionally been used as refractory lining for primary aluminium treatment furnaces. Due to the reducing effects of molten aluminium alloys, these materials are susceptible to the formation of corundum. The temperatures at the sidewalls around the bellyband can reach at least 1200°C. To meet the more challenging demands, a variety of methods of enhancing the corrosion resistance have been developed for castables. These include the use of additives, pore blocking agents, alternative aggregates and different bonding system. This chapter presents that different additives with castables were found to show good corrosion resistance.

3.1. Boron-bearing Compounds and AlPO_4

3.1.1. Introduction

In aluminum treatment furnaces, service temperature may exceed 1200°C to speed up melting rates. Additives so far in use are known not survive beyond about 1100°C. Novel additives are needed to protect refractory against corrosion in such high temperature operating conditions.

The result of this study has indicated that when used as additives in alumino-silicate castables, boric compounds and AlPO_4 show excellent resistance for corundum corrosion. These boric compounds are BN, ZrB_2 , TiB_2 , B_4C , and CaB_6 . In order to explain this phenomenon, a series of analysis and tests including XRD, pore size distribution and micrograph, have been done. New phase $9\text{Al}_2\text{O}_3 \cdot 2\text{B}_2\text{O}_3$ exists in boron-bearing castables after fired at 1200°C. AlPO_4 does not decomposed after 1200°C for 4 hours heat-treatment.

The ways of protecting silica from corrosion need to be further investigated for boron-bearing and phosphorus-bearing additives.

3.1.2. Experimental Procedures

3.1.2.1. Sample Preparation

Two commercial castables were used as refractory bases. Five wt% potential additives are added inside these castables. Castable samples were made through usual process. The samples were pre-fired at 1200°C for 5 hours before testing.

Table 3.1.1: Castables Chemical Composition

Composition (wt%)	C-6070-3	C-7080-4
Al ₂ O ₃	57.29	70
SiO ₂	30.26	23,1
Fe ₂ O ₃	0.84	0,8
CaO	1.42	2,8
MgO	0.07	0,3
TiO ₂	1.43	1,7
ZrO ₂	3.29	
Alkalis	0.09	0,2

Each refractory sample is a square plate with 50×55mm² size and 12 mm height, containing a central cylindrical hole ($\Phi=13$ mm).

Alumina crucible is made in house by slip-casting. Upper inside diameter (I.D):32mm, height: 42mm, bottom inside diameter (I.D):30mm.

38 g Al-5%Mg-5%Zn alloy was put into the alumina crucible. Alumina mortar was used for sealing off the air access between refractory sample and crucible.

The set-up used for evaluation of refractory resistance to corundum growth is showed in Figure 2.1.

3.1.2.2. Porosity, Density and Amount of Water

With the addition of additives, castables need different amount of water. These result in the change of porosity and density. Refractory samples with or without additives were tested after fired at 1200°C for 5 hours.

3.1.2.3. Corrosion Tests

Oxidization Procedure:

The samples were put on a platform inside the furnace. The distance between the platform and lid was 1/4 of overall depth. The furnace cover is made up of insulating board (24mm thick) drilled with 9 holes of 15mm diameter. An alumina tube and rubber pipe are used for leading compressed air into the furnace so that the inside furnace maintains oxygen-rich atmosphere. Under 1200°C, the set-ups were soaked for 40 hours. Figure 2.17 and Figure 2.18 show the heat-treatment equipment.

Corundum mushroom is observed after the alloy is oxidized completed. Figure 2.4 shows a set-up with corundum mushroom.

Cutting and Comparison:

After tested under 1200°C×40hrs, the set-ups were cut longitudinally to compare their cross-sections with original refractory bases.

The cut section of refractory sample is shown in Figure 3.1.1. The shadowy triangle area was considered as potential corundum corrosion area.



Figure 3.1.1: Potential Corundum Corrosion Area in Refractory Sample

3.1.2.4. Characterization Techniques

In order to clarify the effect of boron-bearing compounds and AlPO_4 on $\text{Al}_2\text{O}_3\text{-SiO}_2$ refractories, further tests and analysis are done as follows.

3.1.2.4.1. Pore Size Distribution Analysis

In the mercury intrusion porosimetry method, a cylindrical pore model is assumed, and the size of pores is principally calculated using the Washburn equation:

$$D = 14 \gamma (\cos \theta / P)$$

Where D is the apparent diameter of the pore being intruded, γ the surface tension of mercury, θ the contact angle between mercury and the material and P the absolute pressure causing the intrusion. This equation can be used to convert pressure to pore diameter. The pore-size distribution can be determined by measuring the volume of mercury intruded into the pores as a function of pressure.

Micromeritics PoreSizer 9320 determines macropores, mesopores, cracks, and crevices contained in powdered or bulk sample. The PoreSizer then creates detailed reports of porosity with data describing pore sizes (0.006 to 360 μm diameter), their number, volume, area, and size distributions.

PoreSizer 9320 collects data with the high resolution and precision required for industry and research. High-tech pressurization systems generate pressures from 0 to 30,000 psi with an accuracy of 0.1% psi of full scale. State-of-the-art A/D converters resolve each data point to one part in 200,000. Even the intrusion/extrusion volumes are resolved to within a fraction of a microliter using ultra-sensitive capacitance transducers.

The scanning and equilibration modes, in conjunction with pressure points and/or a mercury intrusion increment, let the operator design the analysis to fit the sample. The result is a report that more precisely represents sample characteristics.

During analysis, specially designed penetrometers contain the sample and mercury. Since mercury is non-wetting for most materials, it must be forced into the sample pores with hydraulic pressure. The volume of mercury penetrating the pores is measured directly as a function of applied pressure. As pressure increases, mercury intrudes into smaller and smaller pores.

The volume of intruding mercury is measured by the change in electrical capacitance of a cylindrical coaxial capacitor formed by the penetrometer stem. The outer penetrometer stem is clad with a metallic skin; an inner-core capillary holds mercury. During intrusion/extrusion, the mercury moves in the capillary like mercury in a thermometer. This allows measurement of capacitance change caused by the movement of mercury in the capillary. Intrusion/extrusion volumes are detected within a fraction of a microliter.

3.1.2.4.2. X-Ray Diffraction Analysis

The phase analyses of refractory samples were done using XRD.

3.1.2.4.3. Optical Microscopy (OM) and Scanning Electron Microscopy (SEM)

The refractory samples were mounted in the bakelite, polished and examined under optical microstructural evaluations. The microstructural changes were carried out using SEM.

3.1.3. Results and Discussion

3.1.3.1. Corrosion Tests

The corundum corrosion results are shown in Figure 3.1.2.

These figures display that the presence of boron-bearing compounds and AlPO_4 in Al_2O_3 - SiO_2 refractories can resist corundum attack in Al_2O_3 - SiO_2 refractories.

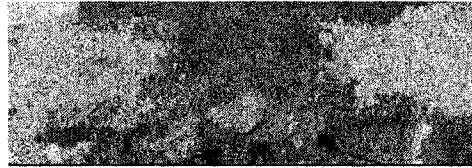
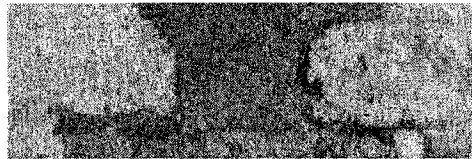
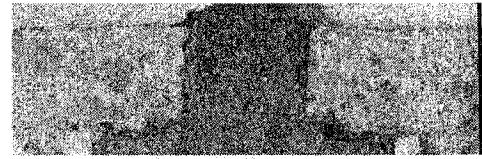
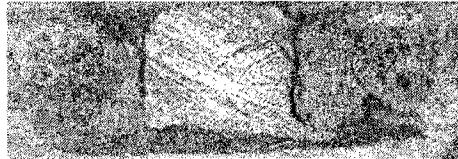
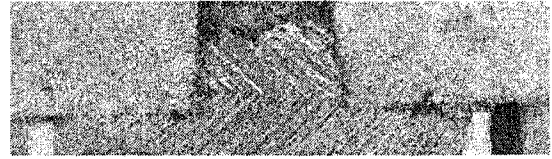
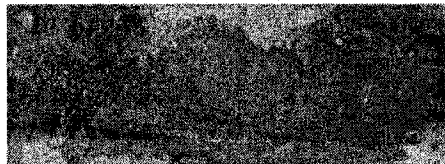
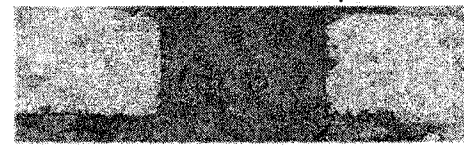
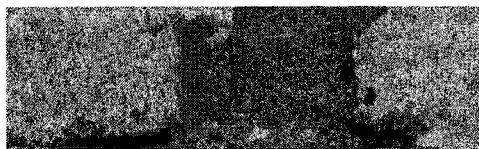
**C-6070-3****C-7080-4****C-6070-3+5%BN****C-7080-4+5%BN****C-6070-3+5%CaB₆****C-7080-4+5%CaB₆****C-6070-3+5%B₄C****C-7080-4+5%B₄C****C-6070-3+5%ZrB₂****C-7080-4+5%ZrB₂****C-6070-3+5%TiB₂****C-7080-4+5%AlPO₄****C-6070-3+5%AlPO₄**

Figure 3.1.2: Corundum Corrosion Test Results: C-6070-3 Series and C-7080 Series

3.1.3.2. Porosity, Density and Amount of Water

Table 3.1.3 displays that boron-bearing additives make castables having a lower porosity except the one with B_2O_3 . When B_2O_3 is used as additive, castables required much more water to cast. This results in the porosity up and density down.

Table 3.1.2: Porosity and Density after $1200^{\circ}C \times 5hrs$ Heat-treatment

	Water(%)	Porosity (%)	Density (g/cm ³)
C-6070-3	5.7	15.9	2.59
C-6070-3+5%B ₄ C	7	15.83	2.45
C-6070-3+5%BN	7.3	14.86	2.51
C-6070-3+5%ZrB ₂	5.7	13.03	2.67
C-6070-3+5%TiB ₂	4.6	10.57	2.71
C-6070-3+5%CaB ₆	8.3	13.82	2.57
C-6070-3+5%B ₂ O ₃	10.8	32.24	1.99
C-6070-3+5%AlPO ₄	8	22.8	2.42
C-7080-4	6.0	17.7	2.63
C-7080-4+5%B ₄ C	8.4	11.9	2.6
C-7080-4+5%BN	7	12.9	2.59
C-7080-4+5%ZrB ₂	6	12.41	2.77
C-7080-4+5%CaB ₆	11.8	16.31	2.45
C-7080-4+5% AlPO ₄	7	20.82	2.46

With BN, B₄C, CaB₆, castables have lower porosity and lower density. It means presence of more closed pore inside refractories.

ZrB₂ and TiB₂ bring about low porosity and high density.

Lower porosity does not have a beneficial effect on penetration.

From the manufacture point of view, ZrB_2 and TiB_2 are suitable additives for Al_2O_3 - SiO_2 castables.

Since $AlPO_4$ is a fine and light powder, which has adsorption and separation properties, more water is needed when used as additive. This results in porosity rise and density drop. This higher porosity and lower density do not influence to corundum corrosion.

Brondyke^[49] reported a significant degradation of porous alumina-silica refractories installed in furnaces containing molten aluminium. He reported that the porosity of refractories had little influence on the extent of aluminium penetration in refractories. Most of the interactions between alumina-silica bricks and the melt were shown to be related to the reduction of silica in contact with molten aluminium and transport of silicon into the melt.

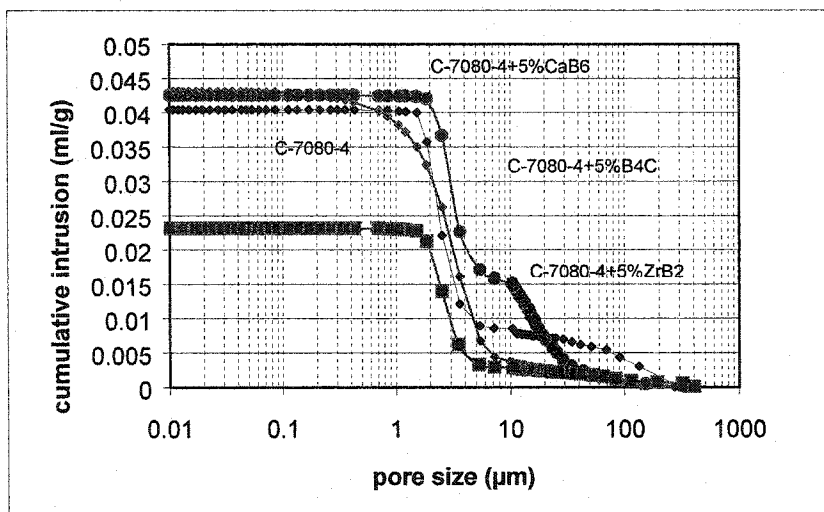
3.1.3.3. Pore Size Distribution Analysis

Through pore size distribution analysed, microstructure change can be evaluated.

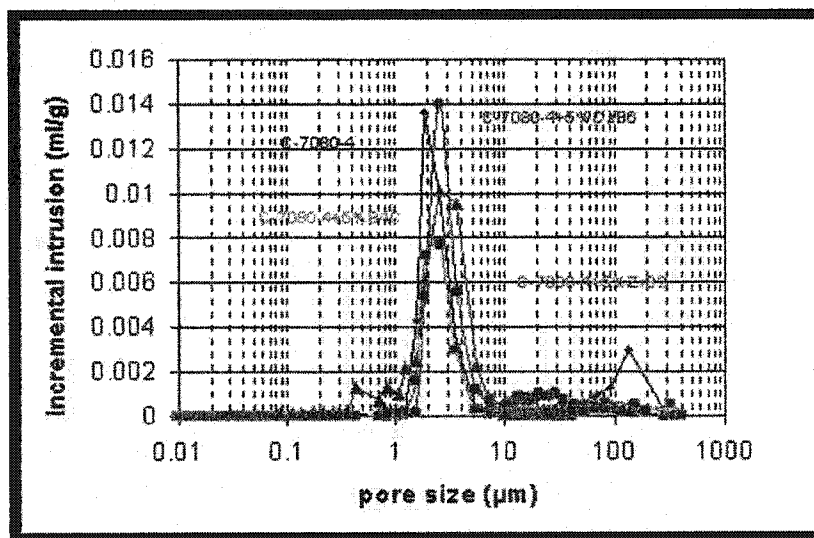
Figure 3.1.3 shows the pore size distribution evolution for C-7080-4 samples with or without additives. The cumulative intruded mercury volume increases slightly when additives are CaB_6 and B_4C . In the case of C-7080-4+5% ZrB_2 , there is a lower total volume of pores, indicating an overall less open microstructure. From (incremental intrusion vs. Pore size) figure, the main pore sizes are bigger slightly (2-3 μm) and there are no pores (>100 μm) after adding these additives.

Figure 3.1.4 indicates that pore size distributions for C-6070-3 with additives are different from without additives. In case of cumulative intrusion vs. Pore size, C-6070-3 displays a larger volume pores, indicating a more open structure. In case of incremental intrusion vs. Pore size, the pore size is larger (2-3 μm) and pore of 10-30 μm are also present when H_3BO_3 and TiB_2 are used as additives.

Figure 3.1.5 illustrates a similar trend displayed by $AlPO_4$ as additive in C-7080-4.

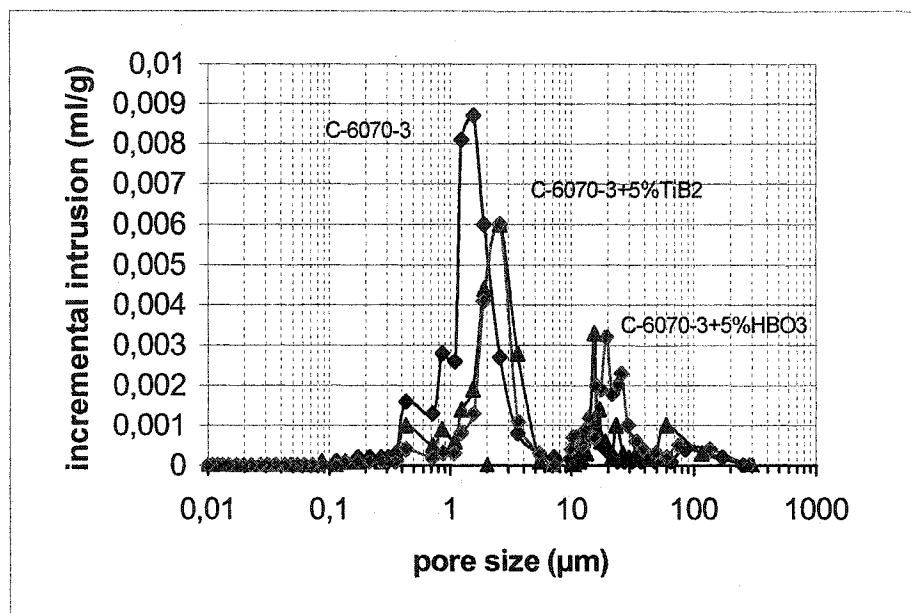


(a) Cumulative Intrusion vs. Pore Size

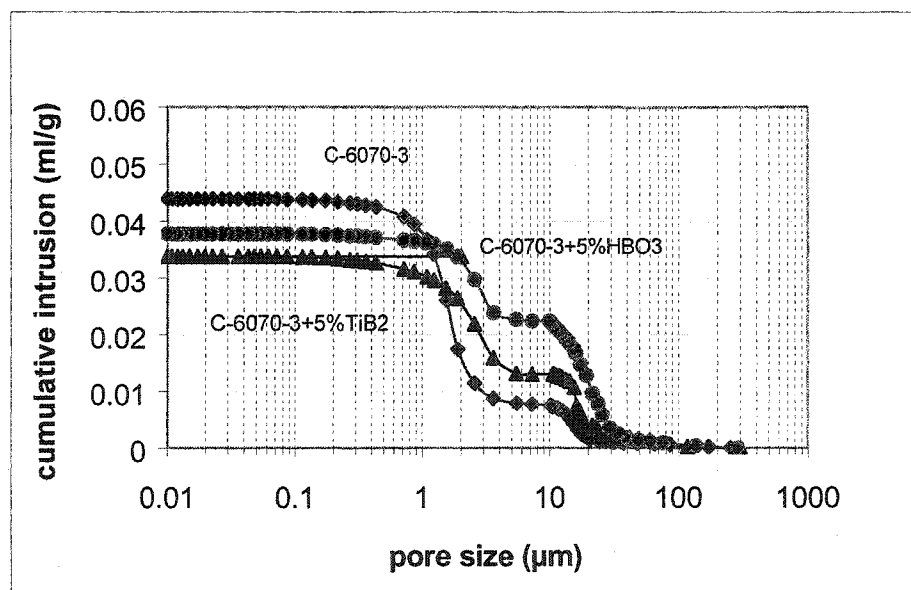


(b) Incremental Intrusion vs. Pore Size

Figure 3.1.3: Pore Size Distribution for C-7080-4 With or Without Additives

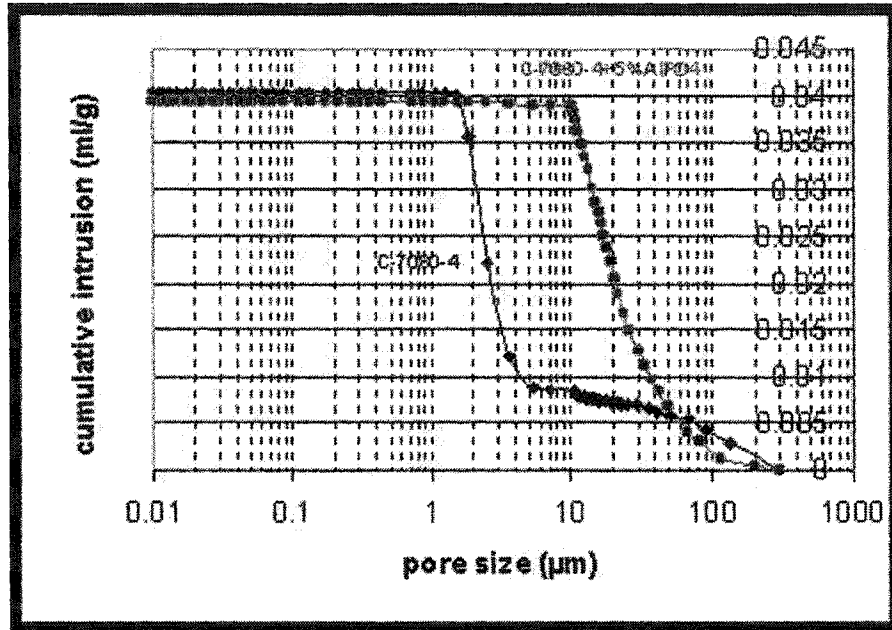


(a) Cumulative Intrusion vs. Pore Size

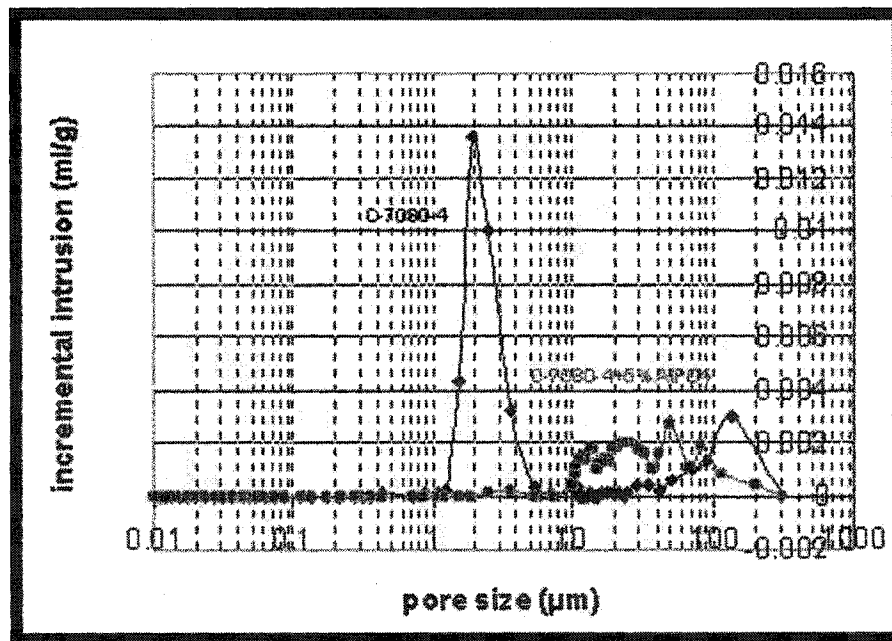


(b) Incremental Intrusion vs. Pore Size

Figure 3.1.4: Pore Size Distribution for C-6070-3 With or Without Additives



(a) Cumulative Intrusion vs. Pore Size



(b) Incremental Intrusion vs. Pore Size

Figure 3.1.5: Pore Size Distribution for C-6070-3 With or Without AlPO_4

C-7080-4+5%AlPO₄ displays a similar volume of pores in Figure 3.1.5, indicating a similar open structure with C-7080-4. However, in case of with AlPO₄, there are bigger pores, indicating a more open pores microstructure. Figure 3.1.5 (b) illustrates a C-7080-4+5%AlPO₄ has larger open pores than C-7080-4. The medium pore diameter of C-7080-4+5%AlPO₄ is around 11 μm while the medium pore diameter of original castable C-7080-4 is only 1-2 μm. This is attributed to the looser packing caused by the inclusion of 5%AlPO₄ in substitution of the original similar grain sized matrix.

The pore size of the refractory is the most important parameter governing the metal intrusion into the refractory open pore structure.

It is shown that refractory material open porosity and pore size distribution are of key importance with respect to the penetration and reaction mechanisms of molten aluminum and refractories. The wetting of the refractories and physical properties like porosity and pore size distribution of the refractories determine the extent of the aluminum contact and infiltration^[41,66].

Some researchs^[21,22,23] indicate that when pore diameter exceeds 1-2μm, aluminium penetration and subsequent reactions between metal and refractories occur. Aluminio-silicate refractories can be made to resist aluminium attack when the pore radius of the material is kept below 0.5-1.0μm.

Adding AlPO₄ results in enlarging open pores. On the other hand, AlPO₄ play key roles in resisting to corundum corrosion. This also implies that pore size and volume of pores are not effective on resisting to corundum corrosion.

Pore Size Distribution Analysis can not explain well on why boron-base and phosphorus-base additives show better corundum corrosion resistance. Further research is to be done to clarify the corrosion resistance mechanism.

3.1.3.4. X-Ray Diffraction Analyses

As shown in Table 3.1.3, boron-bearing castables have a common new phase after being fired at 1200°C for 5 hours. It is aluminum borate ($9\text{Al}_2\text{O}_3 \cdot 2\text{B}_2\text{O}_3$).

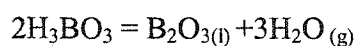
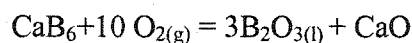
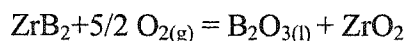
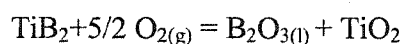
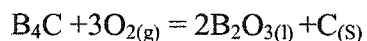
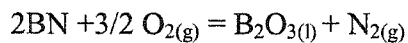
Table 3.1.3: Mineralogical Phases Analysis for C-6070-3 Samples

Phases	C-6070-3	C-6070-3+5%B ₄ C	C-6070-3+5%B ₂ O ₃	C-6070-3+5%TiB ₂
Mullite($3\text{Al}_2\text{O}_3 \cdot 2\text{SiO}_2$)	major	major	major	major
Corundum(Al_2O_3)	minor-major	minor	minor	minor
Celsian($\text{BaO} \cdot \text{Al}_2\text{O}_3 \cdot \text{SiO}_2$)	minor-major	trace?	trace	trace
Kyanite($\text{Al}_2\text{O}_3 \cdot \text{SiO}_2$)	trace?			
Zircon($\text{ZrO}_2 \cdot \text{SiO}_2$)	minor	minor-major	minor-major	minor-major
Zirconia(ZrO_2)	trace			trace
Baddeleyite(ZrO_2)				
Cristobalite(SiO_2)	minor-major	minor	minor	minor-major
$9\text{Al}_2\text{O}_3 \cdot 2\text{B}_2\text{O}_3$			trace-minor	
$4\text{Al}_2\text{O}_3 \cdot \text{B}_2\text{O}_3$		trace?		minor
Rutile(TiO_2)	trace	trace	trace	trace
Amorphous		trace-monor	trace	

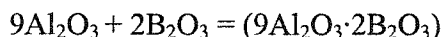
During the sintering process, Al_2O_3 reacts with B_2O_3 coming from boron-bearing additives oxidation to form needle shaped ($9\text{Al}_2\text{O}_3 \cdot 2\text{B}_2\text{O}_3$) crystals. It is possible that this new phase helps in resisting corundum attack.

In the equilibrium system Al_2O_3 - B_2O_3 , there are only two new phases, ($9\text{Al}_2\text{O}_3 \cdot 2\text{B}_2\text{O}_3$) and ($2\text{Al}_2\text{O}_3 \cdot \text{B}_2\text{O}_3$). It has been accepted here that ($4\text{Al}_2\text{O}_3 \cdot \text{B}_2\text{O}_3$) is ($9\text{Al}_2\text{O}_3 \cdot 2\text{B}_2\text{O}_3$).

Boron-bearing compounds oxidation occurs, forming B_2O_3 as shown by following reactions:



These reactions are followed by the formation of the aluminum borate ($9\text{Al}_2\text{O}_3 \cdot 2\text{B}_2\text{O}_3$) whose crystallization increases the volume occupied by Al_2O_3 and B_2O_3 of about 9%:

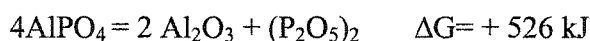


B_4C and B_2O_3 can reduce slag penetration resistance in Al_2O_3 - SiO_2 - SiC - C refractory^[12].

It is considered that it result from formation of a more fluid boron-containing liquid.

Similarly, it is assumed that formation of a more fluid boron-containing liquid and new phase ($9\text{Al}_2\text{O}_3 \cdot 2\text{B}_2\text{O}_3$) or ($4\text{Al}_2\text{O}_3 \cdot \text{B}_2\text{O}_3$) are responsible for Al penetration resistance.

Based on the FactSage thermodynamic calculation, it is deduced that the following reactions can not occur at 1200°C.



It is confirmed that AlPO_4 cannot be decomposed, as XRD results show.

Table 3.1.4: Mineralogical Phases Analysis for C-7080-4 Samples

	C-7080-4	C-7080-4 +5%B ₄ C	C-7080-4 +5%ZrB ₂	C-7080-4 +5%BN	C-7080-4 +5%CaB ₆	C-7080-4 +5% AlPO ₄
Mullite (3Al ₂ O ₃ ·2SiO ₂)	major	major	major	major	major	major
Corundum (Al ₂ O ₃)	major	major	major	major	major	major
Kyanite (Al ₂ O ₃ ·SiO ₂)		trace?				

Zircon (ZrO ₂ ·SiO ₂)			minor- major			
Baddeleyite (ZrO ₂)			minor			
Cristobalite (SiO ₂)	minor- major	minor	minor- major	minor- major	minor	minor- major
9Al ₂ O ₃ ·2B ₂ O ₃		trace- minor	trace-minor	trace?	trace- minor	
4Al ₂ O ₃ ·B ₂ O ₃			trace-minor			
Anorthite(CaO· Al ₂ O ₃ ·2SiO ₂)	minor			trace	trace	
Rutile(TiO ₂)		trace	trace	trace	trace	trace
Amorphous			trace			trace
Aluminum Phosphate (AlPO ₄)						minor- major

3.1.3.5. Micrograph Analyses (OM, SEM)

Two types of corundum forms through corundum corrosion test at 1200°C. Direct oxidization corundum through $\text{Al(s)} + \text{O}_2 = \text{Al}_2\text{O}_3\text{(s)}$, and re-ox reaction corundum is from equation $3\text{SiO}_2\text{(s)} + 4\text{Al(l)} = 2\text{Al}_2\text{O}_3\text{(s)} + 3\text{Si(s)}$ or $3(3\text{Al}_2\text{O}_3 \cdot 2\text{SiO}_2)\text{(s)} + 8\text{Al(l)} = 13\text{Al}_2\text{O}_3\text{(s)} + 6\text{Si(s)}$.

Figure 3.1.6 displays refractory corrosion area. New corundum formation after re-ox reaction results in forming cracks and pores due to volume changes (decrease). Corundum through direct oxidization corundum forms loose and layered structure

(Figure 3.1.8). There is an obvious interface between direct oxidization corundum and re-ox reaction corundum (Figure 3.1.9, Figure 3.1.13, and Figure 3.1.21).

Figure 3.1.19, Figure 3.1.20, Figure 3.1.24, Figure 3.1.26, Figure 3.1.27, Figure 3.1.28, and Figure 3.1.32 illustrate the presence of new phase in pores of boron-bearing refractory. It looks like a transparent glass fiber, supposed to be $9\text{Al}_2\text{O}_3\cdot 2\text{B}_2\text{O}_3$ or $\text{Al}_2\text{O}_3\text{-SiO}_2\text{-B}_2\text{O}_3$ glass fiber.

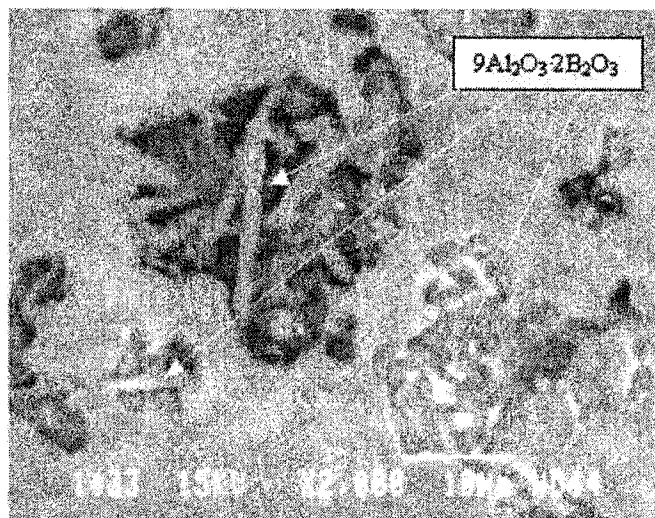


Figure 3.1.6: SEM Observation Shows $9\text{Al}_2\text{O}_3\cdot 2\text{B}_2\text{O}_3$ (needle like)
in C-7080-4+5%CaB₆ Sample After 1200°C×5hrs

Rarely, needle like $9\text{Al}_2\text{O}_3\cdot 2\text{B}_2\text{O}_3$ is focused through SEM as shown in Figure 3.1.6, which represents C-7080-4+5%CaB₆ sample after 1200°C×5hrs.

The corrosion process takes place via various mechanisms including oxidation of molten aluminium in direct contact with oxygen from air (formation of corundum), molten aluminium infiltration through corundum and refractory-aluminium reactions. These

three processes occur simultaneously. The overall result is dictated by a large number of variables including the furnace atmosphere (P_{O_2}) and temperature; the chemical and mineralogical composition of the refractory; its porosity, density and permeability.

Infiltration by Metal Aluminium

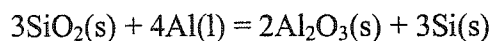
The degree to which the refractory is infiltrated by molten aluminium depends strongly on the furnace temperature and atmosphere, as well as on the composition of the aluminium melts itself. Above 1100°C, molten aluminium wets both mullite, an essential compound of alumino-silicate and high-alumina refractory lining^[42].

Figure 3.1.19 shows molten aluminium goes through the area where corundum is formed by direct oxidation. Figure 3.1.20 and 3.1.23 display corundum corrosion occur after molten aluminum penetration.

Corrosion of refractory sample at more than 1200°C arises from contact of the sample with molten aluminium infiltrating through corundum. Molten Al penetrates through re-ox reaction corundum (shown in Figure3.1.21), and stops at a pore where corundum through direct metal oxidation is formed (Figure 3.1.23 and Figure 3.1.26). Figure3.1.33 indicates clearly this situation.

Reduction Oxidation Reactions

Silica (SiO_2) and mullite ($3Al_2O_3 \cdot 2SiO_2$), which are the two major components of the refractory matrix, and silica-rich vitreous phases, are reduced upon contact with molten aluminium or its alloys and decompose at higher temperatures through the following reactions:



The standard Gibbs energies (ΔG°) of above Equations are highly negative ($\Delta G^\circ_{1500K} = -460kJ$ and $-865kJ$, respectively).

The solubility of Si in molten aluminium is temperature dependent. Upon contact with the refractory lining, the aluminium saturates with silicon and causes it to precipitate as metal silicon.

All these reactions are strongly exothermic and expansive, and involve the formation of gaseous intermediates phases such as SiO, AlO and AlO₂, so that the reducing atmosphere and high temperature of the furnace highly accelerates their kinetics^[43].

Volume changes associated to these reactions lead to the formation of differential diffusion channels inside the molten metal-ceramic compound, which favours the corrosion process.

Figure 3.1.10, Figure 3.1.11, Figure 3.1.13, Figure 3.1.14, Figure 3.1.15, Figure 3.1.16, Figure 3.1.18, Figure 3.1.20, Figure 3.1.22, Figure 3.1.25, Figure 3.1.29 and Figure 3.1.30 show attacked areas and unaltered areas.

Research into corrosion mechanisms has traditionally been focused on correlating available data for physical (density, porosity, and permeability), chemical and mineralogical properties of the material with its service life.

Several researches prove that phosphoric acid-bonded castables show minimal deterioration after two years of continuous operation^[5,67,68].

Here, AlPO₄ is used as additive. Figure 3.1.21 shows sample after corrosion by molten aluminum. Alumino-silicate refractories have been transformed to porous corundum composites.

Figure 3.1.32, Figure 3.1.33 and Figure 3.1.34 indicate interface between corroded areas and un-corroded areas in different magnification.

It is very interesting that glass fiber is also found in pores of C-7080-4+5%AlPO₄ sample. It's mineral phases are yet to be determined.

3.1.4. Conclusions

The corundum corrosion tests have been conducted at 1200°C in an air atmosphere in order to clarify the effect of boron-bearing compounds and AlPO_4 on the resistance of corundum attack for Al_2O_3 - SiO_2 castables.

No direct relationship can be observed between the apparent porosity, density and resistance to molten aluminium or corundum corrosion.

Boron-bearing additives do not apparently change pore size distribution. Adding AlPO_4 results in pore size enlarger, but the volume of pores does not change.

By addition of BN, B_4C , ZrB_2 , TiB_2 , CaB_6 and AlPO_4 5mass%, to Al_2O_3 - SiO_2 castables, C-7080-4 and C-6070-3, the corundum corrosion extent decreases dramatically.

$9\text{Al}_2\text{O}_3 \cdot 2\text{B}_2\text{O}_3$ is formed when boric compounds are used as additives in Al_2O_3 - SiO_2 castables.

In case of AlPO_4 , there is no new phase formation. AlPO_4 cannot be decomposed and does not react with SiO_2 .

Both penetration and oxidation-reduction reaction have a great impact on corrosion.

Boron-bearing and phosphorus-bearing additives do not react with SiO_2 and the mechanism of these additives protecting alumino-silicate refractories from molten aluminium or corundum is further to be studied.



Figure 3.1.7:
C-6070-3 new corundum after ox-re

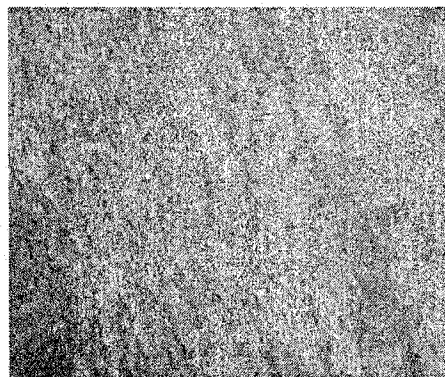


Figure 3.1.8:
C-6070-3 direct oxidation
corundum layer structure

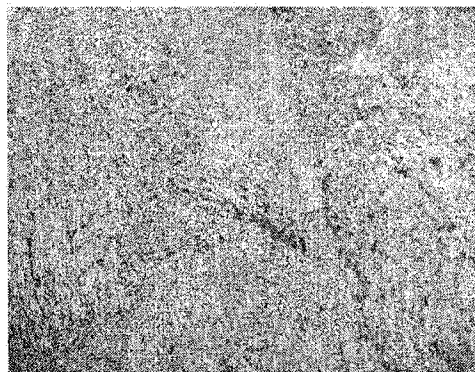


Figure 3.1.9:
C-6070-3 area between direct oxidation
corundum (left) and ox-re corundum (right)

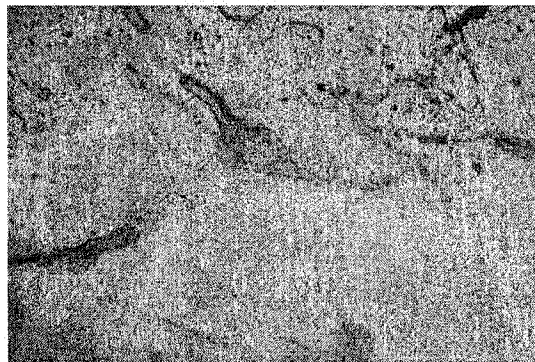


Figure 3.1.10:
C-6070-3 refractory attacked by
corundum and molten Al



Figure 3.1.11:
C-6070-3+5%TiB₂ corroded area with
more pores and cracks(dark area)
and regular (bright area)

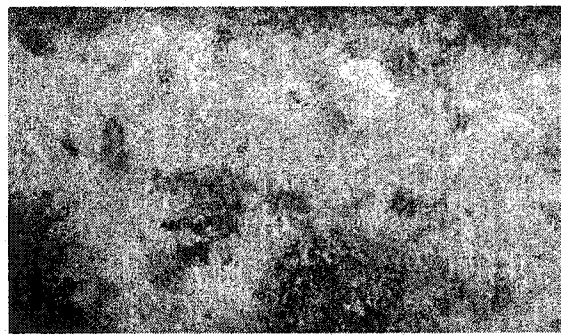


Figure 3.1.12:
C-6070-3+5%TiB₂
oxidized area (matrix,black)
and regular (white big grain)

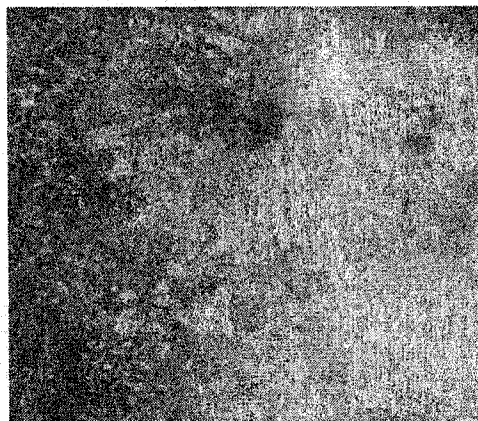


Figure 3.1.13:
C-7080-4 Refractory(right) corroded
by corundum(left) $\times 5$

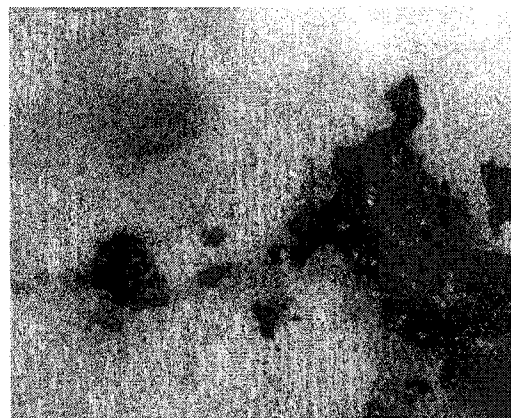


Figure 3.1.14:
C-7080-4 Refractory corroded
by corundum(black) $\times 10$

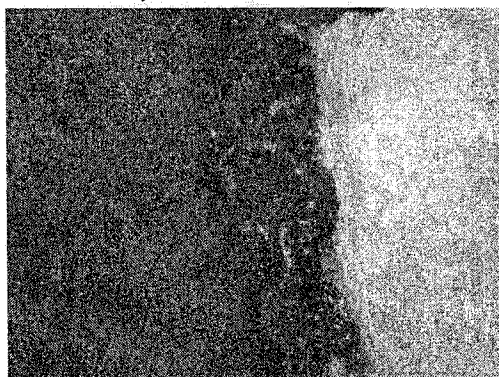


Figure 3.1.15: C-7080-4+5%ZrB₂
Refractory corroded by corundum(black) $\times 10$
Left: direct oxidized corundum
Middle: re-ox reaction corundum
Right: original refractory



Figure 3.1.16: C-7080-4+5%ZrB₂
Refractory corroded
by corundum(black) $\times 20$

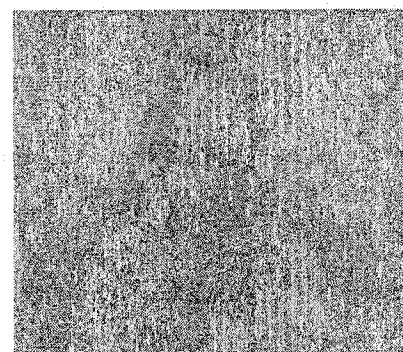
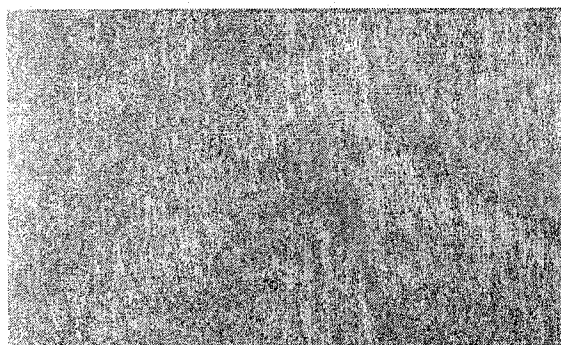


Figure 3.1.17: (a) (b) C-7080-4+5%ZrB₂ New phase---glass fiber $\times 50$

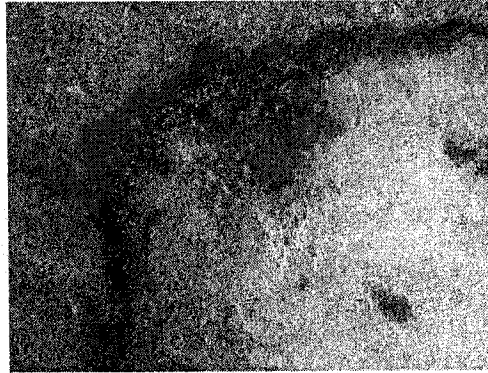


Figure 3.1.18 : C-7080-4+5%CaB₆
Refractory corroded by corundum ×10
Left: direct oxidized corundum(dark);
Middle: re-ox reaction corundum(black)

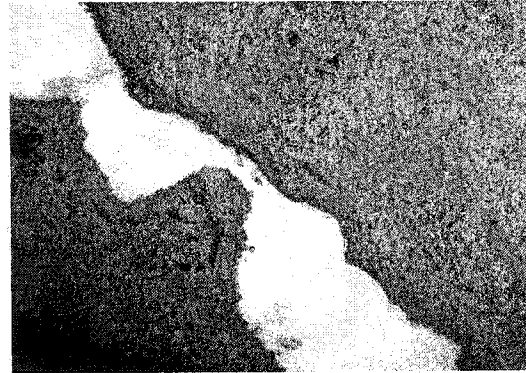


Figure 3.1.19 : C-7080-4+5%CaB₆
Molten Al goes through corundum ×10

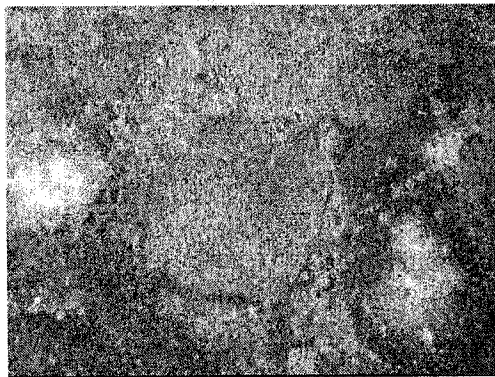


Figure 3.1.20: C-7080-4+5% B₄C
Refractory corroded
by corundum(more pores) ×50



Figure 3.1.21: C-7080-4+5%CaB₆
Refractory corroded by corundum ×100
Molten Al goes through channel and
attacks inside refractory

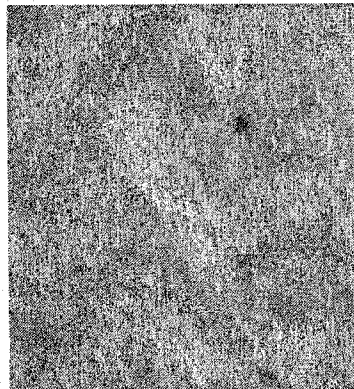


Figure 3.1.22: C-7080-4+5%CaB₆
New phase---glass fiber ×500



Figure 3.1.23: C-7080-4+5%B₄C
Molten Al penetrates through
capillary channel and new phase
(glass fiber) grows ×200

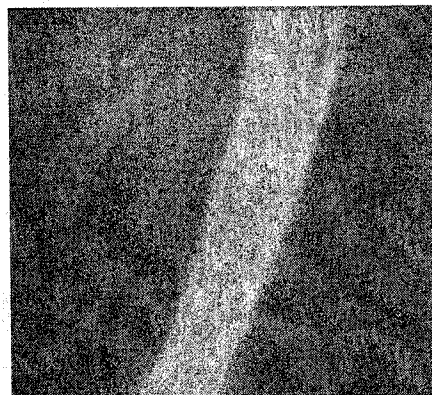
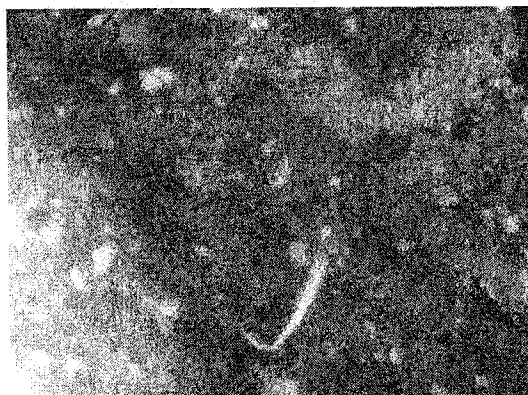


Figure 3.1.24: C-7080-4+5%B₄C New phase---glass fiber is formed (a)×20 (b)×100

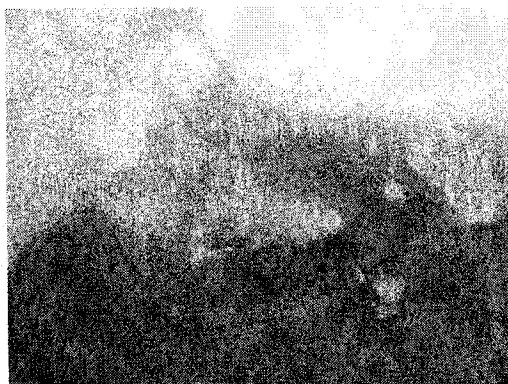


Figure 3.1.25: C-7080-4+5%BN
Refractory corroded by corundum
Molten Al penetrates through re-ox reaction
corundum, and stops at a pore.
Bottom: re-ox reaction corundum;
Middle: direct oxidized corundum(black) ×500

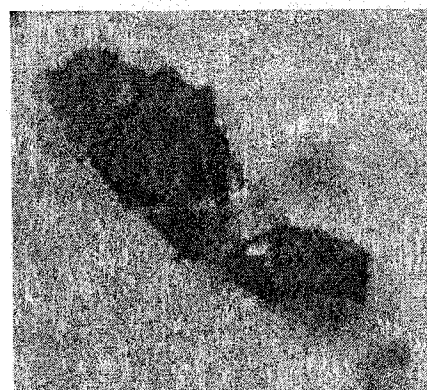


Figure 3.1.26: C-7080-4+5%BN
Corundum is formed in a
closed pore ×200



Figure 3.1.27: C-7080-4+5%BN
contaminated refractory inside
(caused by molten Al penetration) ×100

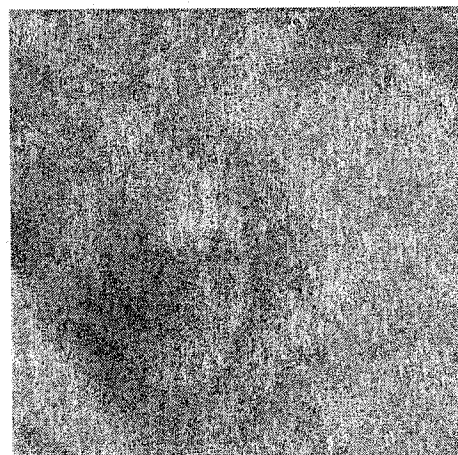


Figure 3.1.28: C-7080-4+5%BN
New phase is formed in a pore ×500

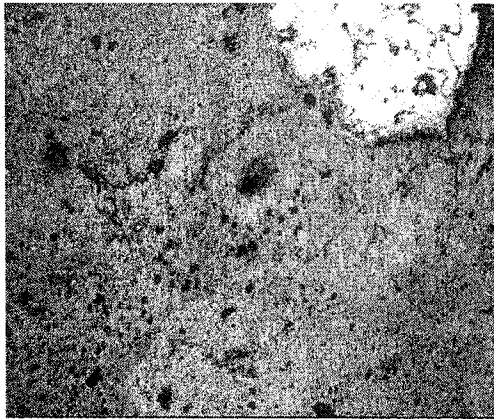


Figure 3.1.29: C-7080-4+5%B₄C
Refractory corroded by corundum and molten Al
Direct oxidized corundum(upper left)
re-ox reaction corundum(lower left and lower right,
more pores), molten Al(upper right,light) ×50

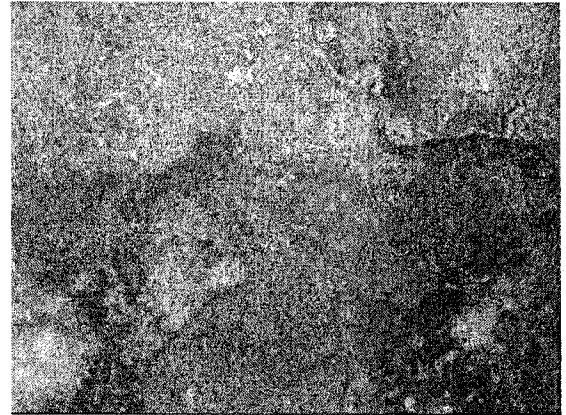


Figure 3.1.30: C-7080-4+5%B₄C
Refractory corroded by
corundum and molten Al ×100

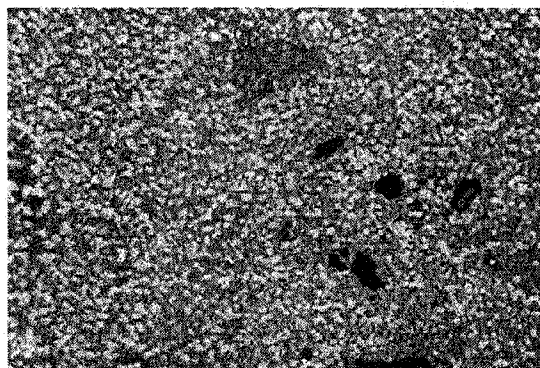


Figure 3.1.31: C-7080-4+5%AlPO₄
Ox-Re Reaction Corundum Area ×50

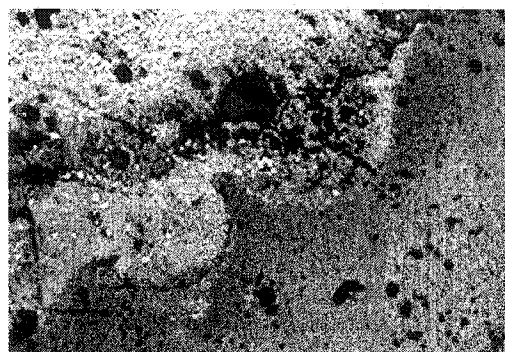


Figure 3.1.32: C-7080-4+5%AlPO₄
Interface between Corroded
area and Un-corroded area ×10

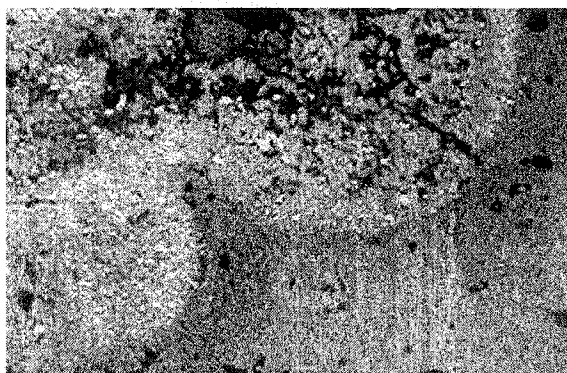


Figure 3.1.33: C-7080-4+5%AlPO₄
Interface between Corroded
area and Un-corroded area ×20

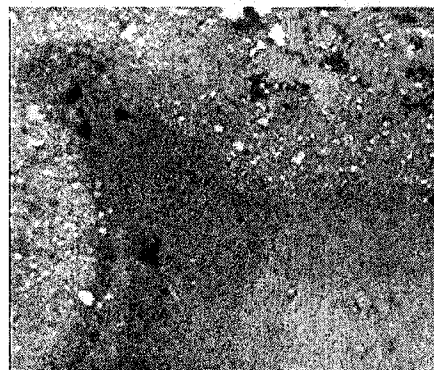


Figure 3.1.34: C-7080-4+5%AlPO₄
Interface between Corroded
area and Un-corroded area ×50

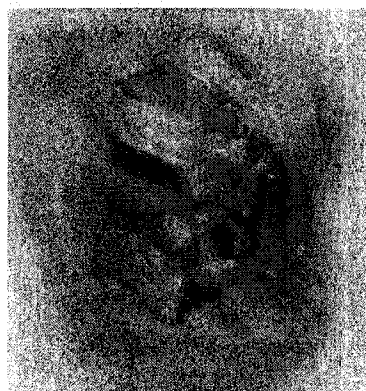


Figure 3.1.35: C-7080-4+5%AlPO₄
Interwine glass fiber in a pore ×20



Figure 3.1.36: C-7080-4+5%AlPO₄
Glass fibers in a pore ×20

3.2. Alkaline Earth Metal Oxides and Rare Earth Oxides

3.2.1. Introduction

In order to enhance the corrosion resistance of alumino-silicate castables, some specific additives are generally employed by refractory producers. Among these additives, BaSO_4 and CaF_2 are the most common ones.

An attempt has been made to characterize the proper role of barium sulfate in the protection mechanism of refractories. It has been pointed out that barite, by reacting with alumina and silica among the fine particles of the refractories, forms hexa-celsian and/or celsian in the firing temperature ranging between 900°C to 1200°C . Such transformations reduce the amount of free silica within the matrix and should consequently improve the corrosion resistance of the refractory. However, the protective effect of barium sulfate appeared to be significantly reduced when firing temperatures exceeded 1050°C . Adding CaF_2 favored the anorthite formation. Parallel to corrosion resistance improvement, the amount of anorthite appeared to be increased with firing temperature ^[19,20,21,22]. The efficiency of these additives, to protect the castable, is in their potential role in converting silica to some alumino-silicates based crystalline phases that are more resistant to aluminum attack.

The purpose of this study was to analyse the effect of alkaline earth metal oxides and rare-earth oxides such as BaCO_3 , CaCO_3 , Y_2O_3 , HfO_2 , MgO and dolomite as additives to protect low cement castables against corundum attack at 1200°C for 40 hours.

3.2.2. Experimental Procedures

Experimental procedures are described in section 3.1.2.

3.2.3. Results and Discussion

3.2.3.1. Corrosion Tests

Figure 3.2.1 shows that corundum corrosion resistance of low cement castable with/without oxide-base additives.

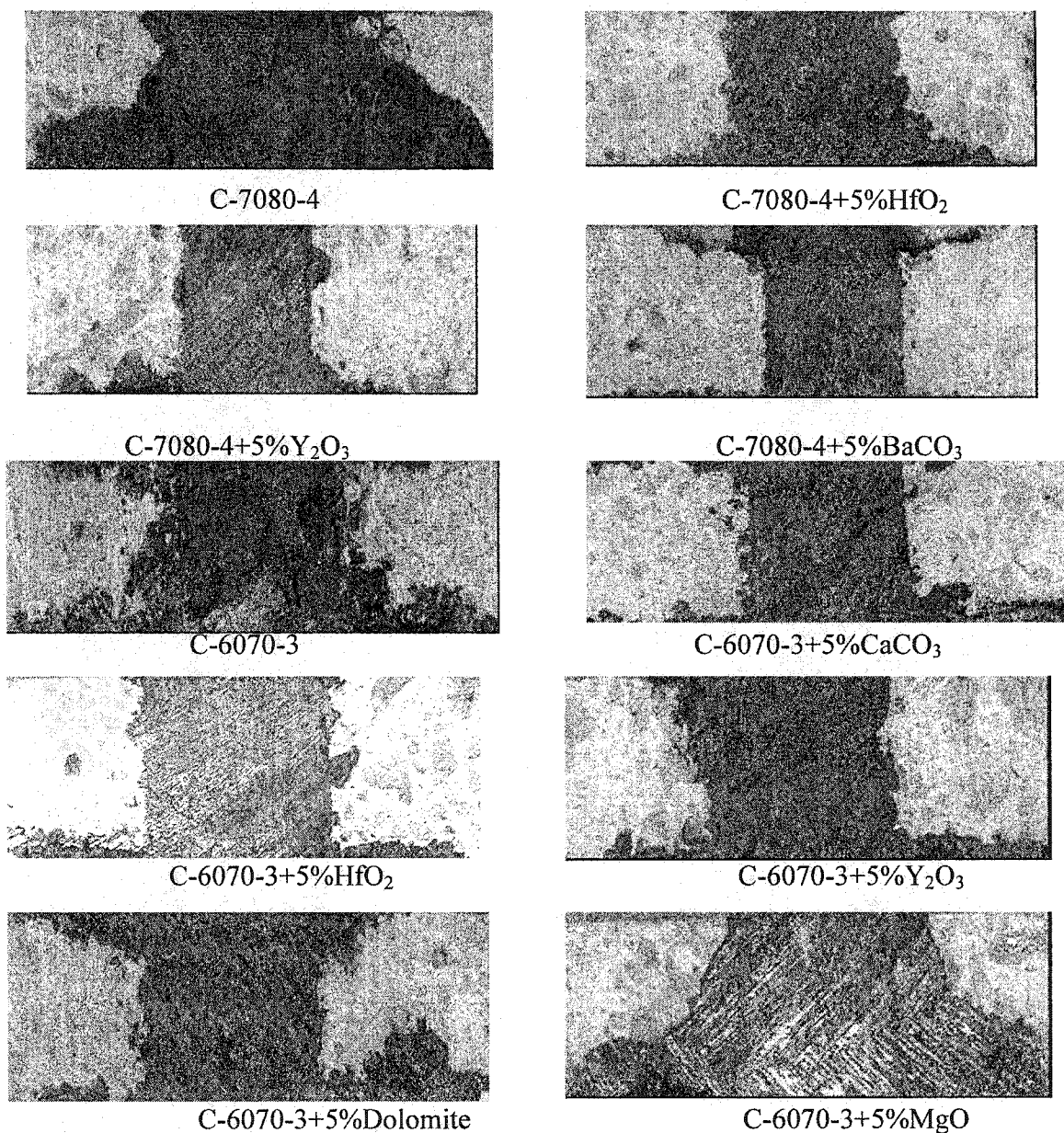


Figure 3.2.1: Corundum Corrosion Resistance of Low Cement Castable
With/Without Oxide-base Additives

It is clear that BaCO_3 , CaCO_3 , Y_2O_3 and HfO_2 are effective additives in aluminosilicate castables. As for dolomite is concerned, it is difficult to show good corundum corrosion resistance. With MgO , the castables show more corrosion than the original castables.

3.2.3.2. Porosity and Density

More water results in porosity rise and density drop in Table 3.2.1. Higher porosity and lower density do not influence the corundum corrosion.

Table 3.2.1: Porosity and Density after 1200°C×5hrs Heat-treatment

Sample	Water (%)	Porosity (%)	Density (g/cm ³)
C-6070-3	5.7	15.9	2.59
C-6070-3+5%CaCO ₃	6.4	20.83	2.41
C-6070-3+5%MgO	9.5	25.88	2.32
C-6070-3+5% Dolomite	9.5	23.12	2.36
C-6070-3 +5%Y ₂ O ₃	5.7	18.56	2.58
C-6070-3+5%HfO ₂	6.0	16.95	2.66
C-7080-4	6.0	17.7	2.63
C-7080-4+5%BaCO ₃	9.5	23.17	2.47
C-7080-4+5%Y ₂ O ₃	6.0	17.98	2.65
C-7080-4+5%HfO ₂	6.0	17.31	2.70

Adding rare-earth oxides Y₂O₃ and HfO₂ to original castables (C-6070-3 and C-7080-4) don't change the density but the porosity increases when the amounts of water are at the same level.

More water is necessary when MgO and/or dolomite were added. Adding CaCO₃, MgO, dolomite and BaCO₃ result in porosity increase and density drop.

Under same water level and same castable base, additive dolomite shows better corundum corrosion resistance than magnesia in Figure 3.2.1. C-7080-4+5%BaCO₃ includes more water, but it shows the best corundum corrosion resistance. C-7080-4+5%CaCO₃, C-7080-4+5%Y₂O₃, and C-7080-4+5%HfO₂ show good corrosion resistance to external corundum growth.

Adding additives change the porosity and density of the castables, but there is no direct relationship between porosity, density and corrosion resistance.

3.2.3.3. Pore Size Distribution

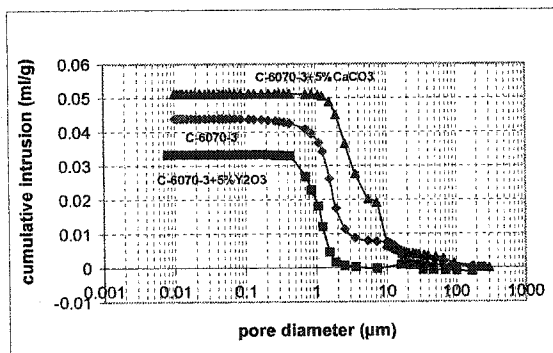


Figure 3.2.2: Pore size distribution for C-6070-3 with or without additive (Cumulative intrusion vs. Pore size)

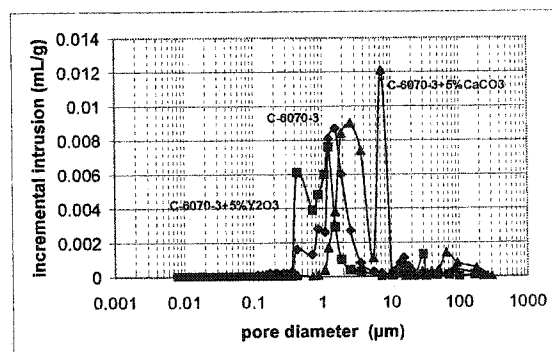


Figure 3.2.3: Pore size distribution for C-6070-3 with or without additive (Incremental intrusion vs. Pore size)

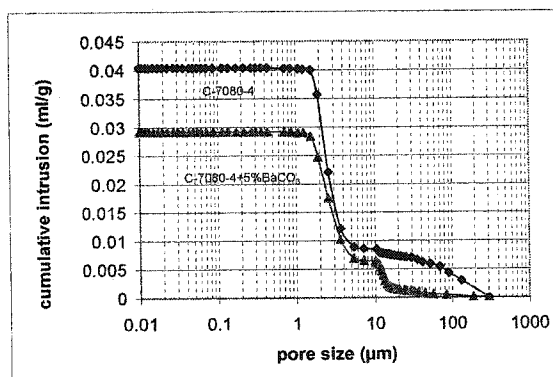


Figure 3.2.4: Pore size distribution for C-7080-4 with or without additive (Cumulative intrusion vs. Pore size)

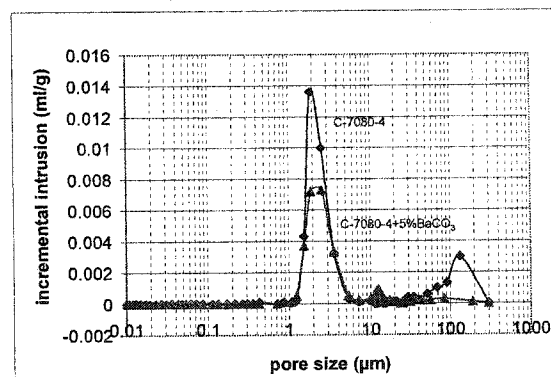


Figure 3.2.5: Pore size distribution for C-7080-4 with or without additive (Incremental intrusion vs. Pore size)

C-6070-3+5%CaCO₃ displays a larger volume of pores in Figure 3.2.2, indicating a more open structure. Figure 3.2.3 illustrates, sample C-6070-3+5%CaCO₃ has a larger open pores than C-6070-3. Contrary to C-6070-3+5%CaCO₃, C-6070-3+5%Y₂O₃ displays a smaller volume of pores, indicating a less open structure.

Figure 3.2.4 and Figure 3.2.5 show a similar trend displayed by with or without BaCO₃ in C-7080-4 castable base. However, in case of castable with BaCO₃, there is a lower total volume of pores, indicating an overall less open microstructure. This occurrence is attributed to higher packing caused by the inclusion of 5%BaCO₃ in mix with same grain size distribution.

Adding CaCO₃ results in enlarging open pores. In case of castable with Y₂O₃ and BaCO₃, there is a lower total volume of pores. Both Y₂O₃, BaCO₃ and CaCO₃ play good role in resisting corundum corrosion. This implies that pore size and volume of pores are not main factors in resisting corundum corrosion.

3.2.3.4. X-Ray Diffraction Analysis

Refractory samples with or without additives are tested after 1200°C for 5hours.

From Table3.2.2, it is observed that when CaCO₃, dolomite and BaCO₃ are used as additives, new phases such as anorthite, spinel and celsian are formed respectively.

When Y₂O₃ is used as additives, new phases of Y₂O₃·SiO₂ are formed.

Based on the FactSage thermodynamic calculation^[56], following reactions are possible at 1200°C.

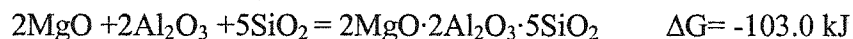
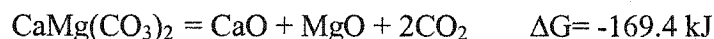


Table 3.2.2: Mineralogical Phases Analysis for C-6070-3 Samples

Phase	C-6070-3	C-6070-3 +5% CaCO ₃	C-6070-3 +5% Dolomite	C-7080-4	C-7080-4 +5% BaCO ₃	C-7080-4 +5%Y ₂ O ₃
Mullite (3Al ₂ O ₃ ·2SiO ₂)	Major	major	major	major	major	major
Corundum (Al ₂ O ₃)	minor- major	major	minor- major	major	major	major
Celsian (BaO·Al ₂ O ₃ · SiO ₂)	minor- major	minor- major	minor		minor	
Kyanite (Al ₂ O ₃ ·SiO ₂)	trace?					
Zircon (ZrO ₂ ·SiO ₂)	Minor	trace				
Zirconia(ZrO ₂)	Trace					
Baddeleyite (ZrO ₂)		Trace- minor	minor			
Cristobalite (SiO ₂)	minor- major	Minor	minor- major	minor- major	minor	Minor- major
Anorthite (CaO·Al ₂ O ₃ ·2SiO ₂)		Trace	trace- minor	minor	trace	trace
Spinel (MgO·Al ₂ O ₃)			Trace?			
Y ₂ O ₃ ·SiO ₂						trace
Rutile (TiO ₂)	Trace	Trace	trace		trace	trace
Amorphous		Minor	trace- minor			

Afshar and Allaire postulated that the efficiency of non-wetting additives, to protect the castable, is in their potential role in converting silica to some alumino-silicates based crystalline phases that are more resistant to aluminum attack.^[20]

Barium carbonate has a melting point of 1350°C, yet it reacts with silica. The formation of barium orthosilicate and metasilicate occurs at temperatures as low as 900°C. If Na₂O is present, these reactions may begin as early as 400°C.^[58]

Some characteristics of HfO₂ are given below: Melting point 2790°C; softening temperatures 1100-1500°C; density 9.7 g/cm³; CTE (250-1300°C) 5.8 x 10⁻⁶/°C. White powder when pure, undergoes monoclinic transition at 1700°C. Chemically resistant but reacts with hydroxides at elevated temperatures. There is a compound between HfO₂-SiO₂, it is HfSiO₄.^[58]

Y₂O₃ reacts with SiO₂ from alumino-silicate castables at elevated temperature, and the product Y₂O₃·SiO₂ has been confirmed by XRD results.

From the view of XRD analysis, it is observed that alkaline earth metal oxides and rare earth oxides react with silica, and new crystalline phases such as anorthite (CaO·Al₂O₃·2SiO₂), barium anorthite (BaO·Al₂O₃·2SiO₂), and Y₂O₃·SiO₂ are formed. This transformation reduces the amount of free silica within the matrix of refractories. Refractory protection is achieved through these new crystalline phases rather than reaction between silica and aluminium metal.

3.2.3.5. Microstructure Analyses (Optical Micrographs)

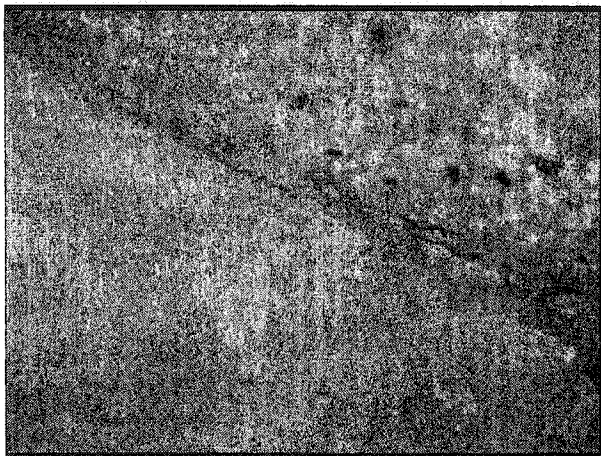


Figure 3.2.6: C-7080-4 + 5%Y₂O₃
Interface between corroded area
and un-corroded area ×20

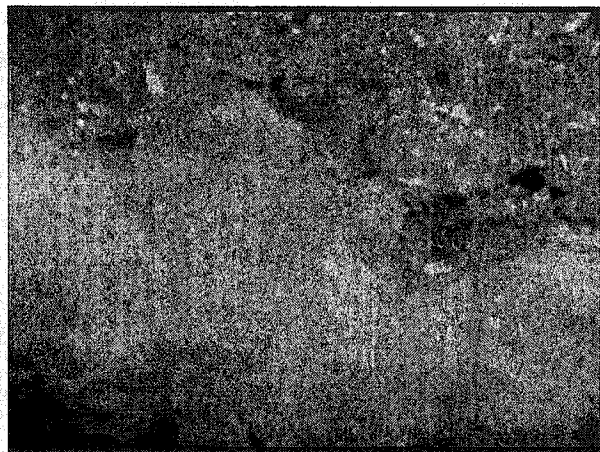


Figure 3.2.7: C-7080-4 + 5%Y₂O₃
Interface between corroded area
and un-corroded area ×50

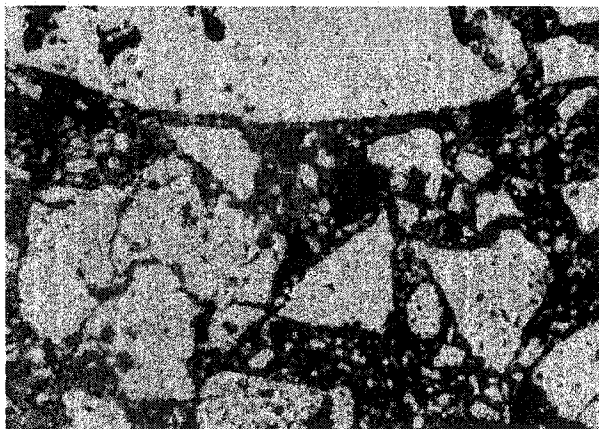


Figure 3.2.8: C-7080-4+5%BaCO₃ ×50

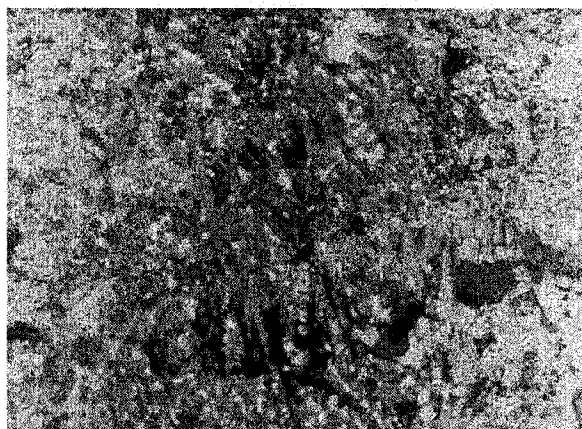


Figure 3.2.9: C-7080-4+5%BaCO₃
Corroded Area ×50

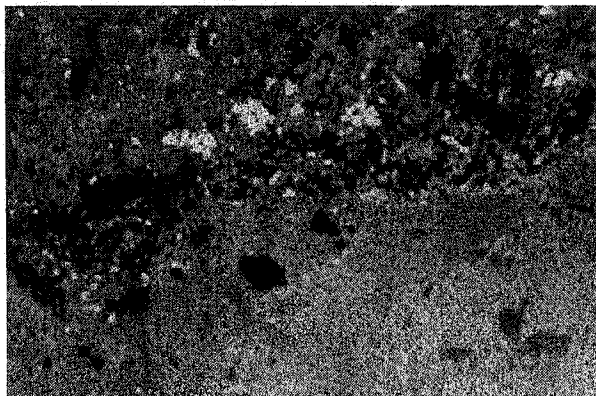


Figure 3.2.10: C-6070-3-5%CaCO₃
Interface between corroded area
and un-corroded area ×20

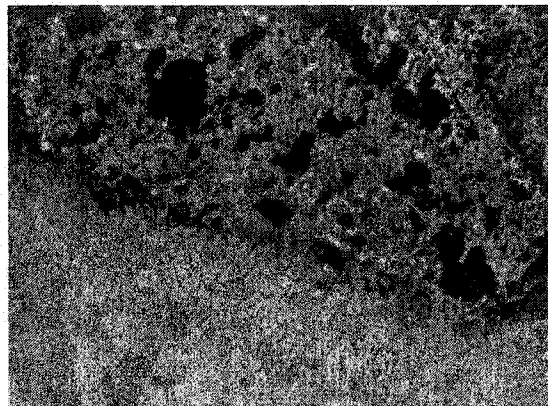


Figure 3.2.11: C-6070-3-5%CaCO₃
Interface between corroded area
and un-corroded area ×50

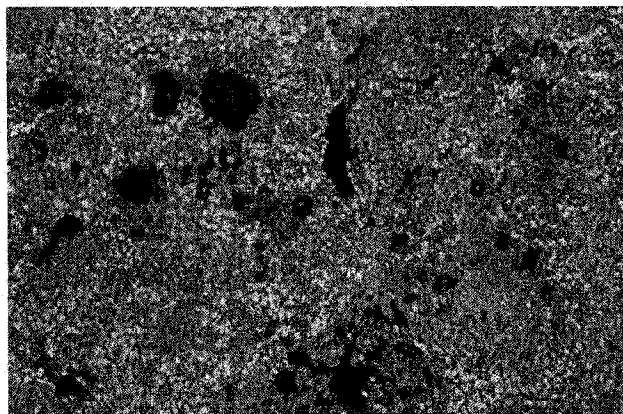


Figure 3.2.12: C-6070-3+5%Dolomite
Corroded Area ×20

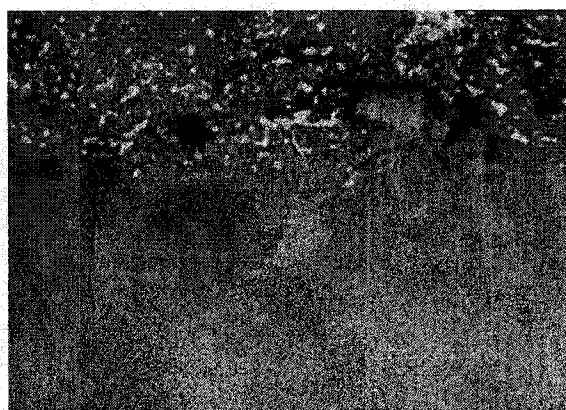


Figure 3.2.13: C-6070-3+5%Dolomite
Interface Between Corroded Area
and Un-corroded Area ×50

There is an interface between corroded zone and uncorroded zone, and the corroded zone is more porous than the original uncorroded zone, as shown in Figure 3.2.6,7, 10,11,12,13.

The corroded zone is heterogeneous, and has a loose structure (compare Figure3.2.8 and Figure3.2.9)

Corrosion involves a combination of different mechanisms, such as dissolution and invasive penetration (where diffusion, grain boundary, and stress corrosion may all be present), and oxidation-reduction reactions (where absorption, adsorption, and mass transport phenomena all come into play) ^[59].

These microstructural pictures also imply that oxidation-reduction reaction is the main factor that results in corrosion for alumino-silicate castables containing alkaline earth metal oxides and rare earth oxides.

3.2.3.6. Thermodynamic and Kinetic Analysis

Selection of additives of alumino-silicate refractories to be used for aluminium foundry furnaces is often done on the basis of thermodynamic equilibrium diagram. For example, an Ellingham diagram is looked at to check whether a given oxide could be reduced by molten aluminium, but magnesia should be stable, as well as calcia (Figure 3.2.14). Actually, this is not always true.

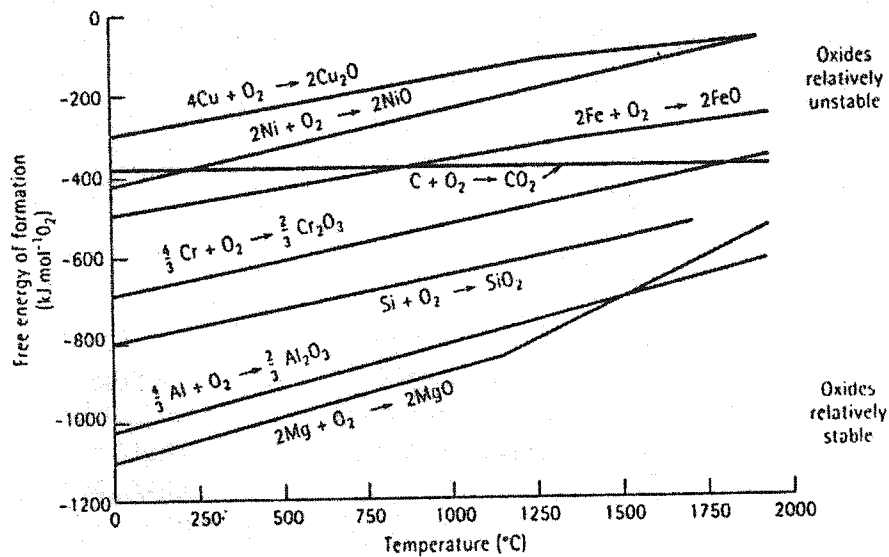


Figure 3.2.14: Ellingham Diagram for Oxides

It has been shown in Figure 3.2.1, that metallic Al-5%Mg-5%Zn alloy infiltrates and corrodes C-6070-3+5%MgO sample.

Magnesia does not play a role in resisting molten Al alloy or corundum under this test condition.

Here the real cause that lies behind the metal infiltration is the solid volume reduction during the corrosion reaction: to 11.255 cm³ (molar volume) of MgO, correspond only 9.941 cm³ of spinel. Transformation of MgO into MgAl₂O₄ can be described in the following manner:

--dissolution of magnesia by molten aluminium: $\langle \text{MgO} \rangle = [\text{Mg}^{2+}] + [\text{O}^{2-}]$

--partial reduction of Mg²⁺ by aluminium: $3[\text{Mg}^{2+}] + 2\{\text{Al}\} = 3[\text{Mg}] + 2[\text{Al}^{3+}]$

--precipitation of spinel from dissolved species: $[\text{Mg}^{2+}] + 2[\text{Al}^{3+}] + 4[\text{O}^{2-}] = \langle \text{MgAl}_2\text{O}_4 \rangle$

To conclude, the reaction rim thickness depends on the diffusion rate of magnesium dissolved in infiltrated aluminium, out of the cracks^[57].

3.2.4. Conclusions

Alkaline earth metal oxides such as BaCO_3 , CaCO_3 and dolomite, and rare earth oxides such as Y_2O_3 and HfO_2 are effective additive for aluminosilicate castables C-7080-4 and C-6070-3 to resist to corundum corrosion when the test temperature is 1200°C .

Alkaline earth metal oxides and rare earth oxides can react with silica, and new crystalline phases such as anorthite ($\text{CaO}\cdot\text{Al}_2\text{O}_3\cdot 2\text{SiO}_2$), barium anorthite ($\text{BaO}\cdot\text{Al}_2\text{O}_3\cdot 2\text{SiO}_2$), and $\text{Y}_2\text{O}_3\cdot\text{SiO}_2$ are formed. This transformation reduces the amount of free silica within the matrix of refractories. Refractory protection is achieved through these new crystalline phases rather than reaction between silica and aluminium metal.

Magnesia does not play a role in resisting to molten Al alloy or corundum under this test condition even though Ellingham diagram shows magnesia is more stable than alumina. Transformation of MgO into MgAl_2O_4 should be responsible for this phenomenon.

Oxidation-reduction reaction is the main factor which results in corrosion for aluminosilicate castables containing alkaline earth metal oxides and rare earth oxides.

Adding additives can change the porosity and density of the castables, but there is no direct relationship between porosity, density and corrosion resistance.

Pore size and volume of pores are not main factors of refractory castables in corundum formation.

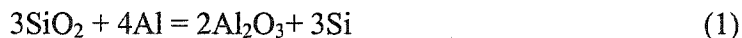
CHAPTER 4: THE CORROSION RESISTANCE OF SILICA GLASSES TO MOLTEN ALUMINUM

4.1. Introduction

Launder lining castable is main refractory in launder system. Launder system products include launder lining castable refractory, trough socks and filtration for wash reduction, gasket, rope and tadpole seals.

Fused silica refractory castable with optimized packing density results in a high strength and erosion resistant material. High thermal shock resistance at high service temperatures, smooth cast surface, preheating unnecessary and easily cleaned are other advantages of such refractory materials. For these characteristics, the fused silica refractories found several applications in aluminum industry, including launder linings, transfer and stub troughs, filter boxes, control pins and furnace tubes.

However, the low chemical resistance of silica against aluminum attack represents the major inconvenience in the use of such refractory products. Indeed, as it is well known, liquid aluminum reduces silica to a metallic state along with the conversion of aluminum to corundum. This type of reaction can be represented as



The conversion of alumino-silicate refractories, also referred to as corrosion, can cause several problems, such as a sharp decrease in the mechanical properties of the refractory, contamination of the molten bath, aluminum loss and enormous heat loss. That is why several attempts have been focused to improve the resistance of the refractories to aluminum attack and penetration.

This chapter presents results regarding the effect of sodium, phosphorus and boron in silica glasses on their resistance to corrosion by Al-5%Mg-5%Zn alloy. The results are profitable to develop potential building material for launders, which should be inert to molten aluminum and its alloys, and offer outstanding non-wetting additives improving the chemical resistance of castables at elevated service temperatures.

4.2. Materials and Properties

Three kinds of material were prepared in laboratory as follows:

I - A typical soda-lime glass (window glass)

This starting material is designated below as W-glass.

Composition:

70% SiO₂, 10% CaO, 15% Na₂O, 5% MgO/Al₂O₃

It was prepared by heating a mixture of silica (SiO₂), Na₂CO₃ and CaCO₃ in a furnace at 1400°C:



Properties:

It is not a very expensive kind of glass. It is easy to work. It breaks and gets scratched easily. It has a low melting/softening point.

Uses:

Bottles, windows, flat glass sheets.

II - Boron-bearing glass

Compositions:

It is a mixture of borosilicate. It is usually prepared from silica, boron oxide (B₂O₃), aluminum oxide (Al₂O₃) and sodium oxide (Na₂O). Three following compositions was used in this work:

- 1: a typical chemical composition of Pyrex glass: 80% SiO₂, 13% B₂O₃, 4% Na₂O, 3% Al₂O₃;
- 2: 5g B₂O₃ with 5g SiO₂ sand;
- 3: 4g B₄C with 8g W-glass (window glass).

Properties (Pyrex):

It has high temperature strength, low coefficient of thermal expansion, good thermal shock resistance, high softening temperature and bears high temperature.

Uses (Pyrex):

Cooking, chemical glassware, laboratory wares, beakers, test tube, flask etc.

III- Phosphorus-bearing glass

The following mixes were prepared:

- 1: 8g W-glass and 4g P₂O₃ powder;
- 2: 3g P₂O₅ and 6g fumed silica
- 3: 4g Bone Ash (Tri-calcium phosphate: Ca₃(PO₄)₂) with 8g W-glass;
- 4: 3g AlPO₄ with 6g W-glass.

4.3. Test and Results

Each glass powder was put inside an alumina crucible with the addition of 10g of Al-5%Mg-5%Zn alloy (as solid pieces) on top of it.

Figure 4.1 to 4.8 show the results after heating at 1200°C and keeping at this temperature for 40 hours.

Soda-lime glass totally reacted with Al alloy (Figure 4.1). New phases are formed and most of them are corundum. Soda-lime glass is not found any more in the crucible. The light dark grain shown in left lower part of Figure 1 is solid silicon resulting from corrosion reactions.

There is a clear interface between Pyrex glass and corundum from the oxidation of Al-5%Mg-5%Zn alloy (Figure 4.2). This layer has a dark appearance and its thickness is about 2-3mm. This interfacial layer is analyzed by scanning electron microscope in order to verify the presence of aluminum attack (see Figures 4.9 to 4.12).

Figure 4.3 shows SiO_2 -- B_2O_3 mixture and Al alloy after heat-treatment. A milky white, high viscosity liquid has formed, with drastic expansion. On the right side of the figure, there is opal SiO_2 and B_2O_3 liquid mixture. It seems that there is no corrosion reaction between SiO_2 -- B_2O_3 mixture and Al alloy or its oxides.

Figure 4.4 illustrates B_4C and window glass mixture in contact with the aluminum alloy after heating. Similar to the two previous boron-based materials, some un-reacted glass has been found after the corrosion test.

Figure 4.5 displays window glass and P_2O_5 mixture in contact with the aluminum alloy after the corrosion test. A milky white and high viscosity liquid phase has formed during heating. Any trace of corrosion or metal infiltration is not observed in the glass.

Figure 4.6, 4.7 and 4.8 show P_2O_5 + fumed silica, bone ash (Tri-calcium phosphate: $\text{Ca}_3(\text{PO}_4)_2$) and AlPO_4 glasses respectively, which apparently well resisted to the aluminum alloy attack.

These results indicate that both boron-bearing and phosphorus-bearing glasses are having good resistance to aluminum alloys penetration and corundum attack at high temperature (1200°C). In other words, boric oxide and P_2O_5 should act as a barrier to aluminum penetration in glass state.

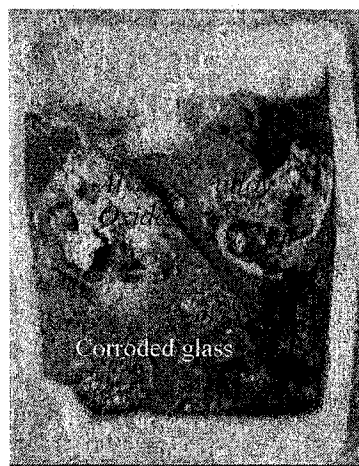


Figure 4.1: Corrosion aspect of W-glass (window glass).

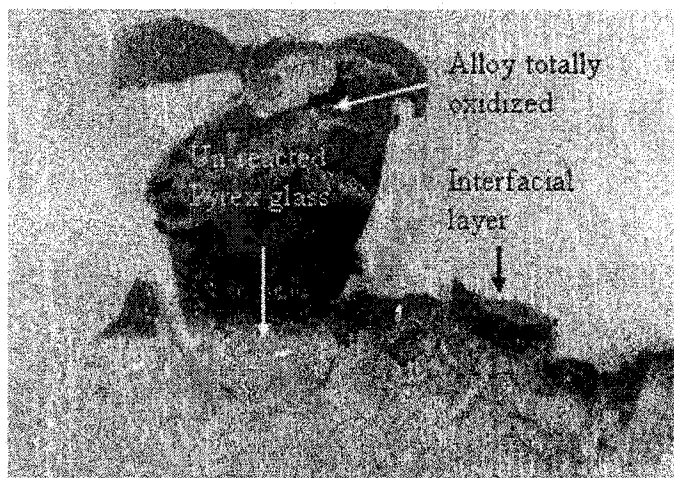


Figure 4.2: Pyrex glass

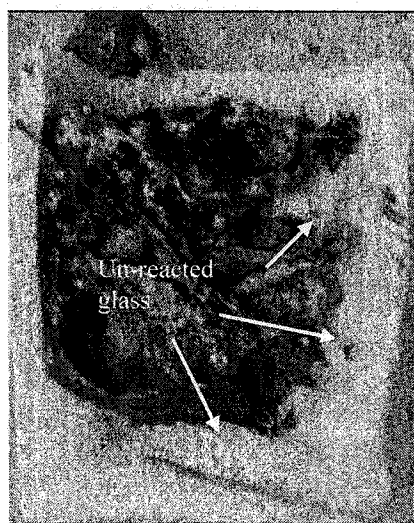


Figure 4.3: B_2O_3 (5g) + SiO_2 (5g)

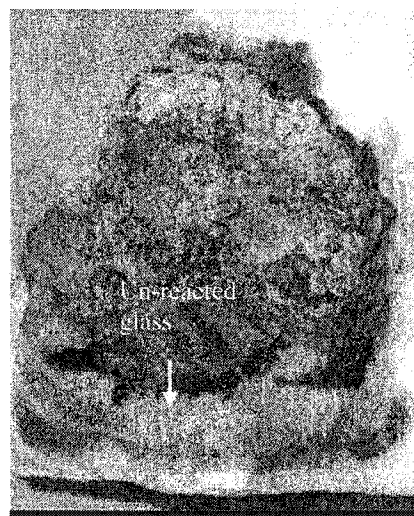


Figure 4.4: B_4C (4g) + W-glass (8g)

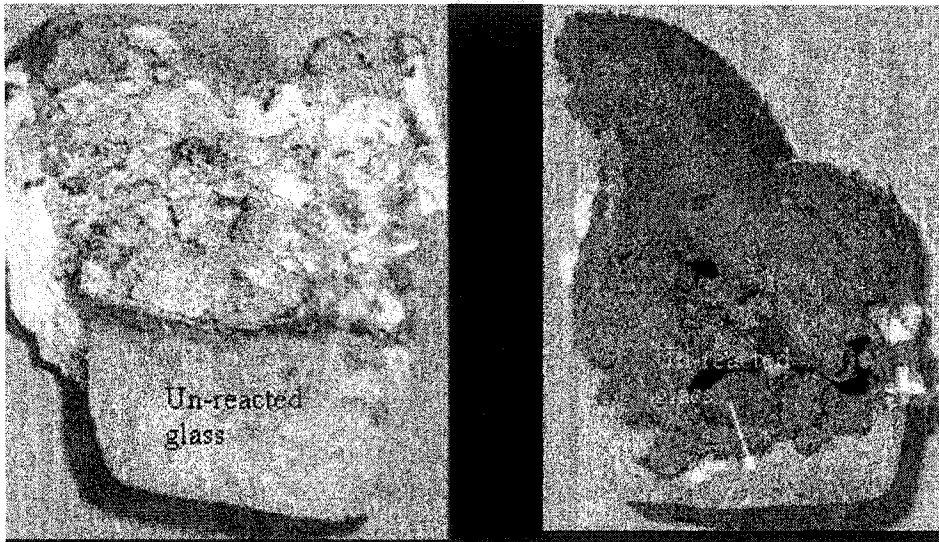


Figure 4.5: P_2O_5 (4g) + W-glass (8g) Figure 4.6: P_2O_5 (3g) + Fumed silica (8g)

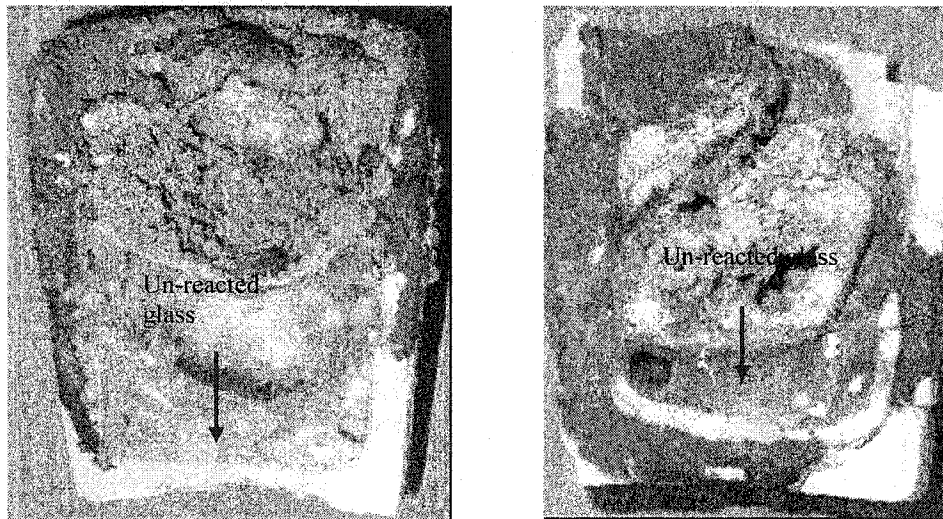


Figure 4.7: Bone Ash (4g) + W-glass (8g) Figure 4.8: $AlPO_4$ (3g) + W-glass (6g)

In order to understand why boron improves the resistance of glasses to aluminum penetration and corrosion, SEM and EDX analysis were performed on the interfacial dark layer obtained during the corrosion test of Pyrex glass sample (see Figure 2). Figure

4.9 shows three zones that were analyzed in this sample. The elemental analysis results are given for these zones in Figures 4.10 to 4.12.

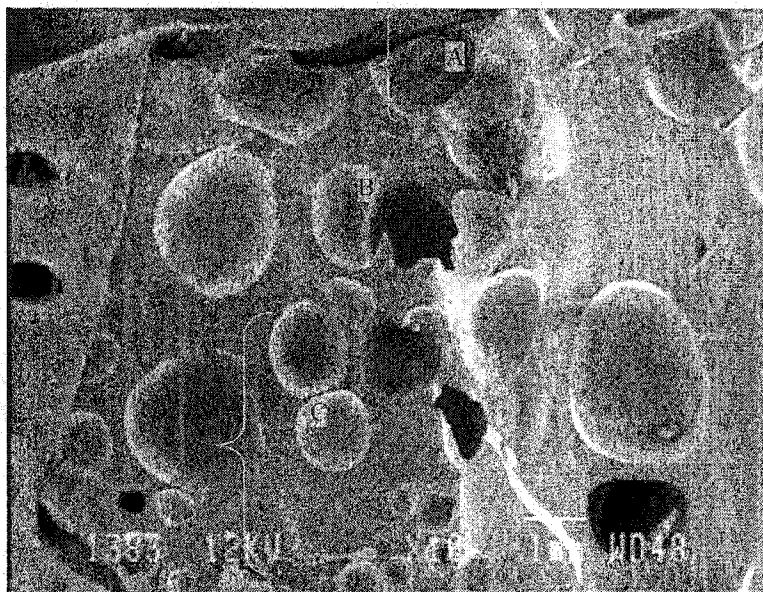


Figure 4.9: Stereoscopic view of the three zones analyses:
A (dark), B (transition), C (clear)

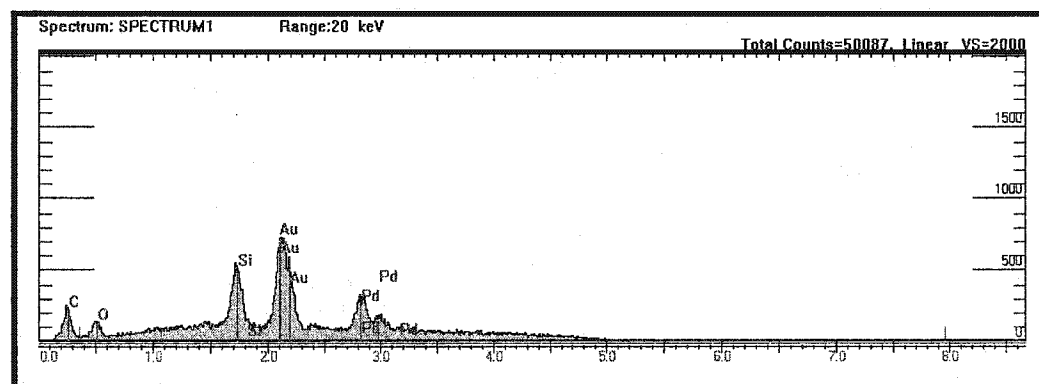


Figure 4.10: Results showing the presence of C, O and Si in the zone A.

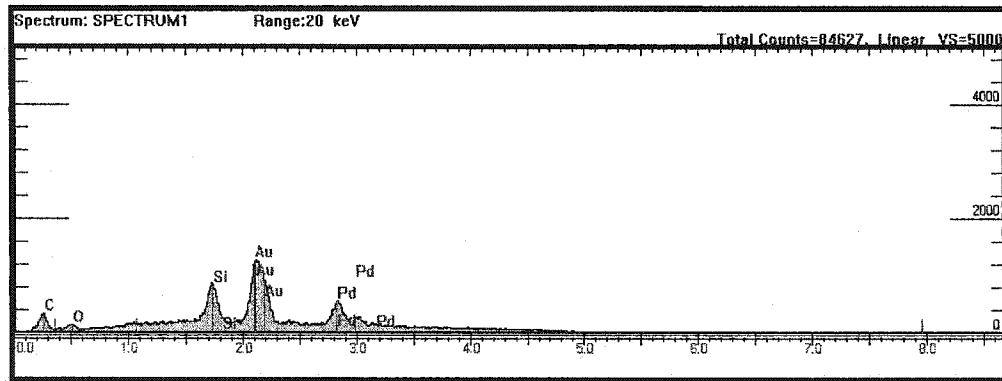


Figure 4.11: Results showing the presence of C, O and Si in the zone B.

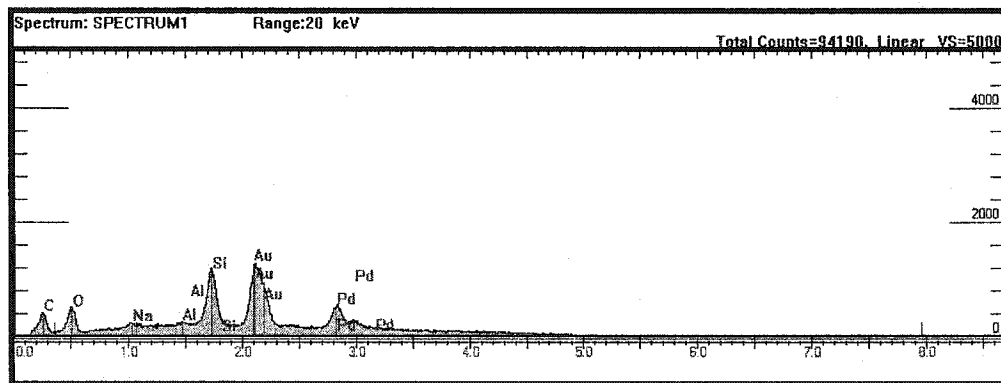


Figure 4.12: Results showing the presence of C, O, Si, Na and Al in the zone C.

Unfortunately, the presence of boron in the glassy phase could not be traced by the present analysis. This may be due to the untraceability of this element. However, the present analysis (Figures 4.9 to 4.12), shows clearly the absence of metal penetration in the dark layer of the Pyrex glass contacting molten alloy.

4.4. Discussion

Referring to Figure 4.13, the main component of glass (the backbone structure) is called a network former. Network formers include mostly SiO_2 , B_2O_3 , and P_2O_5 . To break down the stiff and viscous backbone structure, network modifiers are commonly added which include Na_2O , K_2O , Li_2O and CaO . Network modifiers are often called fluxes in the glass trade ^[61-65].

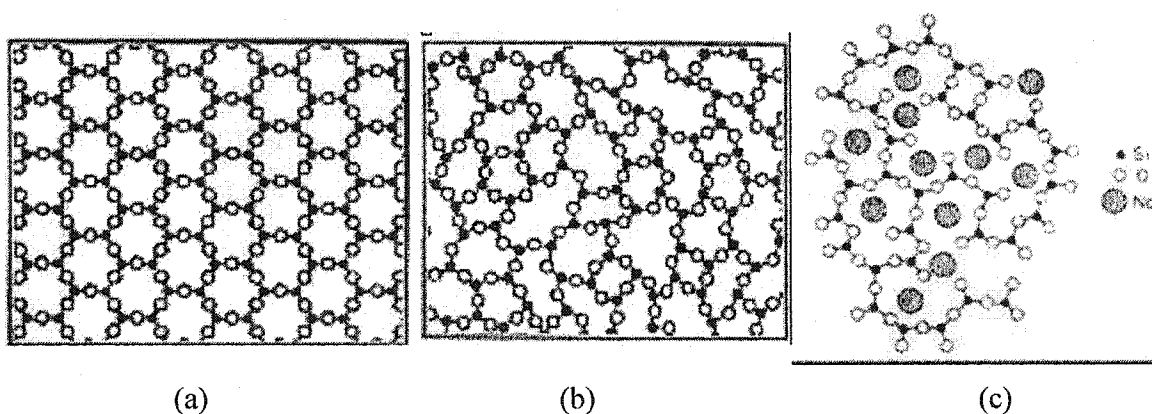
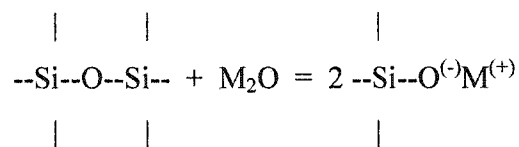


Figure 4.13: Schematic representation of the structure of (a) - ordered crystalline: quartz crystal (b) - random-network glassy form: fused silica glass (c) - sodium silicate glass

There is a wide glass forming range in the binary alkali silicate system (alkali ions $M = \text{Li, Na, K, Rb, Cs}$). The network modifiers (alkali ions) enter the glass as singly charged cations and occupy interstitial sites. Their charge is compensated by NBOs (non-bridging oxygen) created by breaking bridges between adjacent SiO_4 tetrahedra. This "reaction" may be written as:

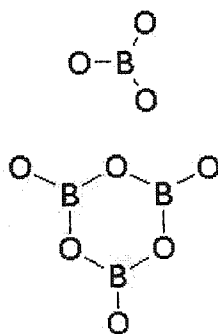


The same is depicted in Figure 4.13-(C). Every alkali ion creates one NBO. The creation of NBOs reduces the connectivity of the glass network, and hence the thermal expansion coefficient, fluidity (inverse of viscosity), diffusion, electrical conduction, and chemical corrosion. All of those increases with increasing modifier content.

Coordination number and bond strength of oxides are shown in Table 4.1. It is known that for glass formers such as SiO_2 , B_2O_3 , and P_2O_5 , the cation coordination number is small (3 or 4). But their single-bond strength and dissociation energy are much larger than for modifiers such as Na_2O .

Table 4.1: Coordination Number and Bond Strength of Oxides

	M in MO _x	Valence	Dissociation Energy per MO _x (kcal/mole)	Coordination Number	Single-Bond Strength (kcal/mole)
Glass Formers	B	3	356	3	119
	Si	4	424	4	106
	B	3	356	4	89
	P	5	442	4	111-88
Glass Modifiers	Na	1	120	6	20
	K	1	115	9	13
	CaO	2	257	8	32

Figure 4.14: Sketch of the Triangular Structure of B₂O₃ glass.

In B₂O₃ glass, the oxygen coordination number of boron is 3. The basic structural unit is a BO₃ triangle, with the boron atom slightly above the plane of the three bridging oxygen atoms. There is experimental evidence that these units arrange to form boroxol rings.

Vitreous B₂O₃ possesses unusually an intermediate range structure involving linked triangles forming planar rings. Boroxol rings glass possesses some aspects of “sheet-like” structure properties (akin to graphite), strong intra-ring bonds and weak Van der

Waal's inter-ring bonds. The very well defined structure of Boroxol rings does not occur in crystalline B_2O_3 polymorphs. B_2O_3 glass is very difficult to crystallize (probably because of these rings) ^[65].

The network structure of phosphate glasses is based upon a tetrahedral PO_4 structural unit. However, the structural behavior of phosphate glasses is markedly different from that of most tetrahedral glassy networks, such as silicate glasses. The reason for this is that the fifth valence electron of the P atom forms an additional "p" bond with one of the oxygen neighbors, making this a terminal bond. The excess of terminal oxygen atoms makes phosphate glasses well suited for accommodation of various modifier cations which themselves may stabilize the network.

In phosphate glasses, the primary network former in the glass is P_2O_5 . The P_2O_5 provides the backbone of the glass structure, forming tetrahedra composed of one phosphorous ion surrounded by four oxygen ions (see Figure 4.15). It differs from the other classic glass formers in that, although it forms a tetrahedral three-dimensional network (because phosphorus is pentavalent) one of the four oxygen ions is doubly bonded, i.e., not coupled to the network. Although a silica-like structure is possible, as in aluminium phosphate, normal alkali and alkaline-earth glasses tend to have chainlike structures because of this pentavalency.

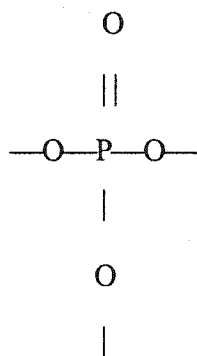


Figure 4.15: Sketch of the tetrahedron structure of P_2O_5 glass showing one $P=O$ nonbridging double bond and three bridging $P-O-P$

Thus, it seems likely that the structure of glassy P_2O_5 is a three-dimensional network of these phosphorous-oxygen tetrahedral as in vitreous silica. It is also possible that sheets of PO_4 tetrahedra exist in some phosphate glass, although there is no direct evidence for them^[61].

4.5. Conclusions

Boron-bearing and phosphorus-bearing silica glasses are more resistant to corrosion than ordinary sodium-bearing glasses.

These results imply that boron-bearing and phosphorus-bearing glass phases are contributed to effectiveness of boron-base and phosphorus-base additives in aluminosilicate refractories.

In soda-lime glass, network modifiers such as Na_2O and CaO enter inside the SiO_2 network, which result in breaking bridges between adjacent SiO_4 tetrahedra. The creation of NBOs reduces the connectivity of the glass network, and hence chemical corrosion occurs and increases with increasing modifier content.

In B_2O_3 glass, linked triangles form planar rings are boroxol ones. Glass possesses some aspects of "sheet-like" structure properties (akin to graphite) and thus strong intra-ring bonds and weak Van der Waal's inter-ring bonds. This structure results in non-wetting with molten aluminum alloy.

The network structure of phosphate glasses is based upon a tetrahedral PO_4 structural unit. However, the structural behavior of phosphate glasses is markedly different from that of most tetrahedral glassy networks, such as silicate glasses. The reason for this is that the fifth valence electron of the P atom forms an additional p bond with one of the oxygen neighbors, making this a terminal bond. It is also possible that sheets of PO_4 tetrahedra exist in some phosphate glass. This unique character of phosphate glass is related to its corrosion resistance to aluminum alloy at elevated temperature.

CHAPTER 5: GENERAL CONCLUSIONS

The major conclusions from the present investigation are:

1. A new corundum corrosion test method was developed.

From several tests, it was proven that the new method is effective for evaluation of refractory resistance to external corundum growth.

Best corundum corrosion test conditions were:

Refractory sample: $50 \times 50 \times 12 \text{mm}^3$ (refractory sample pre-fired at $1200^\circ\text{C} \times 5\text{hrs}$),

Alloy: Al-5%Mg-5%Zn 38g,

1200°C for 40 hours.

With the new method, nine to twelve refractory samples can be tested simultaneously.

Each materials rating from this test is obtained from 3 tested samples.

2. Four kinds of effective additives (including boron-base, phosphorus-base, alkaline earth metal oxides base, and rare-earth base) were found.

2.1. By addition of BN, B_4C , ZrB_2 , TiB_2 , CaB_6 and AlPO_4 5 wt%, to alumino-silicate system castables (C-7080-4 and C-6070-3), the corundum corrosion extent decreased dramatically.

Boron-bearing and phosphorus-bearing additives can't react with SiO_2 . $9\text{Al}_2\text{O}_3 \cdot 2\text{B}_2\text{O}_3$ is formed when boric compounds are used as additives in a lumino-silicate castables. In case of AlPO_4 , there is no new phase formed. AlPO_4 does not decomposed, and it does not react with SiO_2 .

Boron-bearing additives do not apparently change pore size distribution. Adding AlPO_4 results in pore size larger, but the volume of pores does not change.

2.2 Alkaline earth metal oxides such as BaCO_3 , CaCO_3 , and dolomite, and rare earth oxides such as Y_2O_3 are effective additive for alumino-silicate castables C-7080-4 and C-6070-3 to resist to corundum corrosion when the test temperature is 1200°C .

Alkaline earth metal oxides and rare earth oxides can react with silica, and new crystalline phases such as anorthite ($\text{CaO}\cdot\text{Al}_2\text{O}_3\cdot 2\text{SiO}_2$), barium anorthite ($\text{BaO}\cdot\text{Al}_2\text{O}_3\cdot 2\text{SiO}_2$), and $\text{Y}_2\text{O}_3\cdot\text{SiO}_2$ are formed. These transformations reduce the amount of free silica within the refractory's matrix. Refractory protection is achieved with these new crystalline phases, which protect reaction between silica and aluminium metal.

Magnesia does not appear to play a role in resisting to molten Al alloy or corundum under the tested conditions, even though Ellingham diagram shows magnesia is more stable than alumina.

Transformation of MgO into MgAl_2O_4 should be responsible for this phenomenon.

Oxidation-reduction reaction is the main factor that results in corrosion for alumino-silicate castables containing alkaline earth metal oxides and rare earth oxides.

3. Boron-bearing and phosphorus-bearing silica glasses are more resistant to corrosion than ordinary sodium-bearing glasses.

In soda-lime glass, network modifiers such as Na_2O and CaO enter inside the SiO_2 network, which result in breaking bridges between adjacent SiO_4 tetrahedra. The creation of NBOs reduces the connectivity of the glass network, and hence chemical corrosion occurs and increases with increasing modifier content.

In B_2O_3 glass, linked triangles form planar rings are boroxol ones. Glass possesses some aspects of “sheet-like” structure properties (akin to graphite) and thus strong intra-ring bonds and weak Van der Waal’s inter-ring bonds. This structure results in a non-wetting structure to molten aluminum alloy.

The network structure of phosphate glasses is based upon a tetrahedral PO_4 structural unit. However, the structural behavior of phosphate glasses is markedly different from that of most tetrahedral glassy networks, such as silicate glasses. The reason for this is that the fifth valence electron of the P atom forms an additional p bond with one of the oxygen neighbors, making this a terminal bond. It is also possible that sheets of PO_4 tetrahedra exist in some phosphate glass. This unique character of phosphate glass is related to its corrosion resistance to aluminum alloy at elevated temperature.

Finally, no direct relationship was observed between the apparent porosity, density and resistance to molten aluminium or corundum formation from the tested materials under the conditions used in this study.

REFERENCES

1. Michael H. O'Brien and Mufit Akinc "Reduction in Aluminum Alloy Attack on Aluminosilicate Refractories by Addition of Rare-Earth Oxides" American Ceramic Society Bulletin 73{3}491-95 (1990)
2. T.Reetz "New Ceramic Materials for the Non-Ferrous Industry" CERAMIC NEWS special refractory 7{2}76-79 (2000)
3. O.-J.Siljan "Refractory Materials for the Primary Aluminium Industry" CERAMIC NEWS special refractory 7{2} (2)14-22 (2000)
4. K.-E.Granitzki "Refractories in the Foundry Industry" CERAMIC NEWS special refractory 7{2}24-34(2000)
5. A.K.Chatterjee "Refractories for Non Ferrous Industries" The Refractories Engineer Sept. 2-9(2000)
6. Ana Paula F.A.Pereira and Joao B.Baldo "A Low Cement Aluminum Silicate Refractory Castable With Improved Resistance to Molten Aluminum and Cryolite" UNITECR'97 1667-1676(1997)
7. Duncan Jones, Andrew M.Wynn and T.John Coppack "The Development and Application of an Aluminum Resistant Castable " UNITECR'93 854-861 (1993)

8. Ole-J. Siljan, Gjertrud Rian, Dag T. Pettersen, Arve Solheim and Christian Schoning "Refractories for Molten Aluminium Contact Part I: Thermodynamics and Kinetics" UNITECR-ALAFAR 531-550(2001)
9. Shin-ichi SHIMOMURA, Toshiya KISHIMOTO and Haruo NISHIDA "Al₂O₃-AlN Ceramics as Lining Refractory Materials for Aluminum-Magnesium Melting Furnace" UNITECR'95 289-296 (1995)
10. Dr. Peter Jeschke, Dr. Ingo Elstner, Daniel Grimm and Stefan Pischek "Aluminium Titanate—A New Material for the Non-ferrous Metals Industry UNITECR'93 843-853(1993)
11. D S Perera, R L Jeffries and D C Pender "Fabrication of Aluminium Titanate for Refractory Applications in Non-ferrous Metals Industry" UNITECR'93 877-888(1993)
12. Mireille Fouletier, Dieter Gold "Selective, Accelerated Test for Evaluation of Refractory Lifetime in Contact with Aluminium Alloys" UNITECR'97 1667-1676(1997)
13. C. Allaire and M. Guermazi "A New Method for Testing Refractories for Resistance to Corundum Attack" Advances in Refractories for the Metallurgical Industries III, CIM Proceedings Edited by C. Allaire and M. Rigaud, 91-101, August 1999
14. Mohamed Guermazi and Claude Allaire "Effect of Temperature, Atmosphere, Alloy Composition, and Cryolite On the Corrosion Resistance of Refractories by Molten Aluminum" CIREP-CRNF Report No.27 Dec.1998

15. Mohamed Guerhazi and Claude Allaire "Effect of Wollastonite Additions on the Corrosion Resistance of Refractories for Holding and Melting Furnaces" CIREP-CRNF Report No.021 Mar.1998
16. C.Allaire, M.Guerhazi "The Corrosion of Refractories by Molten Aluminum" Aluminum Transactions {1},163-170(1999)
17. C.Allaire, M.Guerhazi "Protecting Refractories Against Corundum Growth in Aluminum Treatment Furnaces" Light Metals 2000,Edited by R.D.Peterson, TMS Proceedings, 685-691,2000
18. Claude Allaire "Mechanisms of Corundum Growth in Refractories Exposed to Al-Mg Alloys" Aluminum Transactions {1},105-120(2000)
19. Saied AFSHAR and Claude ALLAIRE "Effect of BaSO₄ on the Corrosion Resistance of Refractories" CIREP-CRNF Report No.25 Nov.1998
20. Saied AFSHAR and Claude ALLAIRE "Improvement of Low Cement Castables by Non-Wetting Additives against Aluminum Attack" JOM, NOT SUBMITTED YET
21. M.Allahverdi, C.Allaire and S.Afshar "Effect of BaSO₄, CaF₂,and AlF₃ as well as Na₂O on Aluminosilicates Having a Mullite-like Composition" Journal of the Canadian Ceramic Society 66{3}223-230(1997)
22. Saied Afshar and Claude Allaire "The Corrosion of Refractory Aggregates by Molten Aluminum" JOM 43-46,2000

23. Marie-Eve Perron and Claude Allaire "Validation and improvement of the Bellyband Corrosion Test" CIREP-CRNF Report No.23 Nov.1998
24. Marie-Eve Perron and Claude Allaire "Effect of Several Parameters on Corundum Growth in Aluminum Treatment Furnaces" Journal of the Canadian Ceramic Society 69{2}31-35
25. Marie-Eve Perron and Claude Allaire "Microstructural Study of Different Morphologies of Corundum Formed in the Bellyband Corrosion Test" CIREP-CRNF Report No.24 Dec.1998
26. S.Afshar and C.Allaire "The Corrosion of Refractories by Molten Aluminum" JOM 23-27(1996)
27. Sylvio Quesnel, Claude Allaire and Saied Afshar "Criteria for Choosing Refractories in Aluminum Holding and Melting Furnace" Light Metals 1391-1402(1998)
28. Sylvio Quesnel, Claude Allaire and Saied Afshar "Corrosion of Refractories at the Bellyband of Aluminum Holding and Melting Furnace" Advances in Refractories for the Metallurgical Industries II, CIM Proceedings Edited by C.Allaire and M.Rigaud, 321-327, August 1996
29. M.Allahverdi, S.Afshar and C.Allaire "Corrosion Resistance of Aluminosilicate Ceramics to Molten Al-5%Mg Alloy" Advances in Refractories for the Metallurgical Industries II, CIM Proceedings Edited by C.Allaire and M.Rigaud, 295-303, August 1996

30. M.Allahverdi, S.Afshar and C.Allaire “ Additives and the Corrosion Resistance of Aluminosilicate Refractories in Molten Al-5%Mg ” JOM 30-34(1998)
31. Sylvio Quesnel , Saied Afshar and Claude Allaire “Corrosion of Refractories at the Bellyband of Aluminum Melting and Holding Furnaces” Light Metals 661-667(1996)
32. Tomas Richter, Tomas Veza, Claude Allaire and Saied Afshar “Castable with Improved Corrosion Resistance Against Aluminum” Euogress Aachen(Germany),86-90(1998)
33. Criado,Emilio,Martinez, Rafael and Miranda, Manuel “Corrosion of Refractory Lining in an Aluminum Melting Furnace” UNITECR`99 376-379(1999)
34. Ketchion, Stephen etal “High Temperature Corrosion Resistance of Aluminum Contact Refractories” UNITECR`99 384-385(1999)
35. R.Angers, R.Tremblay L.Desrosiers and .Dube “Interactions Between Dense Alumina-Silica Ceramics and Molten Aluminum” Journal of the Canadian Ceramic Society 66{1}64-71(1997)
36. A.M.WYNN “Testing of Castable Refractories for Resistance to Molten Aluminum Alloy” Br.Ceram.Trans.J.,91. 153-158(1992)
37. M.A.CARVALHO, J.R.FRADE and A.M.SEGADAES “Corrosion of Aluminosilicate Refractories by Molten Salts: Evaluation and Testing” Br.Ceram.Trans.J. 86. 74-76(1987)

38. Claude Allaire and Paul Desclaux "Effect of Alkalies and of a Reducing Atmosphere on the Corrosion of Refractories by Molten Aluminum" J.Am.Ceram.Soc. 74{11}2781-2785(1991)
39. Robert Pompe and Roger Carlsson "ON THE REACTIONS INVOLVING REFRACTORIES FOR ALUMINUM CASTING" UNITECR'89 906-911(1989)
40. Technical Association of Refractories Japan, "Refractory Handbook" Tokyo, Japan, 423-429(1998)
41. Ole-J. Siljan and Christian Schoning "REFRACTORIES FOR MOLTEN ALUMINIUM CONTACT. PART II: Influence of pore size on aluminium penetration" UNITECR-ALAFAR 551-571(2001)
42. Saied Afshar and Claude Allaire "The Corrosion of Refractory Aggregates BY Molten Aluminium" JOM 43-46(2000)
43. Criado, Emilio; Martinez,Rafael and Miranda,Manuel "Corrosion of Refractory Lining in an Aluminium Melting Furnace" UNITECR 376-379(1999)
44. Claudio Zirpoli, Galileu Lopes Da Silva, Silivo Araripe Sucupira "New refractories for aluminium melting furnaces" Refractories Applications and News 7{1}20-25(2002)
45. www.whitstonecement.com
46. Mireille Fouletier, Dieter Gold "Selective, Accelerated Test for Evaluation of Refractory Lifetime in Contact with Aluminium Alloys" UNITECR'97 1667-1676(1997)

47. Stephan Rudolph "Boron Nitride" American Ceramic Society Bulletin, 73 {6} 89-90 (1994)
48. Ernest M Levin, Howard F McMuride "Phase Diagram for Ceramists" The American Ceramic Society, 1964,1972,1981
49. Brondyke,K.J., "Effect of molten aluminium on alumina-silica refractories" J.Am.Ceram.Soc., 36,171-174(1953)
50. Chen-Feng Chan, Bernard B.Argent ,and W.E.Lee "Influence of Additives on Slag Resistance of Al_2O_3 - SiO_2 -SiC-C Refractory Bond Phases under Reducing Atmosphere" Journal of American Ceramic Society 81 {12}(1998)
51. S.K.Rhee."Wetting of Ceramics by Liquid Aluminum" Journal of American Ceramic Society 53,386(1970)
52. F.Gebhardt, G.Boymanns "Experiences with use of Magnesia-Alumina-Spinel Bricks in Aluminium Melting Furnaces " Ceramic News Special Refractories 7 {2} 2000
53. Gabis, Victor "Improvement of high alumina castable resistance to corrosion by aluminium alloy" UNITECR'99 380-383(1999)
54. Miyawaki,M and Hongo,Y.: "Effect of materials and pore diameter controal an the penetration resistance of castables", J.Tech.Assoc.Refr.Japan,20 {2} 115-120(2000)

55. Clavurd, B. and Jost, V.: "Refractories used in melting furnaces for aluminium alloy", *Interceram*, 30, 306-314 (1981)
56. www.factsage.com Ecole Polytechnique of Montreal
57. V. Gabis, J.P. Ildefonse, B. Depussy, M. Richard and M. Stucky "Corrosion of MgO and MgAl₂O₄ by aluminium alloys" *Key Engineering Materials* Vols. 132-136 1653-1656 (1997)
58. *Materials Handbook* www.ceramicindustry.com
59. Michel Rigaud "Corrosion Failures of Industrial Refractories and Technical Ceramics" Volume 11 Failure Analysis and Prevention *ASM HANDBOOK The Materials Information Society* Materials Park, Ohio, 44073-0002 (2002)
60. Ernest M Levin, Howard F McMurry "Phase Diagram for Ceramists" *The American Ceramic Society*, 1964, 1972, 1981
61. ROBERT H. DOREMUS "Glass Science" John Wiley & Sons, Inc. 1973
62. C.R. Kurkjian and W.R. Prindle, "Perspectives on the History of Glass Composition" *J. Am. Ceram. Soc.*, 81 {4} 795-813 (1998).
63. W.D. Kingery, H.K. Bowen, D.R. Uhlmann "Introduction to Ceramics" 2nd Edition A Wiley-Interscience Publication JOHN WILEY & SONS 1975

64. Shelby, James E "Introduction to Glass Science and Technology" Cambridge, England : The Royal Society of Chemistry, 1997
65. Richard K.Brow "Introduction to Glass Science" Department of Ceramic Engineering University of Missouri-Rolla www.umr.edu
66. MASAO MIYAWAKI and YASUO HONGO "Effect of Materials and Pore Diameter Control on the Al-Penetration Resistance of Castables" Journal of the Technical Association of Refractories, Japan 20{2}115-120(2000)
- 67.T.H.Hall and G.wilson "Non-wetting Refractories for Aluminium Furnace Application" Proceedings of the International Symposium on Advances in Refractories for the Metallurgical Industries 225-233 August 23-26,1987 Pergamon Press
- 68.Don Hill and Joe Bidwell "Refractory Material Reduces Furnace Downtime for Aluminum Die Casting and Extrusion Facilities" 68-70 August,2000 Industrial Heating
69. Waldir de Sousa Resende,Claudio Zirpoli,Galileu Lopes Da Silva and Silvio Araripe Sucupira "New Refractories for Aluminium Melting Furnaces" Refractories Applications and News 7{1}20-25(2002)

70. W.E. Lee, R.E. Moore "Evolution of in situ refractories in the 20th century" Journal of American Ceramic Society 81 {6} 1385-1410(1998)

71. J.M. McCollum "Advanced Refractories for Aluminum Melting Furnaces" Light Metal 807-813(1989)

72. Claude Allaire "MÉTALLURGIE DE L'ALUMINIUM" PARTIE II ÉCOLE POLYTECHNIQUE DE MONTRÉAL Janvier 2001

73. Annual book of ASTM standards, Designation. Standard definitions of terms relating to Refractories, C71, Vol15.01, American Society for Testing and Materials, 1998